PRINTING, STABILIZATION AND OPTIMIZATION OF ODOUR-GENERATING SENSORS

PRINTING, STABILIZATION AND OPTIMIZATION OF

ODOUR-GENERATING SENSORS

BY

ZHUYUAN ZHANG, M.ENG., B.SC., B.A.

A THESIS

SUBMITTED TO THE SCHOOL OF GRADUATE STUDIES

OF MCMASTER UNIVERSITY

IN PARTIAL FULFILMENT OF THE REQUIREMENTS

FOR THE DEGREE OF

DOCTOR OF PHILOSOPHY

Doctor of Philosophy (2015)   McMaster University

(Chemical Engineering)   Hamilton, Ontario, Canada

TITLE: Printing, Stabilization and Optimization of Odour-
                    Generating Sensors

AUTHOR: Zhuyuan Zhang

                    B.Sc., (China Agricultural University)

                    B.A., (China Agricultural University)

                    M.Eng., (Tsinghua University)

SUPERVISOR: Professor Carlos D. M. Filipe

                    Professor Robert Pelton

NUMBER OF PAGES: ix, 166

Abstract

This thesis describes the development, production, optimization and use of two types of odour-generating sensors, which in the presence of specific targets release odorous molecules that are easily detectable by the human nose.The first sensor was based on our previous work using an enzyme-based odour-generating system.This sensor consists of two enzymes, pyridoxal kinase and tryptophanase, that when combined lead to the generation of methyl mercaptan (easily detectable by the human nose) in a manner that is proportional to the presence of the target, adenosine triphosphate (ATP). In this thesis, I took three steps towards making this sensor more relevant from an application point of view.

Our previous sensor was solution-based, a format that is not useful from a practical point of view — it is much more appealing to have the sensor in a solid support. My first contribution was to inkjet-print a fully functional sensor on a paper surface to create, what we call "Smell-Tell" paper or swab. Paper is an attractive support for biosensors because it is inexpensive, readily available and can be discarded after use. Inkjet printing is a scalable technology that will allow producing these sensors in large-scale. Printing the sensor on paper is an important step improving sensor usability. The printed paper sensors were active for at least 48 days when stored in the fridge (4°C).

Keeping the sensors refrigerated to preserve activity is a substantial drawback towards usability of these sensors. My second contribution was to demonstrate that the enzymes and substrates needed for the "Smell-Tell" paper could be preserved at room temperature, with minimal loss of activity, when immobilized in a pullulan film. Pullulan is a readily water-soluble nonionic polysaccharide and our group has previously reported the ability of this material to preserve the activity of enzymes and other molecules at room temperature. I have shown that it is also possible to prepare "Smell-Tell" pullulan tablets, which provide an instrument-free one step assay for on-site detection of ATP, and that the tablets are stable for at least 2 months when stored at room temperature.

The two-enzyme system used is quite complex and no previous efforts had been made to optimize the conditions under which it works best, with minimum use of reagents. Fractional factorial design, a statistical method, was used to optimize the system and to investigate the influence of different variables including enzyme concentration, reaction duration, temperature, etc. Based on human smell tests and a designed scoring system, the conditions were optimized in an efficient manner. I found that the most important factor affecting the ability to detect the target (ATP) was the time of reaction (the longest time provided lower detection levels). Using this statistical method, it was possible to decrease the amount of enzymes used by 30% without sacrificing the detection limit.

The second odour-reporting sensor described in this thesis is a dual-signaling sensor that reports the presence of water (as little as 50 µL) through the generation of both odour and colour signals. This type of sensor can be used to report intrusion of water into difficult to reach electrical panels, or to detect and report water leakage in individual boxes stored in large containers (such as those used to ship meat in trucks). In addition to experimentally validating the approach, we used modelling to simulate the evaporation and diffusion of the odorous signal and the results demonstrated the possibility of using an odour signal as the reporting signal even in a large room. Proof-of-concept was therefore obtained for instrument-free multi-sensory reporters employing odorous signals.

Acknowledgements

Abbreviations

TPase	tryptophanase
PLP	pyridoxal phosphate
PKase	pyridoxal kinase
ATP	adenosine 5'-triphosphate
TRP	tryptophan
PL	pyridoxal
SMLC	S-methyl-L-cysteine
ELISA	enzyme-linked immuosorbent assay
IPTG	isopropyl β-D-1-thiogalactopyranoside
LB	lysogeny broth
E.coli	*Escherichia coli*
IgG	immunoglobulin G
LOD	limit of detection
ppm	parts per million
ppb	parts per billion
DNA	deoxyribonucleic acid
RNA	ribonucleic acid
BSA	bovine serum albumin

Contents

Chapter 1

Introduction

The detection of odourants in the environment, which provides information on danger, food, pathogen, predators and mates, is crucial for the survival of most animals. The controlled generation of odourants will benefit taste and smell industries, including perfumes, food & beverage, pesticides (pheromones) and even odour information display.[1] To date, a number of studies have been performed on the development of controlled odour generation. For example, in the late 1980s, Ryōji Noyori, the laureate of the 2001 Nobel Prize in Chemistry, developed the "Takasago process" for the synthesis of (–)-menthol, which today is one of the world's most sold flavour ingredients.[2] In 1991, Linda B. Buck and Richard Axel, who won the 2004 Nobel Prize in Physiology or Medicine, published their landmark paper on olfactory receptors, unraveling how the sense of smell works in molecular level.[3] Recently, the extraordinary abilities of human olfactory system were further disclosed, distinguishing more than 1.7 trillion stimuli with picomolar to millimolar detection limits for many odourants.[4,5] The human nose provides us with an astonishing ability to protect ourselves. After

simple training, humans can effortlessly relate certain odourant signals to corresponding phenomena. An elegant example demonstrating our robust olfactory system is the use of thiols as the odourants to assist in the detection of natural gas leakages. In the last five years, several research groups have been trying to design different sensing systems, especially biosensing systems, by generating odour signals to further exploit the human sense of smell. Fig. 1.1 shows two examples of odour-generating biosensor applications in detecting the presence of an enzyme and an antigen.[6,7] Fig. 1.1.A comes from Mohapatra's and Phillips' paper in 2012, where they reported on a system to detect the presence of the enzyme glucose oxidase and reporting its presence through the generation of a fluorescent molecule and ethanethiol.[6] Ethanethiol, as the human detectable odour signal, permits quick triaging of samples based on smell. The key concept on that work was the synthesis of a substrate molecule that when cleaved by the target created the two signals. Last year, our group reported an enzymatic biosensor, a substantially different approach from that of Mohapatra and Phillips, which explored tryptophanase (TPase) as an odour-generating reporter to produce methyl mercaptan.[7] An ELISA-like assay (Fig. 1.1.B) was developed to detect the presence of a target (an antigen) and linking the presence of the target with generation of methyl mercaptan via the catalytic activity of TPase.
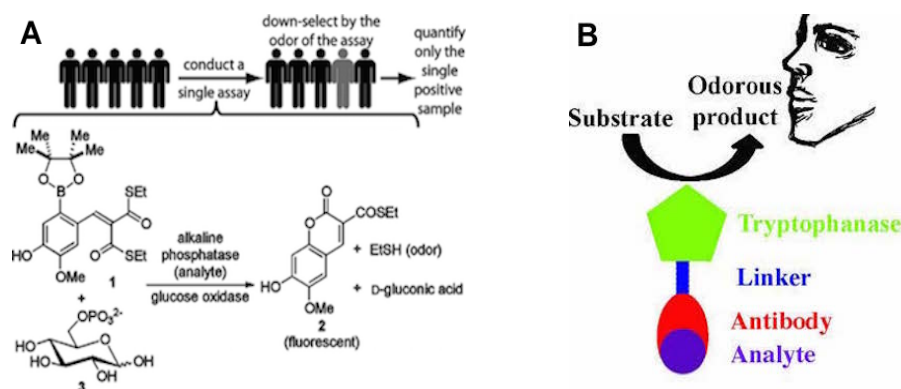
Figure 1.1 Previously reported odour-generating biosensors: (A) the detection of an enzyme using a designed substrate to generate an odour signal for quick screening purpose, adapted from Mohapatra, et al.;[6] (B) the detection of antigen/antibody using tryptophanase based ELISA to generate an odour signal, adapted from Xu, et al.[7]

This chapter will first present a literature review on biosensors, with a focus on odour signal generation and detection, followed by the specific objectives of my research and an outline of the thesis.

1.1 Literature Review

1.1.1 Biosensor Reporting Signals

Biosensors, biological components based analytical devices, have over the past half century been developed for the purposes of environmental monitoring, food quality control and clinical diagnosis.[8,9] A biosensor typically consists of two main elements: a bio-receptor (e.g., enzymes,[10,11] antibodies,[12] nucleic acids,[13] or whole cells[14]) that acts as a target specific recognition element and generates a primary signal; and a transducer that coverts the primary signal into a detectable one.[15–20] Most biosensors

can be categorized into three main groups: electrochemical, optical, and mass sensitive, based on the employed transduction methods and generated final signals.

1.1.1.1 Electrochemical

The basic principle of electrochemical biosensors is the use of chemical reactions to generate or consume electrons, which affects the electrical properties (e.g. electric current or potential).[21] The three main classes of electrochemical biosensors are amperometric, potentiometric, and conductometric.[21] Amperometry is reported to be the most widely used technology in biosensor development.[21] In amperometric biosensors, the potential is set at a value where the current is produced in proportion to the concentration of analyte. These biosensors have been extensively exploited for environmental applications, such as detection of organophosphorus compounds,[22–25] biochemical oxygen demand,[26,27] phenol and substituted phenolic compounds,[28,29] and health applications.[14,30,31] A potentiometric biosensor typically involves the measurement of the potential difference between the indicator electrode and reference electrode.[32] Potentiometric biosensors are widely used, but are often less sensitive and slower than amperometric analogue.[32] Conductometric detection is based on the change in electrical conductivity caused by the ionic species concentration changes and requires no reference electrode.[33] On the other hand, the selectivity of conductometric biosensors is relatively poor.[14,32]

1.1.1.2 Optical

Optical techniques have been employed in many classes of biosensors to provide label free detection. Over the past decades, methods based on colorimetry, fluorescence, chemiluminescence and surface plasmon resonance (SPR) based methods have been the most popular. The colorimetric technique is a simple and straightforward approach for producing signals that can be easily detected by human eyes. A representative example is the commercial pregnancy test strip, which detects human chorionic gonadotrophin and shows up as a colour line. Recently, several research groups including Sentinel Network in Canada,[34–36] Whitesides's group in Harvard University,[37] and Shen's group in Monash University,[38] have been working on the development of user-friendly biosensors, to detect various analytes (e.g. glucose, protein, neurotoxin and human blood type) and generate colorimetric signals. Moreover, there are also elegant concepts using functional nucleic acid to realize detection of heavy metals[39] and bacteria.[40] Fluorescence and chemiluminescence are both luminescence obtained when atoms or molecules relaxing from their excited state to ground state. The difference is the source of energy required to obtain the excited state.[32] Fluorescence requires energy from an external light source, whereas, chemiluminescence demands energy from a chemical reaction.[32] It has been reported that fluorescence or chemiluminescence signal based biosensors have extremely high sensitivity, even at single cell level for bacteria detection.[41,42] However, the fluorescence technique requires time-resolved instrumentations, while chemiluminescence has a relative short lifetime.[32,43] The principle of SPR biosensors is that the adsorption of target molecules results in changes of the refraction index.[44] Various biomaterials have been incorporated with SPR biosensors including nucleic acid[45] and antibody/antigen.[46]

1.1.1.3 Mass Sensitive

Mass sensitive biosensors employ signal generation based on the slight changes in mass to provide label free detection.[32] A mass sensitive biosensor can be fabricated by attaching the recognition element, which recognizes and attaches analytes onto the sensor surface.[47] The two main classes are: (1) quartz crystal microbalance (QCM), or named bulk wave (BW) and (2) surface acoustic wave (SAW).[47] The main difference between QCM and SAW sensors is that the wave created by QCM propagates through the whole volume of the sensor, whereas the SAW wave travels along the sensor surface only. SAW sensors also have smaller sizes and higher operating frequencies.[48]

1.1.2   Odour Signals

In addition to the optical, electrochemical, and mass sensitive signals mentioned in Section 1.1.1, an emerging reporting signal, odour signal, has been investigated recently. Odour signal is different from the three signals described previously in that users do not need to constantly look at the readout for real-time monitoring, since diffusing odour signals can be spontaneously detected by human noses. Detailed previous reports of odour-generating sensors are summarized in Section 1.1.3.

1.1.2.1 Diffusion of Odour Signals

One remarkable advantage of using odour-generating sensors is that the generated odour signals can self-diffuse to detection instruments. Estimation of the diffusion process of odour signals is of large importance for the design and development of odour-generating sensors. Previous studies on gas diffusion simulation are summarized in this section.

Gas emission sources can be characterized by their durations: intermittent or continuous.[49] Alternatively, they can be classified by their dimensions: point, line, area or volume sources.[49] There are several well-established air diffusion models. Most of them, including AERMOD, ATSTEP and CALPUFF, focus on atmospheric systems.[49] Differently, some other models focus on the development of indoor gas diffusion, which is typically for the estimation of indoor air pollutant concentrations and feasible for potential application situations of odour-generating sensors.

A few studies have estimated air pollutant concentrations using the instantaneously well-mixed mass balance model[50–54] or a series of well-mixed divisions to represent different zones[55,56] for the cases where the duration of mixing is much shorter than the time scale of source exposure. In cases where the emission duration is comparable to the exposure time, such as continuous emission, diffusion delay becomes important to consider. In these situations, air pollutant concentrations will be significantly higher in close proximity.[57–59] Fick's law[60,61] and random walk theory[62] have been used to simulate indoor air pollutant concentrations. Additionally, in cases involving forced air flow causing convective diffusion, the advection-diffusion model has been proposed

to predict air pollutant transport from a point source.[63]

Since all aforementationed models depend on some empirical parameters, studies have focused on how to assess the models experimentally. Real time monitors are typically used to simultaneously measure air pollution concentrations. For example, in 2011, Cheng et al.[64] proposed a method to use dozens of monitors to measure CO levels from a continuous indoor point source at different positions (Fig. 1.2). Their results showed that the currently available models could indeed predict indoor concentrations inside naturally ventilated rooms.
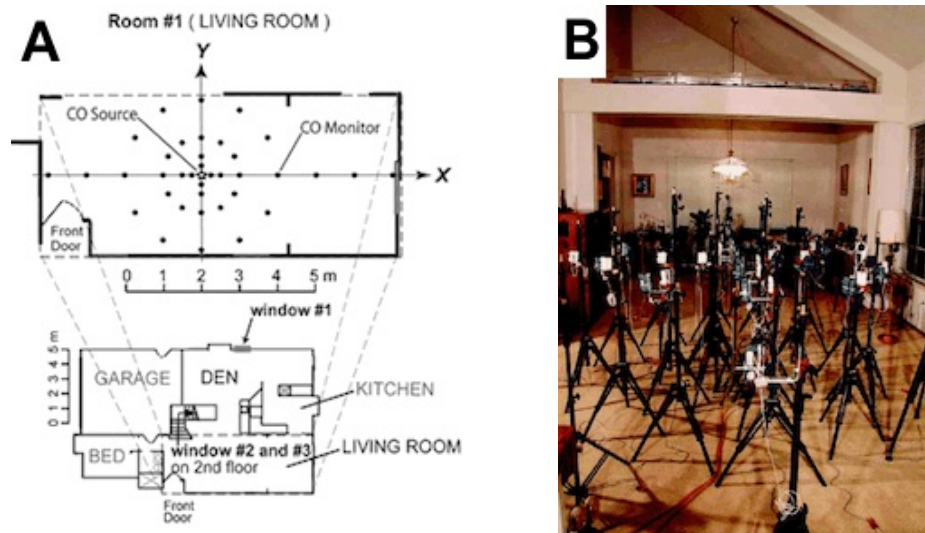
Figure 1.2 Experimental setup assessing models of indoor air pollution diffusion. (A) Schematic of the monitoring array configurations in a residence house; (B) a photo of the setup of real-time monitors for air pollution concentrations determination. Figures are adapted from Cheng et al.[64]

1.1.2.2 Detection of Odour Signals

Human Sense of Smell

Humans have an extraordinarily strong sense of smell, which is provided by olfactory receptor genes, the largest mammalian gene family known.[65-67] The use of odours as reporting signals takes advantage of our strong sense of smell for the following reasons:

1. Odour signals can be rapidly detected by human noses, without use of any instrument;

2. The human olfactory system has extremely low thresholds, the minimum concentration of an odourant that can be detected by humans for many odorous chemicals.[68] Table 4.5 shows several human olfactory threshold examples for odorous chemicals;

Table 1.1 Human olfactory thresholds for some chemical compounds.

Odour Chemical	Human Olfactory Threshold	Reference
Ammonia	5 ppm*	[69]
Indole	0.02 ppb**	[70]
Methyl mercaptan	0.2 ppb	[70]
3-Methyl-1-butnathiol	0.03 ppb	[71]

* ppm: parts per million; ** ppb: parts per billion.

3. The human olfactory system displays super high discrimination between molecules. A recent report shows human noses could discriminate at least 1.7 billion stimuli;[4]

4. Sense of smell is an involuntary ubiquitous human sensation.[72] Eyes shut or open, ears attentive or not, we cannot help but smell. The other senses can be stopped

manually (e.g. closing the eyes or plugging the ears), but we cannot stop breathing;[1]

5. Odourant detection and discrimination can improve with practice;[72,73]

6. Odour signals can work as a supplement to other signals. For example, to provide a supplement for colour signal to assist detection for individuals suffering from optical complications or staying in light-limited situations.

On the other hand, there are also several concerns when only using human noses as the detection instrument:

1. It is hard for humans to quantify the signal strength through olfactory sensing;[74]

2. Humans are bad at identifying the source of odours. Opposed to the elegant spatial abilities in vision and audition, humans have only elementary spatial ability in olfaction;[72]

3. Humans do not place confidence in their noses even though humans have a remarkable olfactory system. Only high odourant concentrations spontaneously shift humans' attention to olfaction;[72]

4. Humans show olfactory adaptation. Three forms of odour adaptation have been reported based on different mechanisms: (1) short-term adaptation, e.g. 6 s for full recovery after a 100 ms brief odour pulse; (2) desensitization, e.g. 1 min for full

recovery after 8 s sustained odour pulse; (3) long-term adaptation, e.g. a few minutes for full recovery after 25 s repetitive odour pulses.[75,76] Out of these, only long-term adaptation influences the olfactory threshold.[75,76]

5. Loss of olfactory acuity due to aging. The loss of olfactory acuity varies between different odourants and individuals.[1]

6. Odour signals are not feasible for individuals suffering from distorted olfactory perceptions such as decreased olfactory sensitivity, the inability to correctly identify the natural smell of an odour, and untrue perception of an odour when there is no odourant inhaled.[77]

Artificial Noses

As there are some health and safety concerns associated with using the human nose as the detection instrument, artificial noses have been developed as a supplement to detect odorous chemicals. These artificial noses have been used in environmental monitoring, food quality control and clinical bio-analysis areas.[78–80] Artificial noses are divided into two main classes: electrical and optical, based on the signal transduction technologies employed. Electrical noses, which convert gas signals into electrical ones, have been explored to mimic the olfactory system. Electrical noses generally exploit materials such as metal oxide semiconductors,[81] conductive polymers,[82] coated quartz vibrators,[83] carbon nanotubes,[84] and graphene.[85] Electronic noses have many advantages, such as short detection time with high sensitivity and reproducibility,

and the ability to recognize complex odours.[86] There are dozens of commercial electronic noses from different companies, with an example shown in Fig. 1.3.A. Even so, electronic noses are generally sensitive to humidity and electromagnetic radiation, which constrains their application in some real fields.[87] Moreover, the aging of sensor surface significantly increases the background noise.[87]
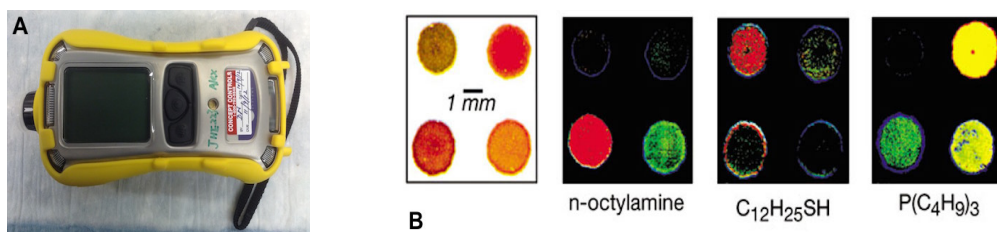
Figure 1.3 Examples of artificial noses: (A) a portable electronic nose used in our lab, which was purchased from RAE systems, Inc.; (B) colour fingerprints of different odour chemicals at the ppm level (adapted from Rakow and Suslick[88]).

The long history of visual indicators in analytical chemistry has promoted the development of optical noses as an alternative to electronic noses to detect odours. Suslick's group reported an optical nose based on the colorimetric approach, in which different types of metal porphyrin showed corresponding constants with different gas molecules, and provided unique colour-change patterns (Fig. 1.3.B).[88] They further demonstrated that this method could discriminate 100 volatile organic compounds,[89] and be used for real time determination of fungal volatile organic compounds.[90] Other examples of optical noses are selective visual detection for TNT (2,4,6-trinitrotoluene),[91] a paper-based colorimetric sensor for volatile organic composites detection,[92] and optical noses for various gases detection based on photonic crystal.[80,93,94]

1.1.3   Odour-Generating Sensors

1.1.3.1 Odour-Generating Biosensor — A Focus on ATP detection

Over the past ten years, besides the two systems shown in Fig. 1.1, there have been three more systems focusing on odour-generating biosensor development. In Melker's 2005 patent, he describes the idea of using nanotubes filled with volatile chemicals which can be released when the target analytes open an RNA aptamer cap on the nanotubes.[95] Nicklin's 2007 patent describes an engineered whole cell based odour-generating biosensor. By comprising genes for the recognition protein and the reporter protein, this sensor generates odorous molecules such as hydrogen sulphide and methanethiol upon exposure to a specific target.[96] In addition, Xu et al.[7] from our group coupled pyridoxal kinase (PKase) with TPase for ATP detection. (Fig. 4.6)
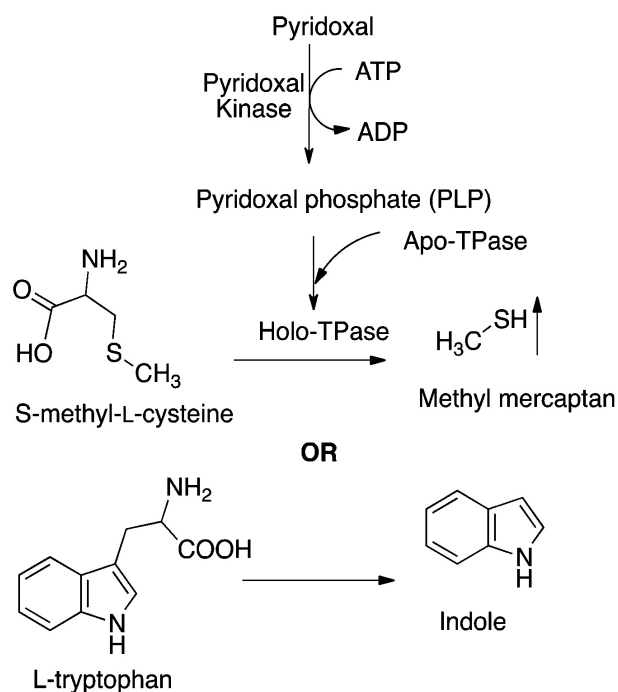
Figure 1.4 Working mechanism of bienzymatic system reported by Xu[7] and Zhang[97] in 2014. Figure adapted from Zhang et al.[97]

ATP is an important biological marker involved in areas of hygiene monitoring, food and water safety monitoring, etc.[7] Several ATP detection strategies have been well developed, including bioluminescence method, electrochemical method, fluorescence method, DNA aptamer method, and atomic force microscopy method.[7] Since the intracellular ATP content is about 10^{-20} to 10^{-18} moles per cell for microbes,[98] some of these ATP assay methods are expected to be used for rapid detection of microorganisms and organic contaminations.[99] Table 1.2 summaries the reported assay principles and their detection abilities since 2009.

Table 1.2 Reported ATP detection methods and detection abilities since 2009.

Assay Principle	LOD*	Reference
Luciferase assay	pM	[100]
Nanoparticle-based fluorescence aptasensor	nM	[101]
Chemiluminescence	nM	[102]
Surface-enhanced Raman scattering**	nM	[103]
Resonance scattering spectral	nM	[104]
Synthetic fluorescent probes	mM	[105]
Circular strand-displacement polymerization based fluorescence aptameric sensor	nM	[106]
Enzyme-assisted fluorescence signal amplification	nM	[107]
Double-stranded DNA based fluorescence	pM	[108]
Metal nanomaterial-based fluorescence aptasensor	µM	[109]

* LOD: limit of detection. ** Surface-enhanced Raman scattering assay bases on the mechanism that Raman scattering intensity of molecules could be greatly improved after adsorbed onto a metal surface.[110]

However, these methods typically involve complicated instruments and well-trained technicians. Different from them, PKase and TPase based bienzyme system was instrument free, with an ATP detection limit of 0.32 µM.[7]

In this bienzyme system, PKase from *E.coli* is a dimeric protein consisting of two $\sim$ 30 kDa subunits (Fig. 1.5.A).[111] It contains 624 residues with unit-cell parameters a = 64 Å, b = 75 Å, c = 109 Å. The active sites of PKase (Fig. 1.5.B & C[112]) contain aspartic acid and glutamic acid, which carry carboxylic groups. From the previous reports, the enzyme kinetic constants are: for L-tryptophan, $K_m = 0.2 \sim 0.273$ mM, $K_{cat} = 1.37$ s^{-1}; for *S*-methyl-L-cysteine (SMLC), $K_m = 2.04$ mM, $K_{cat} = 0.50$ s^{-1}.[113,114]

15
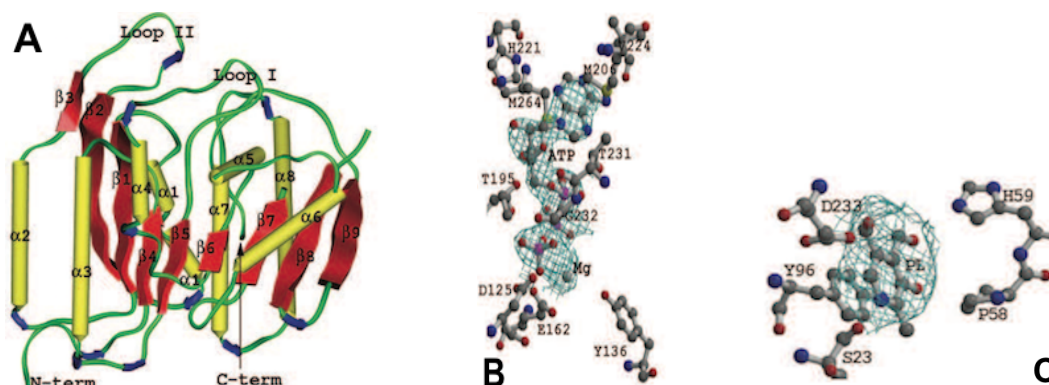
Figure 1.5 (A) Ribbon diagram of the subunit of PKase, with α-helices coloured in yellow and β-strands coloured in red respectively; (B) The ATP binding site of the MgATP-bound complex; (C) The pyridoxal binding site. PL: pyridoxal. Figures are all adapted from Safo et al.[112]

TPase from *E.coli* is a tetramer of four 52.8 kDa subunits (Fig. 1.5A).[115,116] Pyridoxal phosphate (PLP) and ions, such as NH_4^+ and K^+, are the cofactors of TPase.[117] TPase contains 1867 residues with the unit-cell parameters a = b = 215.5 Å and c = 107.6 Å. Its active site (Fig. 1.5B[116,118]) contains lysine, which has primary amine groups, and aspartic acid, which has carboxylic groups. The enzyme kinetic constants are: for pyridoxal, K_m = 30 µM, and K_{cat} = 0.75 s^{-1}; for ATP, K_m = 420 µM.[119]
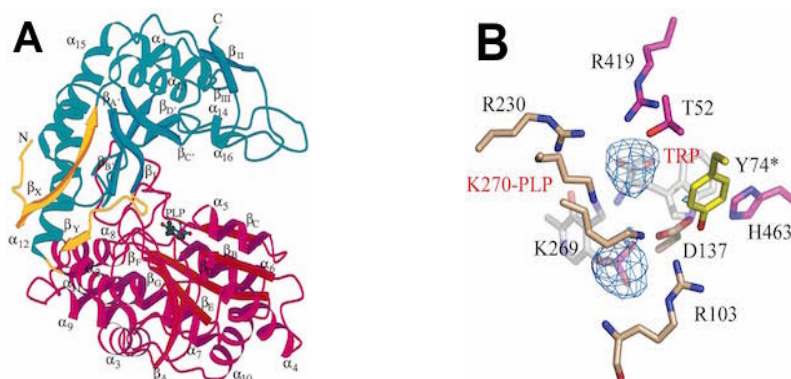
Figure 1.6 (A) Ribbon diagram of the subunit of TPase, with small domain coloured in blue, large domain coloured in red, and N terminus coloured in yellow. Figure adapted from Isupov et al.[116] (B) Active site of TPase with the bound PLP and tryptophan. TRP: tryptophan. Figure adapted from Ku et al.[118]

1.1.3.2 Other Odour-Generating Systems

In addition to the studies of odour-generating biosensors, there are a few reports[120–125] on controlled odour generation, under mild reaction conditions from nonvolatile and odourless precursors. (Fig. 1.7) These processes could be trigged by parameters such as heat,[122] light,[120,126] enzymes,[127–129] oxidizing agents,[130] and pH.[131]
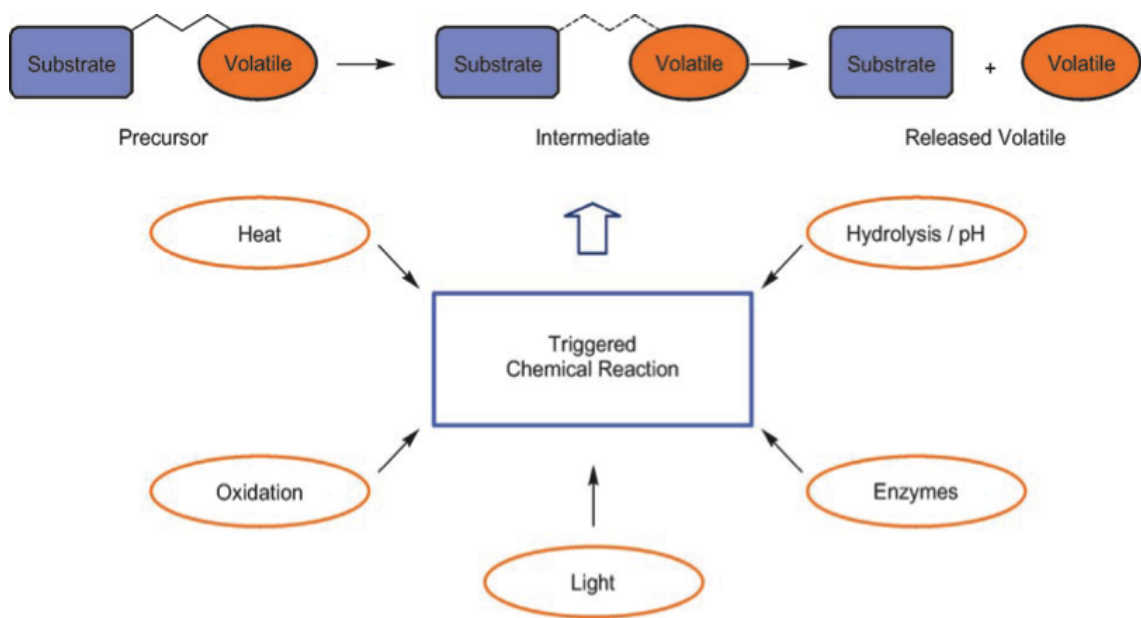
Figure 1.7 Controlled releases of odorous chemicals from nonvolatile and odourless precursors, adapted from Herrmann et al.[122]

Moreover, there are a few studies focused on smell-enhanced technologies, which have the prospective applications including multimedia, ambient displays and games development.[121,123–125] For example, in 2011, Kim et al.[124] reported a matrix odour releasing system controlled by electrically induced heating, which could be used for odour-display.

1.2   Objectives

The use of odours as a reporting signal in the development of sensors, which takes advantage of multiple sensory modalities, is an emerging field. Prior to this thesis being initiated, there was little information about odour-generating sensors suitable

for practical use. The main objective of my work was to develop practically relevant odour-generating sensors, which release human detectable volatile odours when sensors are exposed to odourless targets. The specific objectives of this research were:

1. Verification of the efficiency and viability of the bi-enzymatic odour-generating biosensor consisting of PKase and TPase. The goal was to complete the development of this biosensor, which was demonstrated by a former student, Dr. Xu, in our group.[7] To evaluate the instrument-free detection abilities of this biosensor, human based smell tests were performed.

2. The previously described odour-generating sensor was solution-based. This format has very limited applications outside of the lab. A much more versatile formatting strategy would be to immobilize the enzymatic system on a solid surface, such as paper, which allows enzyme-based biosensors to be easy to store, ship and use. An interesting proof-of-concept demonstration could have the form of a piece of paper that would report the presence of a target by emitting an easily detectable odour — this was one of the objectives of this thesis. In order to achieve this, we had to develop a simple and scalable strategy to assemble the enzymatic system, to which end inkjet printing was utilized. While other strategies are available to immobilize enzymes for a bi-enzymatic sensor (see Table 1.3), inkjet printing is the preferred technology due to the widespread availability of the technology and the implicit ability of this technology to produce sensors in a large-scale operation.

Table 1.3 Immobilization strategies for bi-enzymatic biosensors, reported since 2005.

Bienzyme	Composite Material	Reference
AChE^a & ChO^b	Fe$_3$O$_4$, TiO$_2$, chitosan, graphene and gold nanoparticle	132
α-Amylase & Glucoamylase	Alginate beads with pullulan	133
GOD^c & HRP^d	Gold nanoparticles, L-cysteine and antibody modified carbon electrode	134
AG^g & PyOx^h	Chitosan and carbon nanotubes	135
TYR^e & LACC^f	Matrix comprising iridium nanoparticles and montmorillonite	136
TYR & LACC	TiO$_2$ gel matrix	137
TYR & LACC	Sol-gel material and carbon powder modified electrode	138
APA^i & AChE	Immobilized inside BSA^k membrane and deposited on electrode	139
GOx^j & HRP	DNA nanostructure	140

AChE^a: acetylcholinesterase; ChO^b: coline oxidase; GOD^c: glucose oxidase; HRP^d: horseradish peroxidase; TYR^e: tyrosinase; LACC^f: laccase; AG^g: α-glucosidase; PyOx^h: pyranose oxidase; APA^i: alkaline phosphatase; GOx^j: glucose oxidase; BSA^k: bovine serum albumin.

3. Inkjet-printed paper sensors and solution-based sensors needed to be refrigerated to preserve activity, which is a substantial drawback towards the practical implementation of these sensors. In order to develop a more practical sensor, one objective of this thesis was to preserve the enzymes and substrates needed for the odour-generating sensor at room temperature, with minimal loss of activity as a function of time. Different immobilization methods were to be investigated. Among them, one method proved to be highly effective in achieving the desired stabilizing effects. This method consists of using pullulan, a readily water-soluble odourless polysaccharide, which was previously reported by our group to preserve the activity of enzymes and other molecules at room temperature.[141]

4. Sensors need to be cheap and utilize minimal materials. The bi-enzyme system is quite complex and no previous effort had been made to optimize the working conditions of the sensor. One goal of this thesis was to efficiently optimize the system and to investigate the influence of different variables including enzyme concentration, reaction time, temperature, etc. Fractional factorial designs, a class of experimental designs were applied as a statistical analysis strategy to evaluate the influence of different factors, while at the same time minimizing the number of experiments. This optimization work allowed us to effectively reduce the costs associated with materials needed to achieve reliable sensing.

5. Since enzymes are expensive and some people may not have an acute sense of smell or vision, a much preferable strategy would be to develop enzyme-free systems that report in a multi-sensory manner. The second last goal of this thesis was to develop a simple enzyme-free sensor, which releases odour and colour signals simultaneously when target (water) appears, as a proof-of-concept for instrument-free multi-sensory reporters employing odorous signals.

6. One advantage of the odour-generating sensor is that odorous signal can self-diffuse to the human nose. However, no previous work has been reported on the evaluation of diffused odorous signal detection by the human nose. The last goal of this thesis was to build a model to simulate the odour signal diffusion process and estimate the odour signal concentrations at different distances to the signal source. This work demonstrated the possibility of using an odour as the detectable signal

even in a large room, such as a standard 20 feet intermodal container.

1.3   Thesis Outline

Chapter 1: Presents the research background and the relevant literature of this project. The verification result of the bi-enzymatic system (PKase and TPase), which has been published in *Angewandte Chemie International Edition*, is included in this chapter. The specific objectives and outlines of this thesis are also presented here.

Chapter 2: Describes the preparation of odour-generating bioactive paper based on the bi-enzymatic system, which is named "Smell-Tell" paper. The scale-up technology using a commercial printer to prepare Smell-Tell paper is described. Smell-Tell paper's stability and its efficiency in complex background are characterized. A swab format of the Smell-Tell paper, named Smell-Tell swab, is also proposed for practical applications. This work has been published in *Analyst*, and selected as a hot paper.

Chapter 3: Describes the immobilization of the bi-enzymatic biosensor using pullulan to retain stability in ambient environment. Different strategies to stabilize enzymes, as well as their substrates, are investigated for practical usage. The stabilized bienzyme sensor, named Smell-Tell tablets, retains sensor activity at room temperature and provides a simple on-site one-step assay for ATP detection.

Chapter 4: Describes the optimization of the bi-enzymatic sensor. A method based

on fractional factorial designs and human tests is proposed to investigate the influence of different variables. The biosensor reaction conditions are optimized to reduce material costs.

Chapter 5: Describes the development of a simple dual-signal water detector involving odour and colour signals. The emission and diffusion of odour signal in a large room are simulated to estimate the generated odour signal concentration in potential application situations.

Chapter 6: Summary of the main conclusions and contributions of this project, and the suggestions for future studies.

References

[1] Hoover, K. C. *American journal of physical anthropology* **2010**, *143*, 63–74.

[2] Akutagawa, S. *Topics in Catalysis* **1997**, *4*, 271–274.

[3] Buck, L.; Axel, R. *Cell* **1991**, *65*, 175–187.

[4] Bushdid, C.; Magnasco, M. O.; Vosshall, L. B.; Keller, A. *Science* **2014**, *343*, 1370–1372.

[5] Buck, L. B. *Angewandte Chemie International Edition* **2005**, *44*, 6128–6140.

[6] Mohapatra, H.; Phillips, S. T. *Angewandte Chemie* **2012**, *124*, 11307–11310.

[7] Xu, Y.; Zhang, Z.; Ali, M. M.; Sauder, J.; Deng, X.; Giang, K.; Aguirre, S. D.; Pelton, R.; Li, Y.; Filipe, C. D. *Angewandte Chemie International Edition* **2014**, *53*, 2620–2622.

[8] Sassolas, A.; Blum, L. J.; Leca-Bouvier, B. D. *Biotechnology Advances* **2012**, *30*, 489–511.

[9] Arugula, M. A.; Simonian, A. *Measurement Science and Technology* **2014**, *25*, 032001.

[10] Wang, J. *Electroanalysis* **2001**, *13*, 983.

[11] Moyo, M.; Okonkwo, J. O.; Agyei, N. M. *Sensors* **2012**, *12*, 923–953.

[12] Zeng, X.; Shen, Z.; Mernaugh, R. *Analytical and bioanalytical chemistry* **2012**, *402*, 3027–3038.

[13] Song, K.-M.; Lee, S.; Ban, C. *Sensors* **2012**, *12*, 612–631.

[14] Su, L.; Jia, W.; Hou, C.; Lei, Y. *Biosensors and Bioelectronics* **2011**, *26*, 1788–1799.

[15] Kirsch, J.; Siltanen, C.; Zhou, Q.; Revzin, A.; Simonian, A. *Chemical Society Reviews* **2013**, *42*, 8733–8768.

[16] Vo-Dinh, T.; Cullum, B. *Fresenius' journal of analytical chemistry* **2000**, *366*, 540–551.

[17] Arora, P.; Sindhu, A.; Dilbaghi, N.; Chaudhury, A. *Biosensors and Bioelectronics* **2011**, *28*, 1–12.

[18] Thakur, M.; Ragavan, K. *Journal of food science and technology* **2013**, *50*, 625–641.

[19] Yáñez-Sedeño, P.; Agüí, L.; Villalonga, R.; Pingarrón, J. *Analytica chimica acta* **2014**, *823*, 1–19.

[20] Dwivedi, H. P.; Jaykus, L.-A. *Critical reviews in microbiology* **2011**, *37*, 40–63.

[21] Monošík, R.; Streďanskỳ, M.; Šturdík, E. *Acta Chimica Slovaca* **2012**, *5*, 109–120.

[22] Lee, J. H.; Park, J. Y.; Min, K.; Cha, H. J.; Choi, S. S.; Yoo, Y. J. *Biosensors and Bioelectronics* **2010**, *25*, 1566–1570.

[23] Zhao, W.; Ge, P.-Y.; Xu, J.-J.; Chen, H.-Y. *Environmental science & technology* **2009**, *43*, 6724–6729.

[24] Upadhyay, S.; Rao, G. R.; Sharma, M. K.; Bhattacharya, B. K.; Rao, V. K.; Vijayaraghavan, R. *Biosensors and Bioelectronics* **2009**, *25*, 832–838.

[25] Sharma, S.; Tomar, L.; Acharya, J.; Chaturvedi, A.; Suryanarayan, M.; Jain, R. *Sensors and Actuators B: Chemical* **2012**, *166*, 616–623.

[26] Nakamura, H.; Suzuki, K.; Ishikuro, H.; Kinoshita, S.; Koizumi, R.; Okuma, S.; Gotoh, M.; Karube, I. *Talanta* **2007**, *72*, 210–216.

[27] Dhall, P.; Kumar, A.; Joshi, A.; Saxsena, T. K.; Manoharan, A.; Makhijani, S. D.; Kumar, R. *Sensors and actuators B: Chemical* **2008**, *133*, 478–483.

[28] Kırgöz, Ü. A.; Odacı, D.; Timur, S.; Merkoçi, A.; Pazarlıoğlu, N.; Telefoncu, A.; Alegret, S. *Bioelectrochemistry* **2006**, *69*, 128–131.

[29] Neufeld, T.; Biran, D.; Popovtzer, R.; Erez, T.; Ron, E. Z.; Rishpon, J. *Analytical chemistry* **2006**, *78*, 4952–4956.

[30] Wang, J. *Chemical reviews* **2008**, *108*, 814–825.

[31] Katrlík, J.; Voštiar, I.; Šefčovičová, J.; Tkáč, J.; Mastihuba, V.; Valach, M.; Štefuca, V.; Gemeiner, P. *Analytical and bioanalytical chemistry* **2007**, *388*, 287–295.

[32] Perumal, V.; Hashim, U. *Journal of Applied Biomedicine* **2014**, *12*, 1–15.

[33] Shul'ga, A.; Soldatkin, A.; El'skaya, A.; Dzyadevich, S.; Patskovsky, S.; Strikha, V. *Biosensors and Bioelectronics* **1994**, *9*, 217–223.

[34] Luckham, R. E.; Brennan, J. D. *Analyst* **2010**, *135*, 2028–2035.

[35] Hossain, S. Z.; Luckham, R. E.; Smith, A. M.; Lebert, J. M.; Davies, L. M.; Pelton, R. H.; Filipe, C. D.; Brennan, J. D. *Analytical chemistry* **2009**, *81*, 5474–5483.

[36] Pelton, R. *TrAC Trends in Analytical Chemistry* **2009**, *28*, 925–942.

[37] Martinez, A. W.; Phillips, S. T.; Butte, M. J.; Whitesides, G. M. *Angewandte Chemie International Edition* **2007**, *46*, 1318–1320.

[38] Li, M.; Tian, J.; Al-Tamimi, M.; Shen, W. *Angewandte Chemie International Edition* **2012**, *51*, 5497–5501.

[39] Liu, J.; Lu, Y. *Journal of Fluorescence* **2004**, *14*, 343–354.

[40] Tram, K.; Kanda, P.; Salena, B. J.; Huan, S.; Li, Y. *Angewandte Chemie* **2014**, *126*, 13013–13016.

[41] Ding, C.; Zhong, H.; Zhang, S. *Biosensors and Bioelectronics* **2008**, *23*, 1314–1318.

[42] Velasco-Garcia, M. Optical biosensors for probing at the cellular level: A review of recent progress and future prospects. Seminars in cell & developmental biology. 2009; pp 27–33.

[43] Zhang, Z.; Zhang, S.; Zhang, X. *Analytica Chimica Acta* **2005**, *541*, 37–46.

[44] Nico, J.; Fischer, M. J. *Surface Plasmon Resonance*; Springer, 2010; pp 1–14.

[45] Mannelli, I.; Courtois, V.; Lecaruyer, P.; Roger, G.; Millot, M.-C.; Goossens, M.; Canva, M. *Sensors and Actuators B: Chemical* **2006**, *119*, 583–591.

[46] Park, T. J.; Hyun, M. S.; Lee, H. J.; Lee, S. Y.; Ko, S. *Talanta* **2009**, *79*, 295–301.

[47] Yang, X.; Kirsch, J.; Simonian, A. *Journal of microbiological methods* **2013**, *95*, 48–56.

[48] Berkenpas, E.; Millard, P.; Da Cunha, M. P. *Biosensors and Bioelectronics* **2006**, *21*, 2255–2262.

[49] Jerrett, M.; Arain, A.; Kanaroglou, P.; Beckerman, B.; Potoglou, D.; Sahsuvaroglu, T.; Morrison, J.; Giovis, C. *Journal of Exposure Science and Environmental Epidemiology* **2005**, *15*, 185–204.

[50] Vernez, D.; Bruzzi, R.; Kupferschmidt, H.; De-Batz, A.; Droz, P.; Lazor, R. *Journal of occupational and environmental hygiene* **2006**, *3*, 250–261.

[51] Ott, W. R.; Klepeis, N. E.; Switzer, P. *Journal of the Air & Waste Management Association* **2003**, *53*, 918–936.

[52] Burke, J. M.; Zufall, M. J.; Ozkaynak, H. *Journal of Exposure Analysis and Environmental Epidemiology* **2001**, *11*, 470–489.

[53] Jones, R.; Nicas, M. *Aerosol Science and Technology* **2009**, *43*, 921–938.

[54] Klepeis, N. E. *Environmental Health Perspectives* **1999**, *107*, 357.

[55] Özkaynak, H.; Ryan, P.; Allen, G.; Turner, W. *Environment International* **1982**, *8*, 461–471.

[56] Nazaroff, W. W.; Cass, G. R. *Environmental Science & Technology* **1989**, *23*, 157–166.

[57] Ferro, A. R.; Klepeis, N. E.; Ott, W. R.; Nazaroff, W. W.; Hildemann, L. M.; Switzer, P. *Atmospheric Environment* **2009**, *43*, 706–714.

[58] Ferro, A. R.; Kopperud, R. J.; Hildemann, L. M. *Journal of Exposure Science and Environmental Epidemiology* **2004**, *14*, S34–S40.

[59] McBride, S. J.; Ferro, A. R.; Ott, W. R.; Switzer, P.; Hildemann, L. M. *Journal of exposure analysis and environmental epidemiology* **1999**, *9*, 602–621.

[60] Demou, E.; Hellweg, S.; Wilson, M. P.; Hammond, S. K.; McKone, T. E. *Environmental science & technology* **2009**, *43*, 5804–5810.

[61] Conroy, L.; Wadden, R.; Scheff, P.; Franke, J.; Keil, C. *Applied Occupational and Environmental Hygiene* **1995**, *10*, 620–626.

[62] Nicas, M. *AIHAJ-American Industrial Hygiene Association* **2001**, *62*, 149–158.

[63] Scheff, P. A.; Friedman, R. L.; Franke, J. E.; Conroy, L. M.; Wadden, R. A. *Applied Occupational and Environmental Hygiene* **1992**, *7*, 127–134.

[64] Cheng, K.-C.; Acevedo-Bolton, V.; Jiang, R.-T.; Klepeis, N. E.; Ott, W. R.; Fringer, O. B.; Hildemann, L. M. *Environmental science & technology* **2011**, *45*, 4016–4022.

[65] Mombaerts, P. *Science* **1999**, *286*, 707–711.

[66] Askim, J. R.; Mahmoudi, M.; Suslick, K. S. *Chemical Society Reviews* **2013**, *42*, 8649–8682.

[67] Young, J. M.; Friedman, C.; Williams, E. M.; Ross, J. A.; Tonnes-Priddy, L.; Trask, B. J. *Human molecular genetics* **2002**, *11*, 535–546.

[68] Rodríguez, O.; Teixeira, M. A.; Rodrigues, A. E. *Flavour and Fragrance Journal* **2011**, *26*, 421–428.

[69] Tepper, J. S.; Weiss, B.; Wood, R. W. *Toxicological Sciences* **1985**, *5*, 1110–1118.

[70] Greenman, J.; El-maaytah, M.; Duffield, J.; Spencer, P.; Rosenberg, M.; Corry, D.; Saad, S.; Lenton, P.; Majerus, G.; Nachnani, S. *The Journal of the American Dental Association* **2005**, *136*, 749–757.

[71] Sarrafchi, A.; Odhammer, A. M.; Salazar, L. T. H.; Laska, M. *PloS one* **2013**, *8*, e80621.

[72] Sela, L.; Sobel, N. *Experimental brain research* **2010**, *205*, 13–29.

[73] Li, W.; Howard, J. D.; Parrish, T. B.; Gottfried, J. A. *Science* **2008**, *319*, 1842–1845.

[74] Firestein, S. *Nature* **2001**, *413*, 211–218.

[75] Zufall, F.; Leinders-Zufall, T. *Chemical senses* **2000**, *25*, 473–481.

[76] Kaupp, U. B. *Nature Reviews Neuroscience* **2010**, *11*, 188–200.

[77] Hong, S.-C.; Holbrook, E. H.; Leopold, D. A.; Hummel, T. *Acta oto-laryngologica* **2012**, *132*, S27–S31.

[78] Dymerski, T.; Chmiel, T.; Wardencki, W. *Review of Scientific Instruments* **2011**, *82*, 111101.

[79] Casalinuovo, I. A.; Di Pierro, D.; Coletta, M.; Di Francesco, P. *Sensors* **2006**, *6*, 1428–1439.

[80] Xie, Z.; Cao, K.; Zhao, Y.; Bai, L.; Gu, H.; Xu, H.; Gu, Z.-Z. *Advanced Materials* **2014**, *26*, 2413–2418.

[81] Tomchenko, A. A.; Harmer, G. P.; Marquis, B. T.; Allen, J. W. *Sensors and Actuators B: Chemical* **2003**, *93*, 126–134.

[82] Nambiar, S.; Yeow, J. T. *Biosensors and Bioelectronics* **2011**, *26*, 1825–1832.

[83] Grate, J. W. *Chemical Reviews* **2000**, *100*, 2627–2648.

[84] Esser, B.; Schnorr, J. M.; Swager, T. M. *Angewandte Chemie International Edition* **2012**, *51*, 5752–5756.

[85] Dua, V.; Surwade, S. P.; Ammu, S.; Agnihotra, S. R.; Jain, S.; Roberts, K. E.; Park, S.; Ruoff, R. S.; Manohar, S. K. *Angewandte Chemie International Edition* **2010**, *49*, 2154–2157.

[86] Wilson, A. D.; Baietto, M. *Sensors* **2009**, *9*, 5099–5148.

[87] Ho, C.-M.; Tai, Y.-C. *Annual Review of Fluid Mechanics* **1998**, *30*, 579–612.

[88] Rakow, N. A.; Suslick, K. S. *Nature* **2000**, *406*, 710–713.

[89] Lim, S. H.; Feng, L.; Kemling, J. W.; Musto, C. J.; Suslick, K. S. *Nature chemistry* **2009**, *1*, 562–567.

[90] Zhang, Y.; Askim, J. R.; Zhong, W.; Orlean, P.; Suslick, K. S. *Analyst* **2014**, *139*, 1922–1928.

[91] Mathew, A.; Sajanlal, P.; Pradeep, T. *Angewandte Chemie International Edition* **2012**, *51*, 9596–9600.

[92] Eaidkong, T.; Mungkarndee, R.; Phollookin, C.; Tumcharern, G.; Sukwattanasinitt, M.; Wacharasindhu, S. *Journal of Materials Chemistry* **2012**, *22*, 5970–5977.

[93] Bai, L.; Xie, Z.; Wang, W.; Yuan, C.; Zhao, Y.; Mu, Z.; Zhong, Q.; Gu, Z. *ACS nano* **2014**, *8*, 11094–11100.

[94] Bonifacio, L. D.; Puzzo, D. P.; Breslav, S.; Willey, B. M.; McGeer, A.; Ozin, G. A. *Advanced Materials* **2010**, *22*, 1351–1354.

[95] Melker, R.; Dennis, D. Application of biosensors for diagnosis and treatment of disease. 2005; http://www.google.com.ar/patents/US6974706, US Patent 6,974,706.

[96] Nicklin, S.; Cooper, M.; D, S. Whole cell biosensor using the release of a volatile substance as reporter. 2007; http://google.com/patents/WO2007083137A1?cl=ja, WO Patent App. PCT/GB2007/000,171.

[97] Zhang, Z.; Wang, J.; Ng, R.; Li, Y.; Wu, Z.; Leung, V.; Imbrogno, S.; Pelton, R.; Brennan, J. D.; Filipe, C. D. *Analyst* **2014**, *139*, 4775–4778.

[98] Shama, G.; Malik, D. J. *International journal of hygiene and environmental health* **2013**, *216*, 115–125.

[99] Turner, D. E.; Daugherity, E. K.; Altier, C.; Maurer, K. J. *Journal of the American Association for Laboratory Animal Science: JAALAS* **2010**, *49*, 190.

[100] Fukuba, T.; Aoki, Y.; Fukuzawa, N.; Yamamoto, T.; Kyo, M.; Fujii, T. *Lab on a Chip* **2011**, *11*, 3508–3515.

[101] Zhang, J.-Q.; Wang, Y.-S.; He, Y.; Jiang, T.; Yang, H.-M.; Tan, X.; Kang, R.-H.; Yuan, Y.-K.; Shi, L.-F. *Analytical biochemistry* **2010**, *397*, 212–217.

[102] Li, Y.; Ji, X.; Song, W.; Guo, Y. *Analytica chimica acta* **2013**, *770*, 147–152.

[103] Ye, S.; Xiao, J.; Guo, Y.; Zhang, S. *Chemistry-A European Journal* **2013**, *19*, 8111–8116.

[104] Liang, A.; Ouyang, H.; Jiang, Z. *Analyst* **2011**, *136*, 4514–4519.

[105] Butler, S. J. *Chemistry-A European Journal* **2014**, *20*, 15768–15774.

[106] Song, W.; Zhang, Q.; Xie, X.; Zhang, S. *Biosensors and Bioelectronics* **2014**, *61*, 51–56.

[107] Li, Z.; Song, Y.; Zhu, W.; Deng, L. *Analytical Methods* **2015**,

[108] Lin, C.; Chen, Y.; Cai, Z.; Zhu, Z.; Jiang, Y.; Yang, C. J.; Chen, X. *Biosensors and Bioelectronics* **2015**, *63*, 562–565.

[109] Cai, L.; Chen, Z.-Z.; Dong, X.-M.; Tang, H.-W.; Pang, D.-W. *Biosensors and Bioelectronics* **2011**, *29*, 46–52.

[110] Feng, C.; Dai, S.; Wang, L. *Biosensors and Bioelectronics* **2014**, *59*, 64–74.

[111] Kwok, F.; Churchich, J. E. *Journal of Biological Chemistry* **1980**, *255*, 882–887.

[112] Safo, M. K.; Musayev, F. N.; di Salvo, M. L.; Hunt, S.; Claude, J.-B.; Schirch, V. *Journal of bacteriology* **2006**, *188*, 4542–4552.

[113] Hoch, S. O.; Demoss, R. *Journal of bacteriology* **1973**, *114*, 341–350.

[114] Hoch, J.; Simpson, F.; Demoss, R. *Biochemistry* **1966**, *5*, 2229–2237.

[115] Yoshida, Y.; Sasaki, T.; Ito, S.; Tamura, H.; Kunimatsu, K.; Kato, H. *Microbiology* **2009**, *155*, 968–978.

[116] Isupov, M. N.; Antson, A. A.; Dodson, E. J.; Dodson, G. G.; Dementieva, I. S.; Zakomirdina, L. N.; Wilson, K. S.; Dauter, Z.; Lebedev, A. A.; Harutyunyan, E. H. *Journal of molecular biology* **1998**, *276*, 603–623.

[117] Happold, F. C.; Struyvenberg, A. *Biochemical Journal* **1954**, *58*, 379.

[118] Ku, S.-Y.; Yip, P.; Howell, P. L. *Acta Crystallographica Section D: Biological Crystallography* **2006**, *62*, 814–823.

[119] di Salvo, M. L.; Hunt, S.; Schirch, V. *Protein expression and purification* **2004**, *36*, 300–306.

[120] Wang, Z.; Johns, V. K.; Liao, Y. *Chemistry-A European Journal* **2014**, *20*, 14637–14640.

[121] Obrist, M.; Tuch, A. N.; Hornbæk, K. Opportunities for odor: experiences with smell and implications for technology. Proceedings of the 32nd annual ACM conference on Human factors in computing systems. 2014; pp 2843–2852.

[122] Herrmann, A. *Angewandte Chemie International Edition* **2007**, *46*, 5836–5863.

[123] Yamada, T.; Yokoyama, S.; Tanikawa, T.; Hirota, K.; Hirose, M. Wearable olfactory display: Using odor in outdoor environment. Virtual Reality Conference, 2006. 2006; pp 199–206.

[124] Kim, H.; Park, J.; Noh, K.; Gardner, C. J.; Kong, S. D.; Kim, J.; Jin, S. *Angewandte Chemie International Edition* **2011**, *50*, 6771–6775.

[125] Matsukura, H.; Yoneda, T.; Ishida, H. *Visualization and Computer Graphics, IEEE Transactions on* **2013**, *19*, 606–615.

[126] Charlon, M.; Trachsel, A.; Paret, N.; Frascotti, L.; Berthier, D. L.; Herrmann, A. *Polymer Chemistry* **2015**, *6*, 3224–3235.

[127] Sarry, J.-E.; Günata, Z. *Food Chemistry* **2004**, *87*, 509–521.

[128] Natsch, A.; Schmid, J.; Flachsmann, F. *Chemistry & biodiversity* **2004**, *1*, 1058–1072.

[129] Natsch, A.; Gfeller, H.; Gygax, P.; Schmid, J.; Acuna, G. *Journal of Biological Chemistry* **2003**, *278*, 5718–5727.

[130] Yang, Y.; Wahler, D.; Reymond, J.-L. *Helvetica chimica acta* **2003**, *86*, 2928–2936.

[131] Thompson, R. A.; Allenmark, S. *Journal of colloid and interface science* **1992**, *148*, 241–246.

[132] Wu, X.; Zhong, X.; Chai, Y.; Yuan, R. *Electrochimica Acta* **2014**, *147*, 735–742.

[133] Jadhav, S. B.; Singhal, R. S. *Carbohydrate polymers* **2014**, *105*, 49–56.

[134] Wang, H.; Yuan, R.; Chai, Y.; Niu, H.; Cao, Y.; Liu, H. *Biosensors and Bioelectronics* **2012**, *37*, 6–10.

[135] Odaci, D.; Telefoncu, A.; Timur, S. *Bioelectrochemistry* **2010**, *79*, 108–113.

[136] Zapp, E.; Brondani, D.; Vieira, I. C.; Dupont, J.; Scheeren, C. W. *Electroanalysis* **2011**, *23*, 764–776.

[137] Kochana, J.; Nowak, P.; Jarosz-Wilkołazka, A.; Bieroń, M. *Microchemical Journal* **2008**, *89*, 171–174.

[138] ElKaoutit, M.; Naranjo-Rodriguez, I.; Temsamani, K. R.; Domínguez, M.; de Cisneros, J. L. H.-H. *Talanta* **2008**, *75*, 1348–1355.

[139] Chouteau, C.; Dzyadevych, S.; Durrieu, C.; Chovelon, J.-M. *Biosensors and Bioelectronics* **2005**, *21*, 273–281.

[140] Fu, J.; Liu, M.; Liu, Y.; Woodbury, N. W.; Yan, H. *Journal of the American Chemical Society* **2012**, *134*, 5516–5519.

[141] Jahanshahi-Anbuhi, S.; Pennings, K.; Leung, V.; Liu, M.; Carrasquilla, C.; Kannan, B.; Li, Y.; Pelton, R.; Brennan, J. D.; Filipe, C. D. *Angewandte Chemie International Edition* **2014**, *53*, 6155–6158.

Chapter 2

An Inkjet-Printed Bioactive Paper Sensor that Reports ATP Through Odour Generation

In chapter 2, all experiments were conducted by myself with assistance from Dr. Jingyun Wang, Robin Ng (undergraduate student) and Spencer Imbrogno (undergraduate student). The paper was initially drafted by myself, and edited later to final version by Dr. Yingfu Li, Dr. Zaisheng Wu, Vincent Leung, Dr. Robert Pelton, Dr. John D. Brennan and Dr. Carlos D. M. Filipe. This chapter has been published in **_Analyst_**, 2014, **139**, pp 4775–4778, and selected as a hot paper. Reproduced by permission of The Royal Society of Chemistry. Online link: http://pubs.rsc.org/en/Content/ArticleLanding/2014/AN/c4an01113a#!divAbstract.

Analyst

COMMUNICATION

An inkjet-printed bioactive paper sensor that reports ATP through odour generation†

Zhuyuan Zhang,[a] Jingyun Wang,[a] Robin Ng,[a] Yingfu Li,[b] Zaisheng Wu,[b] Vincent Leung,[a] Spencer Imbrogno,[a] Robert Pelton,[a] John D. Brennan[c] and Carlos D. M. Filipe*[a]

We describe an inkjet printed paper-based sensor that reports ATP by the enzyme catalysed hydrolysis of *S*-methyl-L-cysteine generating an odour (methyl mercaptan) that is easily detectable by the human nose.

Our sense of smell alerts us to spoiled food, gas leaks, fire and other hazards. In spite of these everyday demonstrations of the power of smell, we know of no commercial examples of sensors employing smell reporting. Instead, most commercial biosensors and prototypes, described in the literature, employ colour, fluorescent or digital readouts to report to the user. The disadvantage of these systems is that the user needs to constantly look at the readout for real-time monitoring, while smell-based sensors do not suffer from this limitation. Besides our own work we have found one publication[1] and two patents describing sensors exploiting the sensitivity of the human nose by generating a smell. Melker's 2005 patent describes nanotubes filled with odiferous chemicals that are released with the target opens an aptamer cap on the nanotubes.[2] Nicklin's patent application describes engineered whole, living cells that generate a smell upon exposure to a target.[3] Mohapatra and Phillips[1] recently described a clever reporting system in which a reagent decomposes in the presence of hydrogen peroxide giving a fluorescent chemical plus ethanethiol, an odiferous chemical. They proposed that for point-of-care diagnostics, the initial triage could be based on smell, followed by fluorescent detection if quantification was warranted. Recently we described an alternative smell-based reporting system in which a pair of enzymes, in the presence of ATP (an important

biological cofactor, which is often used as a marker for drinking-water cleanliness and food spoilage), catalyses the hydrolysis of *S*-methyl-L-cysteine (the substrate) to produce methyl mercaptan, CH_3SH.[4] This product has a pungent odour, and can be easily detected by humans with a threshold concentration of 0.2 ppb.[5]

The initial smell-based reporter systems just described were implemented in solution under carefully controlled conditions. Practical biosensors are frequently formatted on solid supports such as paper or porous nitrocellulose. Paper is an attractive support for biosensors because it is inexpensive, available in large quantities light, flexible, can be sterilized and it can be discarded after use by incineration. In this communication we demonstrate a smell-reporting ATP sensor formatted on filter paper giving what we call "Smell-Tell" paper. A critical component of our approach is the immobilization and stabilization of the enzymes in a ~30 nm thick, porous silica layer coating the cellulose fibres.[6]

Scheme 1 summarizes our approach for the generation of methyl mercaptan from *S*-methyl-L-cysteine or indole from L-tryptophan – these were developed previously.[4] Herein methyl mercaptan generation was measured by smell testing whereas indole concentrations were measured spectrophotometrically.

Smell-Tell paper consisted of pyridoxal kinase (PKase) and apotryptophanase (Apo-TPase) immobilized in thin porous silica layers coating paper fibres within the filter paper. Paper-supported silica immobilization was first reported in 2009 [7] and more recently characterized in detail.[6] Silica sol and enzyme inks were formulated for inkjet printing and the formulations are given in ESI file.† A total of four layers of materials were printed in a specific order. In the first printing step, 2.5 μL of silica sol (4 wt% silica equivalent) was printed per square centimeter (superficial) of Whatman #1 filter paper (21 cm × 28 cm). Each sheet was printed with 24 square patterns (2.5 cm × 2.5 cm). Next 5 μL cm^{-2} of 0.5 mg mL^{-1} PKase and 2.5 μL cm^{-2} of 1.5 mg mL^{-1} Apo-TPase were printed sequentially. Finally a top layer of 2.5 μL cm^{-2} silica sol was printed. The printed filter paper was allowed to dry for 15 minutes under ambient

[a]Department of Chemical Engineering, McMaster University, 1280 Main Street West, Hamilton, ON, Canada. E-mail: filipec@mcmaster.ca; Fax: +1 905 521-1350; Tel: +1 905 525-9140 ext. 27278

[b]Department of Biochemistry and Biomedical Sciences, McMaster University, 1200 Main Street West, Hamilton, ON, Canada

[c]Biointerfaces Institute & Department of Chemistry and Chemical Biology, McMaster University, 1280 Main Street West, Hamilton, ON, Canada
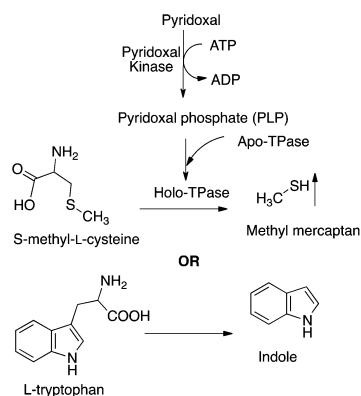
Scheme 1 The generation of methyl mercaptan or indole with a bienzyme reporter scheme developed previously.[4]

conditions between printing steps. Based on Wang's work, porous silica is present as a ~30 nm thick coating on the cellulose fibres.[6] The printed patterns were cut and stored for the following experiments.

Two sample preparation protocols were used to evaluate Smell-Tell paper – incubation in sealed tubes giving the most sensitive and reproducible results, and swab tests, open to the atmosphere simulating a more practical application. The swab fabrication and evaluation are described in a later section. In the sealed-tube protocol, 2.5 cm × 2.5 cm Smell-Tell paper samples were placed in 2 mL centrifuge tubes (TEC 2000-N, Diamed) containing 0.7 mL solution of varying concentrations of ATP (Fig. 1), 0.1 mg mL^{-1} pyridoxal, 0.6 mM MgCl$_2$ and 10 mM L-tryptophan or 1 mM S-methyl-L-cysteine and buffer (0.2 M potassium phosphate and 6.7 mM ammonium sulphate giving a pH of 7.8). The corresponding enzyme contents, from the paper, were 23 μg Apo-TPase and 16 μg PKase. The sealed tubes were incubated at room temperature for one hour in a tube rotator (H011680, VWR) at 18 RPM.

Indole contents were measured spectrophotometrically whereas methyl mercaptan was measured by human smell tests. Following the established protocols,[8] panellists were randomly

selected to indicate which vial emitted an odour signal from a set of three vials, in which one vial was a positive sample and the remaining were blanks. The positive samples contained varying concentrations of ATP while the blank samples had no ATP. The panellists (five panellists took the smell test two times) were asked to smell the entire group of sample sets in the ascending order of ATP concentration to identify the positive samples.

With a view on larger scale manufacturing, our Smell-Tell paper sensors were prepared by inkjet printing enzymes onto filter paper. Initially, we compared thermal (Model PIXMA MP280, Canon) and piezoelectric (Model DMP-2800, Fujifilm Dimatix) inkjet printers for Smell-Tell paper fabrication. Indole generation tests were performed in sealed tubes and the results were compared to control samples where the enzymes were added as solutions and not on paper. For the piezoelectric printed papers, the concentration of indole was about 50% of the control samples whereas only about 10% of the control was observed with thermal inkjet – the detailed results are given in the ESI file (Fig. S4†). Presumably the heat pulse in thermal inkjet process was sufficient to partially denature the enzymes.

The corresponding smell test results are shown in Fig. 1 where we see the same trends as the indole – the piezoelectric inkjet printed Smell-Tell papers facilitated lower ATP limits compared to thermal inkjet printing. Therefore, the piezoelectric inkjet printer was chosen for preparation of Smell-Tell paper.

The ideal bioactive paper sensor should maintain its activity for an extended storage period. To determine how long the Smell-Tell paper could be stored after preparation, we evaluated the 4 °C storage stability of two forms of Smell-Tell paper, with and without porous silica. The indole results in Fig. 2A show about a 50% decline over the first eight days after which the

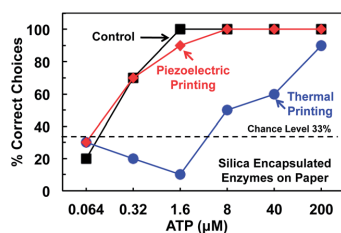**Fig. 1** Comparison of thermal and piezoelectric inkjet printing for Smell-Tell paper fabrication. The results are from a panel of five individuals who chose between three vials, one ATP-spiked and two controls, for each ATP concentration.
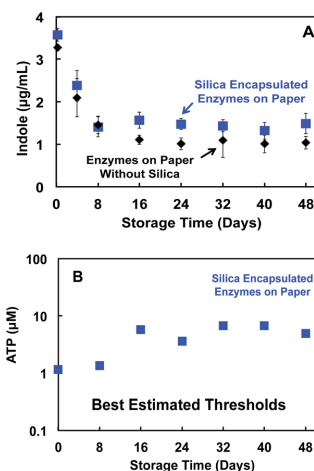
Fig. 2 The influence of 4 °C storage on Smell-Tell paper sensor activity. A – indole concentrations measured spectrophotometrically, B – smell tests results for methyl mercaptan.

Communication   **Analyst**

samples were stable. The porous silica samples were slightly more active based on the indole assay. Longer term, room temperature stability assessments are underway.

The corresponding methyl mercaptan smell test results are shown in Fig. 2B as the best estimated threshold (BET) values. In this protocol, the BET for a panellist was the geometric mean of the lowest ATP concentration detected and the highest ATP concentration not detected. The BET values in Fig. 2B were the geometric mean values of all the panellists. An example BET calculation is shown in the ESI file.†

The smell test results as functions of storage time in Fig. 2B show the same trends as the indole results. The lowest detectable ATP concentrations with fresh Smell-Tell paper in our sealed-tube protocol was 1.6 μM whereas the detection limits degraded to close to 10 μM for the aged samples.

Matrix effects are always a concern when biosensors are used in food safety inspection. To demonstrate the application of Smell-Tell paper for testing food and beverage contamination, we substituted odourless buffer with orange punch. Fig. 3 compares the performance of silica encapsulated Smell-Tell paper in Orange Punch ("Selection" brand frozen juice concentrate, Metro Inc. Canada) to buffer alone. The pH of the orange punch was raised to ~7 by addition of 1 M K_2HPO_4 solution and spike with a range of ATP concentrations. The indole results show that enzymes were not inhibited by any of the components in the orange punch. Similarly, the smell results were not significantly influenced by the odiferous components in the punch.

As discussed by Mohapatra and Phillips,[1] smell-based biosensors are likely to be used as an initial assessment in a limited resource environment. Our sealed-tube sample preparation protocol is too complex for use in the field. As an alternative, motivated by the widely used "Q-tip" cotton swab, we
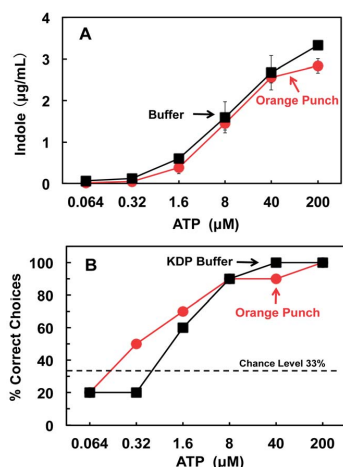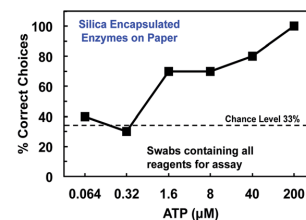
Fig. 4 Smell-Tell paper formatted as swab containing all of the components of the assay (pyridoxal, Mg^{2+}, and S-methyl-L-cysteine, PKase and Apo-TPase). The swab was contacted with a drop of ATP solution and was assessed by a human test panel after sitting on a dish for one hour, open to the atmosphere.

Table 1 A comparison of sealed-tube and open swab results for smell detection of methyl mercaptan generated by Smell-Tell paper with porous silica enzyme immobilization

	BET values (μM)	
	Sealed-tube	Swab
ATP in buffer	1.16	3.05
ATP in Orange Punch	1.36	9.40

prepared test swabs in which 2.5 cm × 2.5 cm of Smell-Tell papers were fixed onto the end of a stick (see photograph in Fig. 4). The remaining components of the assay (70 μg pyridoxal, 420 nmol $MgCl_2$ and 700 nmol S-methyl-L-cysteine) were spotted onto the swab giving a complete Smell-Tell sensor.

In our swab protocol, a 0.7 mL drop ATP in buffer was added as drop on a clean, uncovered 35 mm petri dish. The swab was placed in the dish in an orientation permitting the dry Smell-Tell paper to imbibe some of the drop. The swabs in uncovered dishes were left in a quiescent section of the laboratory with no obvious airflow. After one hour, the samples were evaluated either spectrophotometrically for indole (result shown in Fig. S9†) or by our human test panel for methyl mercaptan. In spite of the open atmosphere and the lack of mixing, the smell tests in Fig. 4 were surprisingly sensitive. The BET value corresponding to these experiments was 3.05 μM.

A more detailed series of comparisons were made between the seal-tube and swab protocols with both buffer solution and Orange Punch. The results are summarized in Table 1.

As expected, the seal-tube values were nearly an order of magnitude more sensitive. Nevertheless, with BET values less than 10 μM, the swab values were encouraging.

Conclusions

In summary, we have developed simple paper and swab-based sensors that generate odour signals that are detectable by the human nose in the presence of ATP. To the best of our knowledge, this is the first report of a bioactive odour-generating paper sensor or swab. Although more sensitive colorimetric ATP sensors exist,[9] this work is a proof of concept showing smell

Fig. 3 Comparison of Smell-Tell ATP sensor performance in Orange Punch and buffer, using both indole spectrophotometric reporting (A) and methyl mercaptan smell reporting (B).

40

Analyst

detection is possible in a practical swab format. The multiple inputs to smell generation (ATP, two enzymes and pyridoxal) provide opportunities to couple this smell-reporting scheme to recognition agents for other targets. Practical biosensors must be amenable to efficient manufacturing and must have a significant shelf life. The Smell-Tell paper sensors were prepared by inkjet printing, a scalable technology. By encapsulating the enzymes in porous silica coatings on the cellulose fibres, the enzymes were protected from proteases and were active after 48 days. Longer term stability testing is underway.

Acknowledgements

Notes and references

1 H. Mohapatra and S. T. Phillips, *Angew. Chem., Int. Ed.*, 2012, **51**, 11145–11148.
2 R. J. Melker and D. M. Dennis, US6974706 B1, 2005.
3 S. Nicklin, M. Cooper and N. D'Souza, WO Patent Application 083137 Al, 2007.
4 Y. Xu, Z. Zhang, M. M. Ali, *et al.*, *Angew. Chem., Int. Ed.*, 2014, **53**, 2620–2622.
5 J. Greenman, M. El-Maaytah, J. Duffield, *et al.*, *J. Am. Dent. Assoc., JADA*, 2005, **136**, 749.
6 J. Wang, D. Bowie, X. Zhang, *et al.*, *Chem. Mater.*, 2014, **26**, 1941–1947.
7 S. M. Z. Hossain, R. E. Luckham, A. M. Smith, *et al.*, *Anal. Chem.*, 2009, **81**, 5474–5483.
8 ASTM, ed., Standard practice for determining odor and taste thresholds by a forced-choice ascending concentration series method of limits, E-679–04, ASTM International, Conshocken, 2008.
9 M. W. Griffiths, *J. Dairy Sci.*, 1993, **76**, 3118–3125; R. A. Deininger and J. Lee, *Field Anal. Chem. Technol.*, 2001, **5**, 185–189.

Electronic Supplementary Information for

An Inkjet-Printed Bioactive Paper Sensor that Reports ATP through Odour Generation

Zhuyuan Zhang,[a] Jingyun Wang,[a] Robin Ng,[a] Yingfu Li,[b] Zaisheng Wu,[b] Vincent Leung,[a] Spencer Imbrogno,[a] Robert Pelton,[a] John D. Brennan,[c] and Carlos D. M. Filipe*[a]

*Corresponding author

[a] Department of Chemical Engineering, McMaster University, 1280 Main Street West, Hamilton, Canada

E-mail: filipec@mcmaster.ca; **Fax:** +1 905 521-1350; **Tel:** +1 905 525-9140 ext. 27278

[b] Department of Biochemistry and Biomedical Sciences, McMaster University, 1200 Main Street West, Hamilton, Canada

[c] Biointerfaces Institute & Department of Chemistry and Chemical Biology, McMaster University, 1280 Main Street West, Hamilton, ON, Canada

1

2

1. Materials

Apotryptophanase from *Escherichia coli* (Apo-TPase, EC 4.1.99.1), Kovac's reagent for indoles, Adenosine 5'-triphosphate (ATP) disodium salt, Pyridoxal, L-tryptophan, *S*-methyl-L-cysteine, Triton X-100, Pyridoxal 5'-phosphate (PLP) hydrate, Whatman #1 filter paper, Sodium silicate solution (SS, 14% NaOH, 27% SiO_2) and Dowex 50WX8-100 ion-exchange resin were purchased from Sigma-Aldrich (Oakville, ON). Anhydrous glycerol, Hispur purification column (Product number 89969), Glassine paper and 1-butanol were purchased from Fisher Scientific (Toronto, ON). Nanosep centrifuge devices were purchased from Pall Corporation.

KDP buffer contains 0.2 M potassium phosphate (pH 7.8) and 6.7 mM ammonium sulfate. Apo-TPase reaction solution for indole generation was prepared by dissolving L-tryptophan (10 mM) and PLP (0.2 mM) in KDP buffer.

Bienzyme reaction solution consisted of KDP buffer containing 0.6 mM $MgCl_2$, 10 mM L-tryptophan, 0.2 mM ATP and 0.1 mg/mL pyridoxal, while *S*-methyl-L-cysteine was used as the substrate instead to generate methyl mercaptan.

"Selection" brand Orange punch was purchased at local grocery store.

2. PKase preparation

Pyridoxal kinase (PKase, EC 2.7.1.35) was prepared according to the following method described in the literature.[1] *E. coli* cells carrying the human pdxK gene (pET22-hPLK) were grown in Luria Birtani media at 30 °C, 130 rpm for 8 h, followed by with the addition of 0.5 mM IPTG. Then, cells were cultured for an additional 7 h at 30 °C, 130 rpm before harvesting. The cell pellets were then washed and ruptured. Subsequently, the His-tagged pyridoxal kinase was purified by processing the supernatant with a Hispur purification column and enriched using

3

Nanosep centrifuge devices (30 K). The concentration of purified PKase was determined using Bradford reagent.

3. Apo-TPase preparation

Some batches of commercial Apo-TPase may have contained the cofactor, PLP, because they had not been adequately purified. Therefore, purchased TPase was dissolved and tested before use. Purification was sometimes needed to obtain pure Apo-TPase. The purification followed the former reports.[1, 2] Apo-TPase solution at a concentration of 1.5 mg/mL was prepared with KDP buffer, while Apo-TPase-glycerol (ATPG) was obtained by mixing Apo-TPase solution at a concentration of 3 mg/mL with equal volume of anhydrous glycerol. The two solutions at the same concentration (1.5 mg/mL) were used throughout unless otherwise indicated.

4. Mechanism of methyl mercaptan generation

Methyl mercaptan generation can be described by reaction 1 and reaction 2. The two closely related enzymatic reactions are shown below.
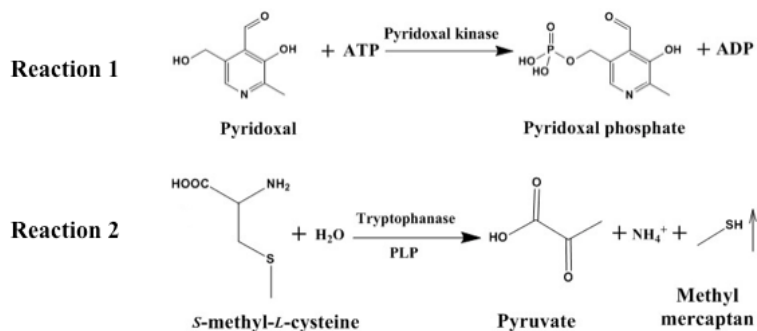
5. Indole generation mechanism and determination

Indole generation

4

Although the reaction mechanism of indole generation is similar to methyl mercaptan generation, the substrate involved in the former is L-tryptophan rather than *S*-methyl-L-cysteine. The indole generation reaction is shown below.
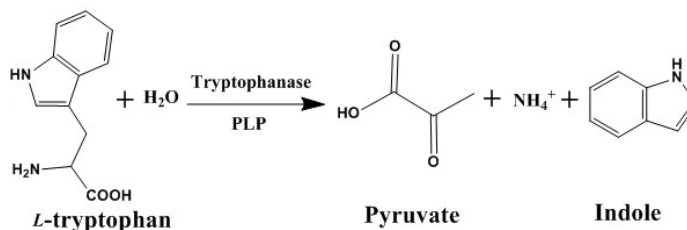
Indole determination

The sample (700 µL) was mixed with 700 µL of water saturated 1-butanol, followed by centrifugation at 1000 g for 30 sec. Then, 400 µL of the supernatant was collected and mixed with 400 µL of Kovac's reagent. After incubating for 5 min, the absorbance of the samples was measured at 570 nm using Beckman Coulter DU800 spectrophotometer. The concentration of indole could be obtained via referring the prepared standard curve.

6. Influence of glycerol for immobilized Apo-TPase activity

In the primary stage, the paper was manually prepared to investigate the feasibility of smell-generating paper. A 15.6 μL droplet of Apo-TPase or ATPG was dropped onto one paper strip with the size of 2.5 cm × 2.5 cm. The resulting strips were allowed to dry for 0.5, 5, 10, 15 or 20 minutes. After the drying, they were placed in the Apo-TPase reaction solution (700 μL) to initiate the enzymatic reaction. The reaction was allowed to proceed for 1 hour and then the amount of indole generated was determined. The experimental results shown in Fig. S1 indicate that no substantial change was detected in the immobilized ATPG activity

5

(line ATPG) after drying at room temperature for 20 min, compared with the rapid decrease in enzyme activity without glycerol (line Apo-TPase). This makes the preparation of the smell-generating paper successful within an acceptable period of time.

7. Enzyme inks preparation

When preparing enzymes inks, glycerol and Triton X-100 were used to adjust the viscosity and surface tension for the purpose of printing.[3] Thus, ATPG and PKase in glycerol (PKG) were prepared via mixing Apo-TPase or PKase with the same volume of anhydrous glycerol. Then, Triton X-100 was added. The resulting solutions were used as the enzyme inks throughout the experiments unless otherwise indicated. The final concentrations of Apo-TPase, PKase and Triton X-100 were 1.5 mg/mL, 0.5 mg/mL and 0.02 wt%, respectively. The activity of PKase in glycerol (PKG) and influence of Triton X-100 were determined for printing purposes. The results (Fig. S2) show that glycerol and Triton X-100 do not deactivate the enzymes and they can be used to prepare enzyme inks with proper properties for printing,

8. Sol-gel material ink preparation and characterization

Sodium silicate sols were prepared following the procedure described by Brennan's group.[3] Sodium silicate solution (2.9 g) was dissolved in 10 mL of ddH$_2$O, and then 5 g of Dowex cation exchange resin was added. The mixture was stirred for 2 min to reach a final pH of 4, followed by filtering. The filtrate was further filtered through a 0.45 μm membrane filter. The resulting solution was mixed with glycerol and Triton X-100 to improve printing performance by controlling viscosity and surface tension.

6

To characterize the coatings on paper substrates, optical profilometry was conducted for paper both with and without the coating of sol-gel material. The photos and peak-to-valley roughness indicate that sol-gel material could make the paper have a uniform surface as shown Fig. S3.

9. Immobilization of enzymes via printing

The thermal inkjet printer was a Model PIXMA MP280 from Canon U.S.A, Inc. and the piezoelectric inkjet printer was a Model DMP-2800 from Fujifilm Dimatix, Inc.

During the printing, enzymes and sol-gel material inks were added into individual cartridges. The coating coverage using the two printers was controlled to be the same (closely). For thermal printing: The amount of printed enzyme ink was controlled by number of layers (via printing more times) and measured by the cartridge weight change. We did that because the cartridge-washing step was avoided during the printing process. The printing amount was also checked with the calculated amount: 14.4 mL/cm^2 per layer. By doing that we could print enzyme / sol-gel material with amounts close to the desired ones. For piezoelectric printing, Enzyme and silica sol inks were added into individual cartridges. The amount of ink printed on the paper was calculated by the drop volume and amount per unit area.

Results in Fig. S4 show a significant enzyme denaturation when using a thermal inkjet printer. When compared with the control, about 90% activity is lost in thermal inkjet printing, while only 50% activity is lost in piezoelectric inkjet printing.

7

10. Activity tracking of immobilized Apo-TPase

The long term stability of the enzymes in solution and on the paper strip was tested over a period of 16 days during which the enzyme solution and enzyme-contained paper strip were stored at 4 °C. Results are shown in Fig. S5.

11. Strategy for bienzyme system immobilization

The dependence of sensing capability of the paper on the order of enzyme printing was investigated. Fig. S6 shows that the optimal method for immobilization of the bienzyme system is printing the ATPG layer above the PKG layer. This might be because the Apo-TPase is the critical parameter (Fig. S7) in this system, and this enzyme should be kept close to the solution.

12. Activity tracking of bienzyme system in solution during storage

Enzyme inks stored at 4 °C were used here. The activity was determined by concentrations of generated indole. The result is shown in Fig. S8.

13. Influence of sol-gel material for the efficiency of Smell-Tell paper

Paper strips, with immobilized bienzyme system, stored in 4 °C for 12 days were used here. The experiment was set up as shown in Table S1. The reaction solution was stored in a bottle, and the enzymatic reaction was initiated by immersing paper strips into the solution. Then, the bottle was sealed and shook gently. The reaction was allowed to last for 1 hour at room temperature before panelists opened the sealed bottle to smell. The detailed results are shown in Table S2. The results indicate 80% of the samples were identified correctly even after storing for 12 days, and sol-gel-contained papers exhibited higher accuracy (90%) compared with the papers without the sol-gel layers (70%). This result shows that sodium silicate material could be used

8

to retain the immobilized enzyme activity and improve the human olfactory detection

of ATP.

Table S1 Setup of the samples for human smell test

	Set 1			Set 2			Set 3			Set 4		
Paper Type	BE	BE	BE	BE	Plain	Plain	BSES	BSES	BSES	BSES	Plain	Plain
ATP in sample	✓	×	×	✓	✓	✓	✓	×	×	✓	✓	✓
Odor signal	Yes	No	No	Yes	No	No	Yes	No	No	Yes	No	No

BE: paper strips with bienzyme layer printed directly on the paper surface. BSES: paper strips with bienzyme layer printed between the layers of sol-gel on the paper surface. Plain: the filter paper without immobilized enzymes. The tick, '✓', means the presence of 0.2 mM ATP in the bienzyme reaction solution, while the cross, '×', indicates no ATP.

Table S2 Results of determination of smell generating test paper

	Correct Judgments of Panelist				
	1	2	3	4	5
Set 1	1	0	1	1	0
Set 2	1	1	1	0	1
Set 3	1	1	1	1	1
Set 4	1	1	0	1	1

There were three bottles for each set shown in Table S1, among which one bottle can give off the smell while the other two cannot emit the olfactory signal. Five panelists were randomly chosen in our lab to smell the gas from the bottle after the reaction. "0" indicates that the panelist did not correctly select the sample out of the three bottles in the set and "1" indicates that the panelist did correctly.

9

14. Human smell test for methyl mercaptan generated by different printers printed Smell-Tell paper

Filter paper (Whatman #1) was used as the paper substrate in this work. For immobilization of pure enzymes, 5 µL/cm^2 of 0.5 mg/mL PKG and 2.5 µL/cm^2 of 1.5 mg/mL ATPG were printed directly onto the paper substrate. For immobilization of enzymes within silica materials, the same amount of each enzyme was printed between two layers of 2.5µL/cm^2 sodium silicate material, which was prepared following our previous reports. Paper strips (2.5 cm x 2.5 cm in size) were used here. Control samples contained the same amount of enzymes, which were in solution.

Table S3. Human smell test for control sample

Panelist	Judgments [a]							
	Concentrations of ATP (µM)						BET	
	0.064	0.32	1.6	8	40	200	Value	Log$_{10}$ of Value
1	0	1	1	1	1	1	0.14	-0.84
2	1	1	1	1	1	1	0.03	-1.54
3	1	0	1	1	1	1	0.72	-0.15
4	0	0	1	1	1	1	0.72	-0.15
5	0	1	1	1	1	1	0.14	-0.84
1	0	1	1	1	1	1	0.14	-0.84
2	0	1	1	1	1	1	0.14	-0.84
3	0	0	1	1	1	1	0.72	-0.14
4	0	1	1	1	1	1	0.14	-0.84
5	0	1	1	1	1	1	0.14	-0.84
Group BET = geometric mean, µM ATP							Average of log$_{10}$ = -0.70	
							BET = 10$^{-0.70}$ = 0.20	
							Log Stand. Dev. = 0.44	

[a] "0" indicates that the panelist identified the wrong sample in the set; "1" indicates the panelist selected the correct sample.

10

Table S4. Human smell test for thermal inkjet printed enzyme samples without sol-gel material (TE)

Panelist	Judgments							
	Concentrations of ATP (μM)						BET	
	0.064	0.32	1.6	8	40	200	Value	Log$_{10}$ of Value
1	0	0	1	0	0	0	447.2	2.65
2	1	0	0	0	1	0	447.2	2.65
3	0	0	0	1	1	1	3.58	0.55
4	0	0	0	0	1	1	17.89	1.25
5	0	0	0	0	0	1	89.44	1.95
1	1	0	1	0	0	0	447.2	2.65
2	1	0	1	0	1	1	17.89	1.25
3	1	1	0	1	1	1	3.58	0.55
4	0	0	1	0	1	1	17.89	1.25
5	0	0	0	0	0	1	89.44	1.95
Group BET = geometric mean, μM ATP							Average of log$_{10}$ = 1.67	
							BET = $10^{1.67}$ = 46.98	
							Log Stand. Dev. = 0.82	

Table S5. Human smell test for thermal inkjet printed enzyme samples with sol-gel material (TSES)

Panelist	Judgments							
	Concentrations of ATP (μM)						BET	
	0.064	0.32	1.6	8	40	200	Value	Log$_{10}$ of Value
1	0	1	0	1	1	1	3.58	0.55
2	1	0	0	1	1	1	3.58	0.55
3	0	0	0	1	0	1	89.44	1.95
4	0	0	0	0	1	1	17.89	1.25
5	1	1	0	0	0	1	89.44	1.95
1	0	0	1	0	1	0	447.2	2.65
2	0	1	0	1	1	1	3.58	0.55
3	1	0	0	1	0	1	89.44	1.95
4	0	0	0	0	1	1	17.89	1.25
5	0	0	0	0	0	1	89.44	1.95
Group BET = geometric mean, μM ATP							Average of log$_{10}$ = 1.46	
							BET = $10^{1.46}$ = 28.99	
							Log Stand. Dev. = 0.74	

11

Table S6. Human smell test for piezoelectric inkjet printed enzyme samples without sol-gel material (PE)

Panelist	Judgments							
	Concentrations of ATP (μM)						BET	
	0.064	0.32	1.6	8	40	200	Value	Log_{10} of Value
1	0	1	1	1	1	1	0.14	-0.84
2	0	0	0	1	1	1	3.58	0.55
3	1	1	1	1	1	1	0.03	-1.54
4	1	0	1	1	1	1	0.72	-0.15
5	0	0	1	1	1	1	0.72	-0.15
1	0	0	1	1	1	1	0.72	-0.15
2	0	0	1	1	1	1	0.72	-0.15
3	0	1	1	1	1	1	0.14	-0.84
4	0	1	1	1	1	1	0.14	-0.84
5	0	0	1	1	1	1	0.72	-0.14
Group BET = geometric mean, μM ATP							Average of log_{10} = -0.42	
							BET = $10^{-0.42}$ = 0.38	
							Log Stand. Dev. = 0.59	

Table S7. Human smell test for piezoelectric inkjet printed enzyme samples with sol-gel material (PSES)

Panelist	Judgments							
	Concentrations of ATP (μM)						BET	
	0.064	0.32	1.6	8	40	200	Value	Log_{10} of Value
1	0	1	0	1	1	1	3.58	0.55
2	0	0	1	1	1	1	0.72	-0.14
3	0	1	1	1	1	1	0.14	-0.84
4	0	1	1	1	1	1	0.14	-0.84
5	1	1	1	1	1	1	0.03	-1.54
1	1	0	1	1	1	1	0.72	-0.15
2	1	0	1	1	1	1	0.72	-0.15
3	0	1	1	1	1	1	0.14	-0.84
4	0	1	1	1	1	1	0.14	-0.84
5	0	1	1	1	1	1	0.14	-0.84
Group BET = geometric mean, μM ATP							Average of log_{10} = -0.56	
							BET = $10^{-0.56}$ = 0.27	
							Log Stand. Dev. = 0.59	

12

15. Details of calculations of best estimation of threshold (BET)

Here, we take table S3 as an example.

In Table S3, six different concentrations of ATP were prepared with a dilution factor of 5. The ATP concentration levels were 0.064 µM, 0.032 µM, 1.6 µM, 8 µM, 40 µM, and 200 µM. For panelist 1 of the first smell test, the best-estimate threshold is $\sqrt{0.32 \times 0.064} = 0.14$ µM ATP. For panelist 2 of the first smell test, he/she could smell the lowest concentration of ATP (0.064 µM). It is assumed that he/she would have been correct at a lower concentration level, where the dilution would have been a factor of 5, which is the space for ATP concentration levels. Consequently, the best-estimate threshold for him/her is $\sqrt{0.064 \times 0.064/5} = 0.03$ µM ATP. All other values follow these same calculations and different panelists received different concentration sets. The BET (the panel threshold) is then calculated as the geometric mean of best-estimate thresholds of the individual panelists.

13

16. Best estimation of threshold (BET) of ATP concentration of stored Smell-Tell paper

BET was calculated following the previous reports.[4] For BET of each panelist, the geometric mean of the highest concentration of ATP that was identified incorrectly and next concentration recognized correctly was calculated. The BET for the entire group (5 people took the tests two times in our case) was then determined as the geometric mean of individual BETs.

Table S8. Determination of BET of ATP concentration after stored for 0 day

Panelist	Judgments							
	Concentrations of ATP (µM)						BET	
	0.064	0.32	1.6	8	40	200	Value	Log$_{10}$ of Value
1	0	0	0	1	1	1	3.58	0.55
2	0	0	1	1	1	1	0.72	-0.15
3	1	0	1	1	1	1	0.72	-0.15
4	0	1	0	1	1	1	3.58	0.55
5	0	0	1	1	1	1	0.72	-0.15
1	0	0	0	0	1	1	17.89	1.25
2	0	0	1	1	1	1	0.72	-0.15
3	1	1	1	1	1	1	0.03	-1.54
4	0	0	0	1	1	1	3.58	0.55
5	0	0	1	1	1	1	0.72	-0.15
Group BET = geometric mean, µM ATP							Average of log$_{10}$ = 0.06	
							BET = $10^{0.06}$ = 1.16	
							Log Stand. Dev. = 0.74	

14

Table S9. Determination of BET of ATP concentration after stored for 8 days

Panelist	Judgments							
	Concentrations of ATP (µM)						BET	
	0.064	0.32	1.6	8	40	200	Value	Log_{10} of Value
1	1	0	1	1	1	1	0.72	-0.15
2	0	1	1	1	1	1	0.14	-0.84
3	1	0	0	1	1	1	3.58	0.55
4	0	0	0	1	1	1	3.58	0.55
5	1	1	1	1	1	1	0.03	-1.54
1	0	0	1	0	0	0	447.21	2.65
2	0	0	1	1	1	1	0.72	-0.15
3	0	0	1	1	1	1	0.72	-0.15
4	1	1	0	1	1	1	3.58	0.55
5	1	0	1	1	1	1	0.72	-0.15
Group BET = geometric mean, µM ATP							Average of log_{10} = 0.13	
							BET = $10^{0.13}$ = 1.36	
							Log Stand. Dev. = 1.10	

Table S10. Determination of BET of ATP concentration after stored for 16 days

Panelist	Judgments							
	Concentrations of ATP (µM)						BET	
	0.064	0.32	1.6	8	40	200	Value	Log_{10} of Value
1	0	1	0	1	0	1	89.44	1.95
2	0	1	1	1	1	1	0.14	-0.84
3	1	1	0	1	1	0	447.21	2.65
4	1	1	0	1	1	1	3.58	0.55
5	0	0	1	1	1	1	0.72	-0.15
1	0	1	0	1	0	1	89.44	1.95
2	1	1	0	1	1	1	3.58	0.55
3	0	0	1	1	1	1	0.72	-0.15
4	0	0	0	1	1	1	3.58	0.55
5	0	0	0	1	1	1	3.58	0.55
Group BET = geometric mean, µM ATP							Average of log_{10} = 0.76	
							BET = $10^{0.76}$ = 5.80	
							Log Stand. Dev. = 1.10	

15

Table S11. Determination of BET of ATP concentration after stored for 24 days

Panelist	Judgments							
	Concentrations of ATP (µM)						BET	
	0.064	0.32	1.6	8	40	200	Value	Log_{10} of Value
1	1	0	0	1	1	1	3.58	0.55
2	1	0	1	1	1	1	0.72	-0.15
3	0	0	0	1	0	1	89.44	1.95
4	0	1	0	1	1	1	3.58	0.55
5	0	0	1	1	1	1	0.72	-0.15
1	0	0	1	1	1	1	0.72	-0.15
2	0	0	1	1	1	0	0.72	-0.15
3	0	1	1	1	1	0	447.21	2.65
4	1	1	0	1	1	1	3.58	0.55
5	1	0	1	1	1	1	0.72	-0.15
Group BET = geometric mean, µM ATP							Average of log_{10} = 0.55	
							BET = $10^{0.55}$ = 3.58	
							Log Stand. Dev. = 0.99	

Table S12. Determination of BET of ATP concentration after stored for 32 days

Panelist	Judgments							
	Concentrations of ATP (µM)						BET	
	0.064	0.32	1.6	8	40	200	Value	Log_{10} of Value
1	0	0	0	0	1	1	17.89	1.25
2	0	0	1	0	1	1	17.89	1.25
3	0	0	0	0	1	1	17.89	1.25
4	0	1	1	1	1	1	0.72	-0.15
5	1	1	0	1	1	1	3.58	0.55
1	0	0	0	0	1	1	17.89	1.25
2	0	0	0	0	1	0	447.21	2.65
3	0	0	0	0	1	1	17.89	1.25
4	0	1	1	1	1	1	0.72	-0.15
5	1	1	0	1	1	1	3.58	0.55
Group BET = geometric mean, µM ATP							Average of log_{10} = 0.83	
							BET = $10^{0.83}$ = 6.81	
							Log Stand. Dev. = 1.05	

16

Table S13. Determination of BET of ATP concentration after stored for 40 days

Panelist	Judgments							
	Concentrations of ATP (µM)						BET	
	0.064	0.32	1.6	8	40	200	Value	Log_{10} of Value
1	0	0	0	1	1	1	3.58	0.55
2	0	0	1	0	1	1	17.89	1.25
3	0	0	1	0	1	0	447.21	2.65
4	0	1	1	0	1	1	17.89	1.25
5	0	0	1	1	1	1	0.72	-0.15
1	1	0	0	1	1	1	3.58	0.55
2	0	1	0	1	1	1	3.58	0.55
3	0	0	0	1	0	1	89.44	1.95
4	0	0	0	1	1	1	3.58	0.55
5	0	1	1	1	1	1	0.14	-0.84
Group BET = geometric mean, µM ATP							Average of log_{10} = 0.83	
							BET = $10^{0.83}$ = 6.81	
							Log Stand. Dev. = 1.00	

Table S14. Determination of BET of ATP concentration after stored for 48 days

Panelist	Judgments							
	Concentrations of ATP (µM)						BET	
	0.064	0.32	1.6	8	40	200	Value	Log_{10} of Value
1	1	0	0	0	0	1	17.88	1.25
2	1	0	0	1	1	1	3.58	0.55
3	0	1	1	1	1	1	0.14	-0.84
4	0	1	0	1	1	1	3.58	0.55
5	1	0	0	1	1	1	3.58	0.55
1	1	0	1	0	0	1	17.89	1.25
2	0	1	0	1	1	1	3.58	0.55
3	1	0	0	1	1	1	3.58	0.55
4	0	0	0	1	1	1	3.58	0.55
5	0	1	1	0	0	1	89.44	1.95
Group BET = geometric mean, µM ATP							Average of log_{10} = 0.69	
							BET = $10^{0.69}$ = 4.93	
							Log Stand. Dev. = 0.72	

17

17. BET of ATP concentration for bienzyme solution and Smell-Tell paper using KDP buffer or orange punch

Table S15. BET of ATP concentration using bienzyme solution with KDP buffer

Panelist	Judgments							
	Concentrations of ATP (µM)						BET	
	0.064	0.32	1.6	8	40	200	Value	Log_{10} of Value
1	0	0	1	1	1	1	0.72	-0.15
2	1	1	1	1	1	1	0.03	-1.54
3	0	1	1	1	1	1	0.14	-0.84
4	0	0	1	1	1	1	0.72	-0.15
5	0	0	1	1	1	1	0.72	-0.15
1	0	0	1	1	1	1	0.03	-1.54
2	0	0	1	1	1	1	0.72	-0.15
3	1	1	1	1	1	1	0.03	-1.54
4	1	1	1	1	1	1	0.03	-1.54
5	0	0	1	1	1	1	0.72	-0.15
Group BET = geometric mean, µM ATP							Average of log_{10} = -0.77	
							BET = $10^{-0.77}$ = 0.17	
							Log Stand. Dev. = 0.70	

Table S16. BET of ATP concentration using bienzyme solution with orange punch

Panelist	Judgments							
	Concentrations of ATP (µM)						BET	
	0.064	0.32	1.6	8	40	200	Value	Log_{10} of Value
1	0	0	0	1	1	1	3.58	0.55
2	1	1	1	1	1	1	0.03	-1.54
3	0	1	1	1	1	1	0.14	-0.84
4	0	1	0	1	1	1	3.58	0.55
5	0	1	1	1	1	1	0.14	-0.84
1	1	0	0	1	1	1	3.58	0.55
2	0	1	1	1	1	1	0.14	-0.84
3	0	1	1	1	1	1	0.14	-0.84
4	1	1	1	1	1	1	0.03	-1.54
5	0	0	1	1	1	1	0.72	-0.15
Group BET = geometric mean, µM ATP							Average of log_{10} = -0.49	
							BET = $10^{-0.49}$ = 0.32	
							Log Stand. Dev. = 0.82	

18

Table S17. BET of ATP concentration using Smell-Tell paper with KDP buffer

Panelist	Judgments							
	Concentrations of ATP (µM)						BET	
	0.064	0.32	1.6	8	40	200	Value	Log_{10} of Value
1	0	0	0	1	1	1	3.58	0.55
2	0	0	1	1	1	1	0.72	-0.15
3	1	0	1	1	1	1	0.72	-0.15
4	0	1	0	1	1	1	3.58	0.55
5	0	0	1	1	1	1	0.72	-0.15
1	0	0	0	0	1	1	17.89	1.25
2	0	0	1	1	1	1	0.72	-0.15
3	1	1	1	1	1	1	0.03	-1.54
4	0	0	0	1	1	1	3.58	0.55
5	0	0	1	1	1	1	0.72	-0.15
Group BET = geometric mean, µM ATP							Average of log_{10} = 0.06	
							BET = $10^{0.06}$ = 1.16	
							Log Stand. Dev. = 0.74	

Table S18. BET of ATP concentration using Smell-Tell paper with orange punch

Panelist	Judgments							
	Concentrations of ATP (µM)						BET	
	0.064	0.32	1.6	8	40	200	Value	Log_{10} of Value
1	0	0	0	1	1	1	3.58	0.55
2	0	1	1	1	1	1	0.14	-0.84
3	1	0	1	1	1	1	0.72	-0.15
4	0	1	1	1	0	1	89.44	1.95
5	0	0	1	1	1	1	0.72	-0.15
1	0	1	0	0	1	1	17.89	1.25
2	0	0	1	1	1	1	0.72	-0.15
3	1	1	1	1	1	1	0.03	-1.54
4	0	1	0	1	1	1	3.58	0.55
5	0	0	1	1	1	1	0.72	-0.15
Group BET = geometric mean, µM ATP							Average of log_{10} = 0.13	
							BET = $10^{0.13}$ = 1.36	
							Log Stand. Dev. = 1.00	

19

18. Indole determination for odour generating swab-like sensor (Smell-Tell swab) tested in open space

The substrates (70 µg pyridoxal, 420 nmol $MgCl_2$ and 7 µmol L-tryptophan) for the enzymatic reaction were immobilized onto the Smell-Tell swab to attain a one-step detection system. The resulting "all in one" Smell-Tell swab was directly placed onto a wet surface to detect ATP on the surface. After the reaction, reaction solution and the swab were transferred into tubes to extract indole for indole determination. The indole determination results were shown in Fig. S9.

19. BET of ATP concentration for Smell-Tell swab tested in open space

Table S19. BET of ATP concentration using Smell-Tell swab with KDP buffer tested in open space

Panelist	Judgments							
	Concentrations of ATP (µM)						BET	
	0.064	0.32	1.6	8	40	200	Value	Log_{10} of Value
1	1	1	0	0	1	1	17.88	1.25
2	1	1	1	1	1	1	0.03	-1.54
3	0	0	1	1	1	1	0.72	-0.15
4	1	1	1	1	0	1	89.44	1.95
5	0	0	1	1	1	1	0.72	-0.15
1	0	0	1	0	1	1	17.89	1.25
2	0	0	1	1	1	1	0.72	-0.15
3	0	0	0	1	1	1	3.58	0.55
4	1	0	0	0	0	1	89.44	1.95
5	0	0	1	1	1	1	0.72	-0.15
Group BET = geometric mean, µM ATP							Average of log_{10} = 0.48	
							BET = $10^{0.48}$ = 3.05	
							Log Stand. Dev. = 1.11	

Table S20. BET of ATP concentration using Smell-Tell swab with orange punch tested in open space

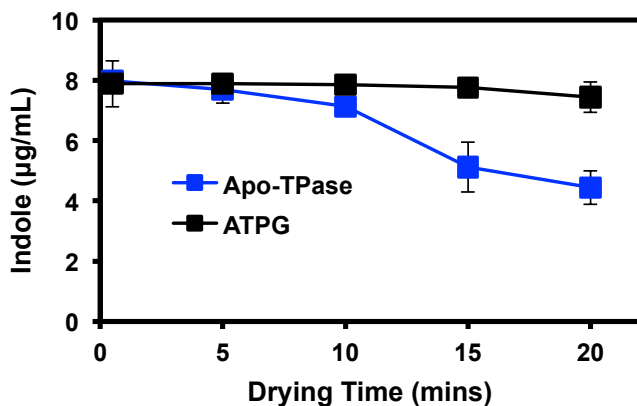| Panelist	Judgments							
	Concentrations of ATP (µM)						BET	
	0.064	0.32	1.6	8	40	200	Value	Log_{10} of Value
1	0	0	0	1	1	1	3.58	0.55
2	0	1	1	1	1	1	0.14	-0.84
3	0	0	1	1	0	1	89.44	1.95
4	0	0	0	1	1	0	447.21	2.65
5	0	1	0	1	1	1	3.58	0.55
1	1	0	0	0	1	1	17.89	1.25
2	0	1	1	1	1	1	0.14	-0.84
3	0	1	1	0	0	1	89.44	1.95
4	0	0	1	1	1	0	447.21	2.65
5	1	0	1	1	1	1	0.72	-0.15
Group BET = geometric mean, µM ATP							Average of log_{10} = 0.97	
							BET = $10^{0.97}$ = 9.40	
							Log Stand. Dev. = 1.33	

21

20. Figures

Fig S1. Influence of glycerol on the activity of immobilized Apo-TPase. Two sets of smell-generating papers were prepared via pipetting 20 µL of Apo-TPase or ATPG onto the paper strips (2.5 cm × 2.5 cm). After air-drying at room temperature for a certain period of time, the TPase-immobilized paper strip was placed into 700 µL of Apo-TPase reaction solution. All the reaction tubes were kept in a tube rotator with rotation speed of 18 rpm at room temperature for 1 h before indole determination.

Fig. S2. Influence of glycerol and Triton X-100 on the bioactivity of enzymes. PT: mixture of pure PKase and pure Apo-TPase; PTGX: mixture of pure PKase and Triton X-100-contained ATPG; PGXT: mixture of Triton X-100-contained PKG and pure Apo-TPase; B-4: mixture of Triton X-100-contained PKG and Triton X-100-contained ATPG. The final concentration of Apo-TPase, PKase and Triton X-100 in bienzyme reaction solution (700 µL) were 33 µg/mL, 22 µg/mL and 0.02 wt%. All of the sample tubes were kept in a tube rotator with rotating speed of 18 rpm under room temperature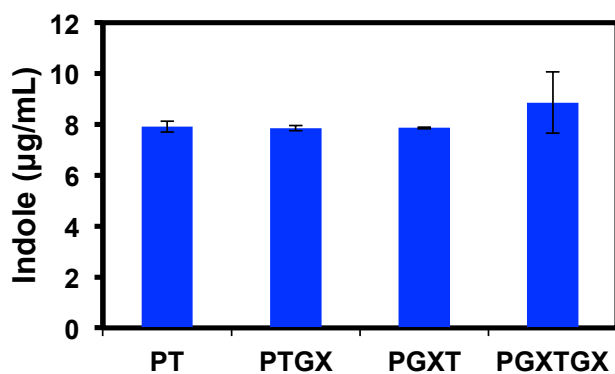 for one hour before indole determination. As shown in the measured data, no significant change in the bioactivity of enzymes was detected in the presence of glycerol and Triton X-100.

22
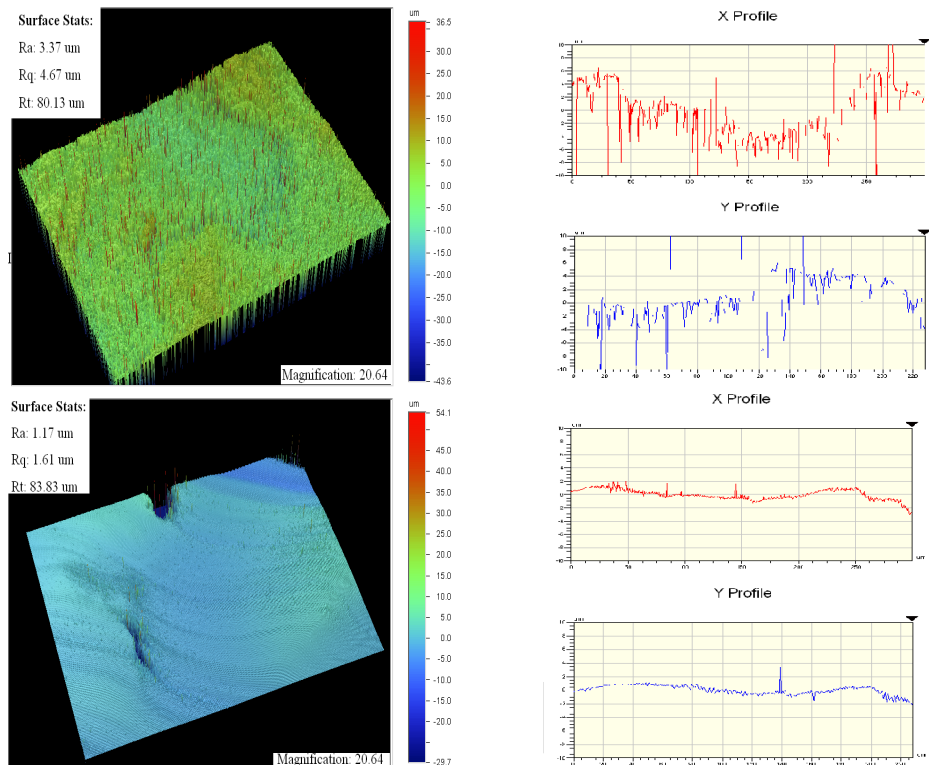
Figure S3. Profilometry images of paper that is uncoated (A) or coated (B) with sol-gel material.
Optical profilometry images were obtained with a WYKO Model NT 1100 Optical Profiling System on the basis of the VSI measurement mode and a magnification of 20 ×.
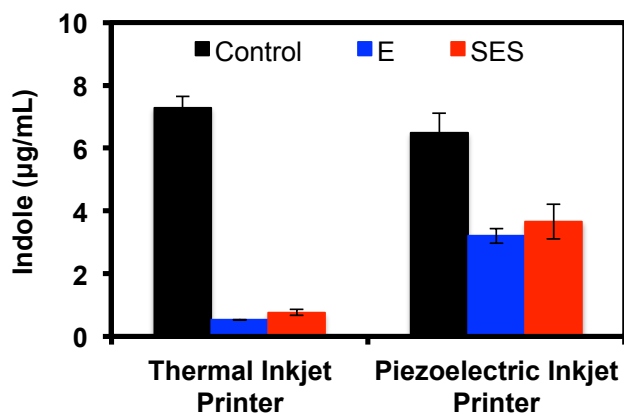
Figure S4. The activity of printed enzymes using different printers based on indole determination.
E: pure enzyme immobilization; SES: enzymes immobilized in a sandwich format using sodium silicate material.

23
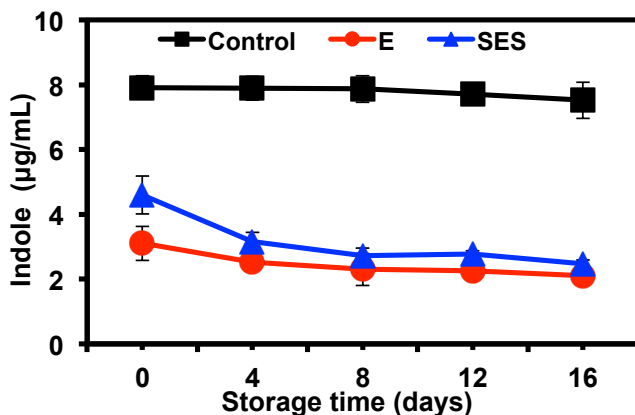
Figure S5. Storage Activities of immobilized Apo-TPase. E: 2.5 µL/cm^2 of ATPG was printed directly onto the filter paper. SES: ATPG was printed between the two layers of 2.5 µL/cm^2 of sol-gel material on the filter paper. After being printed, the enzyme paper was stored at 4°C. Every 4 days, 2.5 cm × 2.5 cm paper strips were cut and placed into Apo-TPase reaction solution. Control: ATPG stored in solution at 4°C. Every 4 days, 15.6 µL control samples were taken out and placed into Apo-TPase reaction solution. The enzyme bioactivity of papers was evaluated using the same method as described in Figure S1.
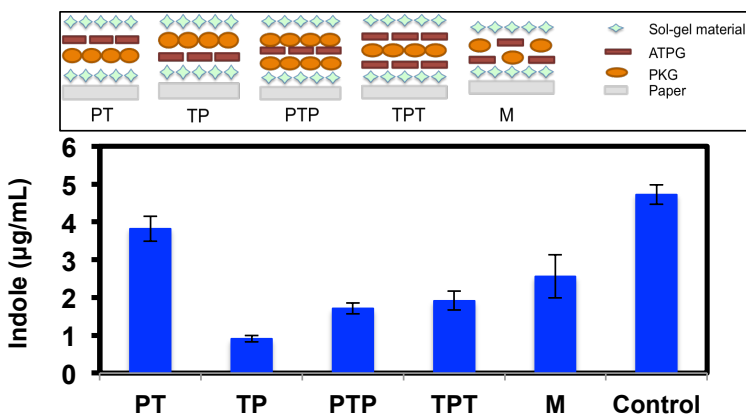
Figure S6. Immobilized bienzyme activities on paper with different enzyme distributing strategies. Different orders to print bienzyme are shown in the upper box (PT: printing PKG layer first and then ATPG layer; TP: printing ATPG layer first and then PKG layer; PTP: printing ATPG layer between two layers of PKG; TPT: printing PKG layer between two layers of ATPG; M: printing the mixture of ATPG and PKG.) Besides the similar sol-gel material layers on the bottom and top, on one paper, the same amount of each enzyme is involved in different layers if the enzyme is printed two times. Moreover, all of papers have the same total amount of enzymes (2.5 µL/cm^2 of ATPG and 5 µL/cm^2 of PKG). Control: 15.6 µL of ATPG and 31.2 µL of PKG solutions mixed with the bienzyme reaction solution.

24
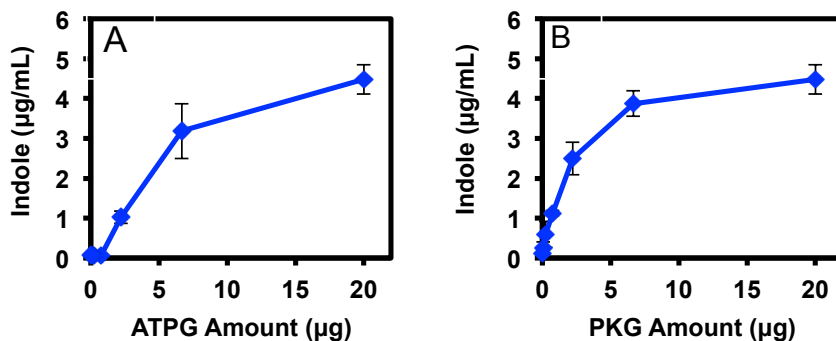
Figure S7. The dependence of bienzyme system efficiency on the amounts of ATPG and PKG. In bienzyme reaction solution (700 μL), when investigating the influence of ATPG concentration, 20 μg of PKase was used, while 20 μg of ATPG was involved to evaluate PKG concentration influence. Indole generated was determined after the enzymatic reaction was allowed to proceed for 1 hour. As shown in section A, the low concentration of ATPG cannot induce the generation of enough indole, and no detectable signal could be collected. Accordingly, the apparent catalytic ability of paper is deemed to be strongly dependent on the Apo-TPase activity.
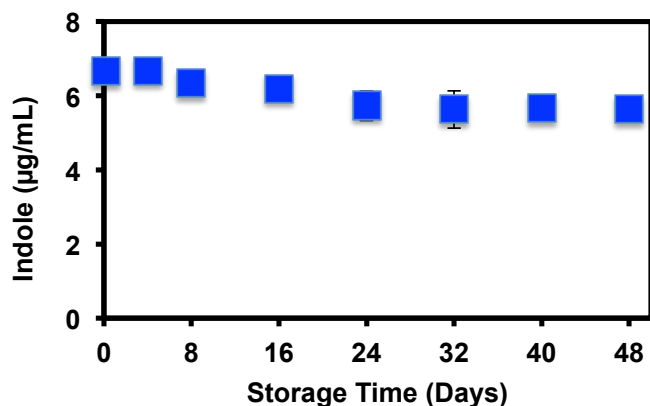
Figure S8. Activity of bienzyme system in solution during storage. Enzyme solutions were stored at 4°C. 15.6 μL of ATPG and 31.2 μL of PKG solutions were used.

25
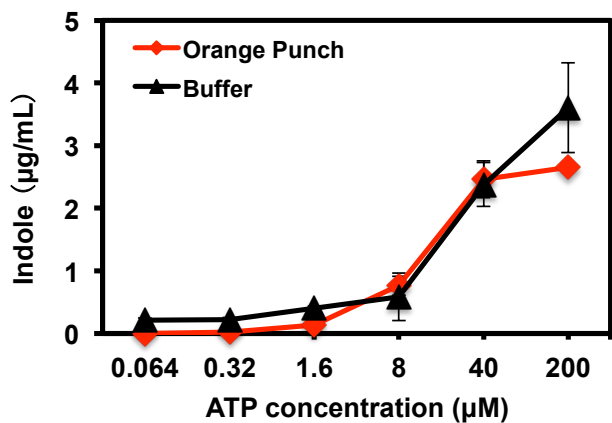
Figure S9. Indole generated by swab with performance in Orange Punch and buffer. The swab contained all of the components of the assay (pyridoxal, Mg^{2+}, and L-tryptophan PKase and Apo-TPase).

Reference

1. M. L. di Salvo, S. Hunt and V. Schirch, *Protein Expression Purif.*, 2004, **36**, 300-306.

2. C. M. Metzler, R. Viswanath and D. E. Metzler, *J. Biol. Chem.*, 1991, **266**, 9374-9381; T. Erez, G. Y. Gdalevsky, C. Hariharan, et al., *Biochim. Biophys. Acta*, 2002, **1594**, 335-340.

3. S. M. Z. Hossain, R. E. Luckham, A. M. Smith, et al., *Anal. Chem.*, 2009, **81**, 5474-5483.

4. ASTM, ed., *Standard practice for determining odor and taste thresholds by a forced-choice ascending concentration series method of limits, E-679-04*, ASTM International, Conshocken, 2008; Y. Xu, Z. Zhang, M. M. Ali, et al., *Angew. Chem. Int. Ed.*, 2014, **53**, 2620-2622.

26

Chapter 3

Bi-Enzymatic Odour-Generating Biosensor with Enhanced Stability: Pullulan Based Smell-Tell Tablets for On-Site ATP detection

In chapter 3, all experiments were conducted by myself and Paul Wigmore (undergraduate student). Xudong Deng, Dr. Sana Jahanshahi-Anbuhi, Vincent Leung, Dr. Robert Pelton and Dr. Carlos D. M. Filipe contributed many helpful suggestions on my experiment design and paper writing.

3.1   Abstract

A pyridoxal kinase and tryptophanase based odour-generating biosensor was reported previously by our group to detect ATP, an important biomarker. The biosensor could be stored in the fridge for weeks, but lost its activity fast in ambient environment. For shipping and storage purposes, in this study, a promising immobilization strategy was investigated to retain the stability of the biosensor at room temperature. Enzymes and three substrates: pyridoxal, L-tryptophan and S-methyl-L-cysteine were all entrapped into pullulan, a natural polysaccharide. Employing this strategy, the two enzymes retained all of their initial activity after being stored at 23°C and 50% relative humidity for one week, at least 100 times better than the free bi-enzyme in buffer stored under the same conditions. The whole biosensor was created in the solid form by entrapping every component within pullulan tablets after the three substrates were proven to be relatively stable using the same approach. The entrapped odour-generating biosensor, named Smell-Tell tablets, could detect 57.1 µM ATP without any instrument, even after being stored at room temperature for two months. This work is the first report on a robust odour-generating biosensor that can be stored in ambient environment for months. The proposed Smell-Tell tablets are easy to ship and handle, providing an uncomplicated platform for easy-to-run single step ATP assay suitable for resource-limited areas.

3.2   Introduction

Humans have an extraordinarily robust olfactory system, with abilities to discriminate at least 1.72 trillion types of stimuli,[1] to detect certain odourants at as low as part per

trillion (ppt) levels,[2–4] and to improve its detection and discrimination with learning and practice.[4–6] Moreover, odour signals are able to reach the human nose by self-diffusion once activated. The distinguished features of the human olfactory system and odour signals make it is reasonable and conceivable to develop odour-generating sensors by turning odourless analytes into volatile odourous signals to exploit the robust human olfactory system.

During the last decade, few researchers were trying to develop odour-generating sensors, which mostly were odour-generating biosensors.[7–12] The previous literature reports revealed the possibility of using aptamers,[7] living cells,[9] designed reagents,[8] and designed enzymatic systems[11,12] to develop odour-generating biosensors. However, there is lack of studies focusing on the development of odour-generating biosensor that can be stored in ambient environment, which is ideal for practical usage. Certainly, enhanced shelf life and stability against denaturation at room temperature and more convenient handling of the biomaterials are necessary for the on-site applications of these biosensors. In this study, we stabilized a bi-enzyme odour-generating biosensor in ambient environment, paving a way to stabilize odour-generating biosensors for room temperature storage and shipping purposes.

Previously, our group have developed a bi-enzyme odour-generating biosensor for ATP detection,[11] which is an important biomarker and useful for hygiene monitoring in industry, such as determining water cleanliness, measuring surface sanitation, etc.[13,14] As summarized in Scheme 1, two enzymes: pyridoxal kinase (PKase) & tryptophanase (TPase), and three small molecule substrates: pyridoxal, S-methyl-L-cysteine (SMLC), and L-tryptophan were used for the fabrication of this biosensor. In the presence of ATP, PKase catalyzes the phosphorylation of pyridoxal, and

generates pyridoxal 5'-phosphate (PLP), converting Apo-TPase (inactive status) to Holo-TPase (active status). Holo-TPase then catalyzes the hydrolysis of SMLC (or L-tryptophan) and produces methyl mercaptan (or indole). Methyl mercaptan is a pungent odourous chemical and can be easily detected by human noses, with an extraordinarily low human olfactory threshold concentration, 0.2 parts per billion (ppb).[11,15] Indole concentration measurement by spectrometry can be used to quantitatively determine the biosensor activity.[11] Our previous studies realized moving this biosensor from solution onto a solid substrate, filter paper, and retained the activities of the immobilized enzymes for at least one month when stored in the fridge at 4°C.[12]
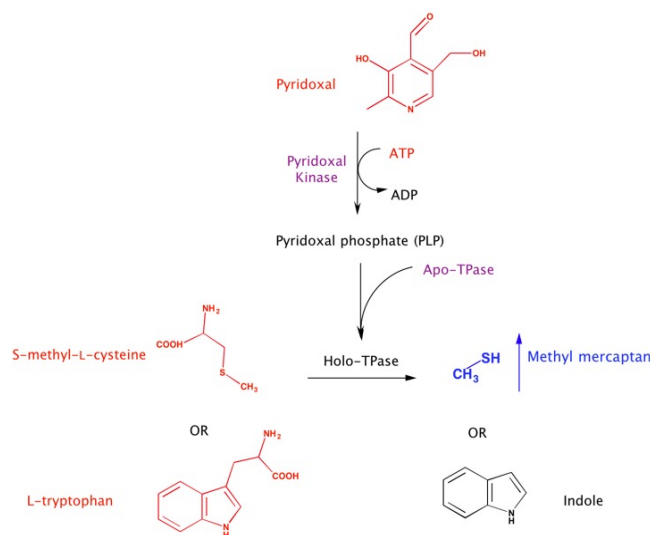
Scheme 1. The generation of methyl mercaptan or indole with a bi-enzyme biosensor scheme developed previously.[11,12] The target (ATP) and three substrates are coloured in red, two enzymes are coloured in purple, and the odour signal is coloured in blue.

To retain the enzyme activities in ambient environment, we investigated the effect of glycerol, pullulan, filter paper, and glassine paper to preserve this bi-enzyme biosensor, which are all odourless. Glycerol, one of the simplest and smallest molecules in

71

the polyol class which is routinely used in food industry[16] and biopharmaceutical formulation,[17,18] was involved to stabilize enzymes in previous studies.[19,20] Pullulan, a natural glucosic polysaccharide, has long been utilized for various applications, ranging from food preservation[21–24] to drug delivery.[25–27] In 2014, Jahanshahi-Anbuhi et al. from our group reported creation of pullulan-tablet based assay system to provide a water-soluble bioassay platform and proved this system could easily entrap and highly stabilize enzymes in ambient environment.[28] Jadhav and Singhal have also reported use of pullulan and alginate beads for entrapment of α-amylase and glucoamylase system.[29] Paper based materials mainly consisted of protein friendly cellulose and worked well as supporting materials for enzyme immobilization.[30] Filter paper and glassine paper were tested in this work, which performed well as carriers for the immobilization of this bi-enzyme system in the previously reported study.[12] In this work, (1) adding protectants (glycerol or pullulan) into enzyme solution, (2) immobilizing enzymes directly on papers, (3) immobilizing enzymes with pullulan or glycerol on papers, and (4) entrapping enzymes in pullulan tablets were exclusively studied. Indole determination by spectrometry and methyl mercaptan determination by human smell tests were applied to measure the retained activity. Entrapping enzymes in pullulan tablets showed the best stabilization effect. The three substrates (pyridoxal, L-tryptophan, and SMLC) were then determined to be relatively stable at room temperature using the same method. The final stabilized biosensor, with all components immobilized in pullulan tablets, was named "Smell-Tell" tablets. The Smell-Tell tablets showed high sensitivity and stability when stored at room temperature, which provides promising simple one-step ATP assay (Scheme 2) specifically appropriate for resource-limited regions.
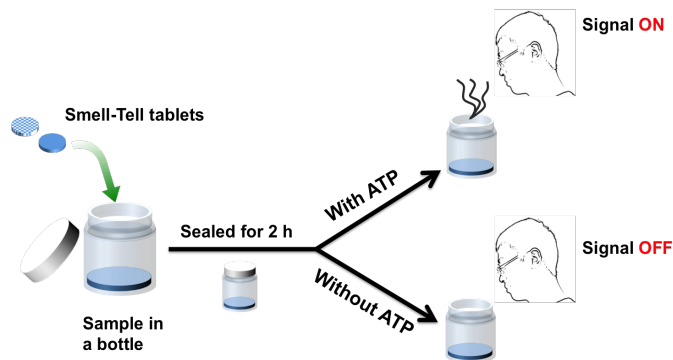
Scheme 2. Simple one-step ATP Yes/No assay using Smell-Tell tablets. Smell-Tell tablets are created by entrapping enzymes and substrates in pullulan tablets. In this assay, the test sample with ATP releases human detectable odour signal, while the sample without ATP does not.

3.3 Materials and Methods

3.3.1 Materials

Crude Apo-TPase from *Escherichia coli* (EC 4.1.99.1), Kovac's reagent for indoles, ATP disodium salt, pyridoxal, L-tryptophan, SMLC, PLP hydrate, and Whatman #1 filter paper, were purchased from Sigma-Aldrich (Oakville, ON). Anhydrous glycerol, hispur purification column (Cat# 89969), glassine paper (Fisherbrand weighting paper, Cat# 09-898-12B) and 1-butanol, were purchased from Fisher Scientific (Toronto, ON). Pullulan (desalinized, Cat# 21115) was purchased form Polysciences, Inc. Tube rotator with rotating speed of 18 rpm (Product# H011680) was purchased from VWR, Canada. Glass bottles with a volume of 40 mL were purchased from a local chemical store. Xerox Phaser Premium Transparency Film (Model#: 1P016194800, polyethylene terephthalate/PET sheet) was purchased on Amazon.com.

PKase (EC 2.7.1.35) and purified Apo-TPase were prepared as reported in previous studies.[31–33] In this work, KDP buffer contained 6.7 mM ammonium sulfate and 0.2 M potassium phosphate. PKase in pullulan solution contained 0.64 mg/mL PKase and 10% w/w pullulan (pullulan concentration higher than 10% leads the tablets difficult to dissolve, while lower concentration is hard for tablets cast). Apo-TPase in pullulan solution contained 1.4 mg/mL Apo-TPase and 10% w/w pullulan. PKase in glycerol solution contained 0.34 mg/mL PKase and 50% v/v glycerol. Apo-TPase in glycerol solution contained 1.4 mg/mL Apo-TPase and 50% v/v glycerol.

Bi-enzymatic reaction system, with a total volume of 1000 µL in KDP buffer, contained 15 µg PKase, 23 µg Apo-TPase, 0.6 mM $MgCl_2$, 10 mM L-tryptophan, 0.2 mM ATP and 0.1 mg/mL pyridoxal, while SMLC was used as the substrate instead of L-tryptophan to generate methyl mercaptan.

3.3.2   Method

Enzyme stability determination

Free enzymes in KDP buffer stored at room temperature (23°C) and in the fridge (4°C) were studied as the benchmarks. 8 µL free Apo-TPase (2.8 mg/mL) in buffer and 23 µL free PKase (0.68 mg/mL) in buffer were used for the bi-enzymatic reaction. The reaction was allowed to proceed for one hour in the rotator (18 rpm) at room temperature before the indole determination. The reaction conditions were the same for the following experiments except otherwise indicated.

To prepare enzymes with pullulan on filter paper or glassine paper, 23 µL PKase in pullulan solution and 16 µL Apo-TPase in pullulan solution (enzyme samples with pullulan); or, 47 µL PKase in glycerol solution and 16 µL Apo-TPase in glycerol

solution (enzymes samples with glycerol), were pipetted onto filter paper and glassine paper strips (with size of 2 cm × 2 cm). The prepared samples were stored in ambient environment: 23°C, 50% relative humidity (RH). For testing, paper strips with enzymes were submerged into bi-enzymatic reaction solution for enzyme reaction and indole determination.

To prepare enzymes in pullulan tablets, 23 µL of PKase in pullulan solution and 16 µL of Apo-TPase in pullulan solution were individually pipetted onto a PET sheet and dried overnight in ambient environment. The prepared enzyme-pullulan tablets were stored at 23°C, 50% RH. For testing, one PKase tablet and one Apo-TPase tablet were used for the bi-enzymatic reaction before the indole determination.

Substrate stability determination

Pyridoxal (7 mg/mL, 10 µL), L-tryptophan (35mM, 50 µL), and SMLC (70 mM, 10 µL) in their pullulan solutions (10% w/w pullulan) were prepared and then pipetted onto a PET sheet individually to prepare substrate-pullulan tablets. After drying overnight, these tablets were stored at 23°C, 50% RH. To determine the stability of substrates in pullulan tablets, the substrate in pullulan tablet was used to run the bi-enzymatic reaction. Equivalent amount of free substrate in solution, stored under the same conditions, was used for the control experiments. The prepared free substrates in solutions and substrates in pullulan tablets were blocked from light during storage, since the substrates are substantially light sensitive when stored at room temperature as reported in the previous publications,[34-37] and proven by results in Fig.S1 of the ESI†.

Indole determination

700 µL of butanol was first mixed with each sample, and then spun down in a centrifuge. Next, 400 µL of the supernatant was extracted and mixed with 400 µL of Kovac's reagent. After incubating for 5 min, the absorbance of the samples was measured at 570 nm using a spectrophotometer (Beckman Coulter DU800). The concentration of indole could be obtained by referring to the prepared standard curve.

Best-estimated threshold (BET) determination

The ATP detection limit based on human noses was indicated by the BET of ATP. The BET value was determined by a triangular forced-choice smell test, which was carried out following ASTM E679-04[38] with slightly modification. ATP with six different concentrations from 0.026 µM to 200 µM (increasing by a factor of 6) was applied to prepare different experiment sets. The reaction was run in 40 mL glass bottles, initiated by adding ATP and then sealed. The reaction was allowed to proceed for one or two hours at room temperature before human panelists opened the sealed bottle to smell. For each experiment set, there were three samples given to a participant, of which only one was positive (with ATP). Five participants, taking each smell test two times, were required to identify the ATP-positive sample from the two other samples that were negative for ATP. The participants were asked to smell the entire group of sample sets in the ascending order of ATP concentration to identify the positive samples, and were forced to indicate a response even if no olfactory difference was detected. BETs for ATP detection were determined and calculated following the previous reports[11,12,38]: The BET of each panelist is the geometric mean of the highest concentration of ATP that was identified incorrectly and next concentration

recognized correctly. The BET for the entire group was determined as the geometric mean of individual BETs.

3.4   Results and Discussion

3.4.1   Enzyme stability in solutions

To move the bi-enzymatic biosensor from the fridge into the ambient environment, the enzyme activities preserved in protectant-added solutions were investigated as the preliminary study. Three different samples: free enzymes in KDP buffer, enzymes in glycerol solution and enzymes in pullulan solution, were sealed in glass vials and stored at 23°C or 4°C before the enzyme activity evaluated by indole determination. Samples stored at 4°C were much more stable compared with those stored at 23°C. Fig. 3.1 shows these three samples all lost more than 99% initial activities in one week when stored at 23°C, strongly suggesting a more effective way to stabilize enzymes in ambient environment is required. Moreover, as indicated by the same initial enzyme activities (generating ~ 5.5 µg/mL indole) on day 1 for these three samples, there is no significant influence from protectants (pullulan and glycerol) on this bi-enzymatic reaction. Therefore, pullulan and glycerol can be used for the future studies.
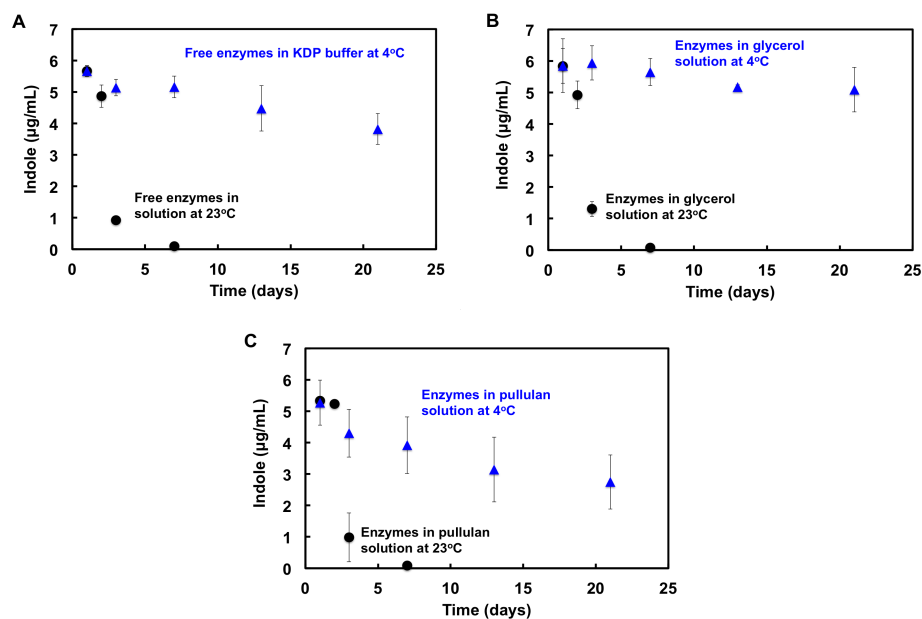
Figure 3.1 Enzyme activities after being stored at 4°C and 23°C. (A) Free enzymes in KDP buffer; (B) enzymes in pullulan solution; (C) enzymes in glycerol solution.

3.4.2 Enzyme stability after immobilization

Previous reports showed immobilized enzymes could retain the enzyme activity.[28,39–43] In this study, we examined 4 different immobilization systems to stabilize this bi-enzymatic biosensor. Free enzymes in KDP buffer directly immobilized on filter paper and glassine paper were first tested. With 95% enzyme activities lost in one day, more effective immobilization protocols were highly desired. Enzymes with pullulan or glycerol immobilized on filter paper (Fig. 3.2A), enzymes with pullulan or glycerol immobilized on glassine paper (Fig. 3.2B), and enzymes entrapped in pullulan tablets (Fig. 3.2C) were then investigated. The activities of these samples after stored at 23°C, 50% RH are shown in Fig. 3.2.
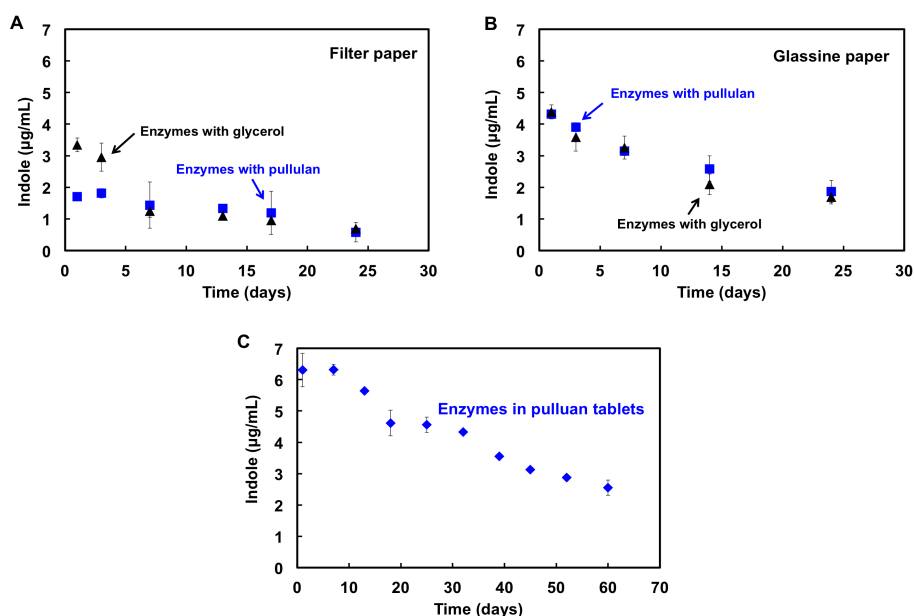
Figure 3.2 Stability tracking of immobilized enzymes after being stored at 23°C, 50% RH. (A) Enzymes with pullulan or glycerol immobilized on filter paper; (B) enzymes with pullulan or glycerol immobilized on glassine paper; (C) enzymes directly entrapped in pullulan tablets.

Compared with enzymes stored in solutions (Fig. 3.1), immobilized enzymes (Fig. 3.2) retained much more activities after being stored in ambient environment. Fig. 3.2A illustrated that, on filter paper, enzymes with glycerol were initially more stable than those with pullulan, but the activities became the same after 7 days and ended up with only 10% activity of fresh free enzymes after 24 days. For glassine paper shown in Fig. 3.2B, there was no significant activity difference between immobilized enzymes with glycerol and with pullulan, which both generated around 30% activity of fresh free enzymes after 24 days. The divergent results of samples on filter paper and glassine paper is probably due to the different morphologies of the paper surfaces. The glassine paper has much less porosity compared to filter paper (0.1 for glassine

paper and 0.87 for filter paper[44]), which reduces the interaction between paper chemicals with enzymes and helps retain enzyme activity. The influence of glycerol and pullulan together showed the similar results (Fig. S2), with less than 35% activity of fresh free enzymes after 24 days storage. Additionally, compared with enzymes in KDP buffer, enzymes immobilized on papers lost part of activities once after immobilization (by comparing the beginning points in Fig. 3.1 and Fig. 3.2A & B). Controvertibly, enzymes entrapped in pullulan tablets (Fig. 3.2C) not only retained all the initial enzyme activities after immobilization, but also preserved considerable enzyme activities when stored in ambient environment for a long time. After being stored for one week at room temperature, the bi-enzyme in pullulan tablets retained $\sim 100\%$ of its activity which is at least 100 times better than the free enzymes stored in solution. Even after being stored for 60 days, the bi-enzyme retained 40% of the initial activity. Put together with the results in Fig. 3.1 and Fig. 3.2, entrapping bi-enzyme in pullulan tablets was demonstrated as the best way to stabilize the bi-enzyme in ambient environment, significantly more robust than enzymes stored in solutions or immobilized on papers. Pullulan tablets were then used in the following work to immobilize the three substrates, in order to move the whole biosensor into the solid phase for easy handling purpose.

3.4.3   Substrates stability tracking in ambient environment
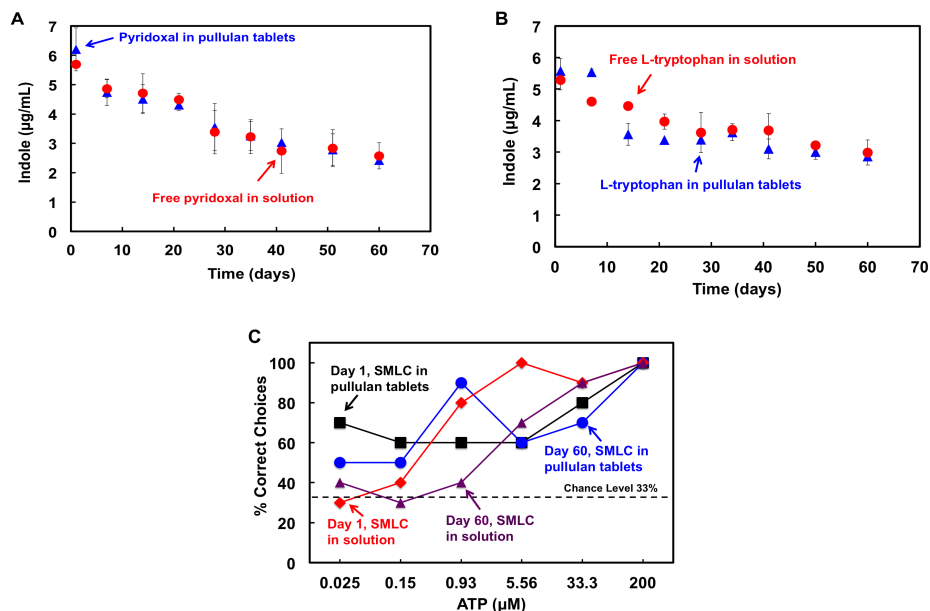
Figure 3.3 Stability tracking of immobilized substrates after stored at 23°C, 50% RH with light blocked. For each sample, free substrate in solution and the substrate entrapped in pullulan tablet were investigated. Stability of (A) pyridoxal and (B) L-tryptophan were determined by indole generation; stability of (C) SMLC was determined by human smell tests. Reaction proceeded for 1 hour at room temperature.

Fig. 3.3 indicates that, pyridoxal, L-tryptophan and SMLC entrapped in pullulan tablets all retained the same activities as the free ones in solution when stored in ambient environment. After being stored for 60 days at 23°C, 50% RH with light blocked, pyridoxal in pullulan tablets retained 43% of the initial activity (Fig. 3.3A), and L-tryptophan in pullulan tablet retained 63% of the initial activity (Fig. 3.3B), which were not significantly different from the corresponding results of free substrates stored in solution: 55% for pyridoxal (Fig. 3.3A) and 57% for L-tryptophan (Fig. 3.3B). Fig. 3.3C shows one day old pullulan tablet of SMLC resulted in a BET of 1.88 µM ATP, and 60 days old sample resulted in a BET of 2.25 µM ATP (detailed

81

results shown in Table S1 & S2 in the ESI†). The results for SMLC stored in solution are slightly better, with BETs of 0.45 µM ATP for one day old samples, and 1.73 µM ATP for 60 days old samples (detailed results shown in Table S3 & S4 in the ESI†). The results indicate SMLC entrapped in pullulan tablets were relatively stable for 60 days. From these results, entrapping substrates in pullulan tablets can help retain the stability of all three substrates in ambient environment with light blocked.

3.4.4   BETs of ATP for Smell-Tell tablets stored at room temperature

For ease of use purpose, substrates were all entrapped in one pullulan tablet, same as the enzymes, to immobilized the whole odour-generating biosensor in pullulan tablets and prepare what we named Smell-Tell tablets, consisted of one tablet containing substrates and another tablet containing two enzymes. (Fig. 3.4)
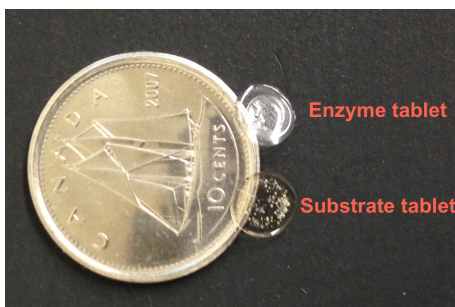
Figure 3.4 A photo of the prepared Smell-Tell tablets with a 10-cent Canadian coin. One tablet contains enzymes, and another tablet contains substrates. The thickness of the tablets is around 0.15 mm.

To investigate the performance of the Smell-Tell tablets when stored in ambient environment, we tracked the efficiency of the Smell-Tell tablets by determining indole

generated and BETs of ATP through human smell tests. Reaction time was prolonged to 2 hours since it requires some time for tablets to dissolve and release the materials inside. The results are shown in Fig. 3.5.
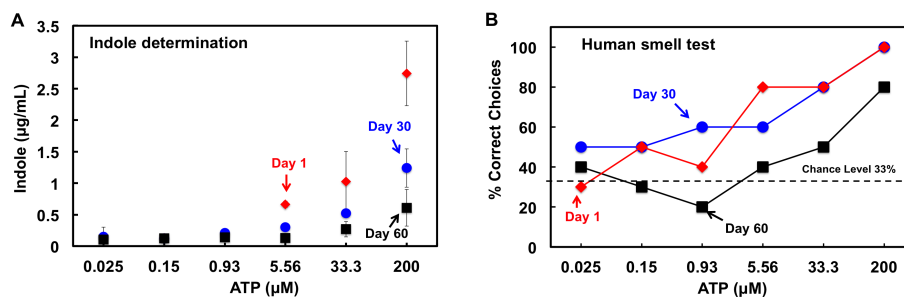
Figure 3.5 Activity tracking for Smell-Tell tablets after stored at room temperature for 1 day, 30 days and 60 days. (A) Indole determination; (B) human smell tests. Reaction proceeded for 2 hours at room temperature.

With all components entrapped in pullulan tablets, the results in Fig. 3.5 illustrate that the Smell-Tell tablets retained high sensitivity when stored at room temperature, even for 2 months. BETs of ATP after storage are: 1.31 µM after 1 day, 1.57 µM after 30 days, and 57.1 µM after 60 days (detailed results shown in Table S5 – S7 in the ESI†).

3.5   Conclusion

We have been working to stabilize two enzymes (PKase and TPase) and three substrates (pyridoxal, SMLC, and L-tryptophan) in ambient environment for practical on-site usage of an odour-generating biosensor. Retained activities of PKase and Apo-TPase are less than 1% initial activity upon 1 week room storage in different

solution cases, including: (1) free enzymes in KDP buffer, (2) enzymes in pullulan solution, (3) enzymes in glycerol solution. Enzyme activities after immobilized with (1) glycerol or pullulan on filter paper, (2) glycerol or pullulan on glassine paper, and (3) directly entrapped in pullulan tablets were also investigated. Among these cases, enzymes directly entrapped in pullulan tablets preserved enzyme activities the best. By entrapping in pullulan tablets, the enzymes retained $\sim 100\%$ activity after stored for 7 days in ambient environment, which is at least 100 times better than the free enzymes in buffer stored in the same conditions. The pullulan entrapped bi-enzyme could retain 40% activity even after stored for 60 days in ambient environment. Three substrates (pyridoxal, L-tryptophan, and SMLC) were also successfully immobilized into the pullulan tablet, making it feasible to immobilize the whole biosensor for easy handling purpose. The developed Smell-Tell tablets show high stable activity even after being stored at room temperature for months, with the BETs of 1.31 µM ATP after one day, 1.57 µM ATP after one month, and 57.1 µM ATP after two months.

This work is the first report on an enzymatic odour-generating biosensor that can be stored at room temperature for months. There is wide range of future applications for the Smell-Tell tablets in on-site safety control and disease diagnostic by providing simple Yes/No ATP assay, especially in resource-limited areas. The multiple inputs (ATP, three substrates and two enzymes) to odour generation also provide opportunities to couple this odour-generating biosensor with recognition reagents for other interesting targets. This immobilization/stabilization strategy may also find potential applications in controlled release of bio-pesticide (pheromone) and odour-display industries by stabilizing vapour-generating biomaterials.

3.6   Acknowledgement

References

[1] Bushdid, C.; Magnasco, M. O.; Vosshall, L. B.; Keller, A. *Science* **2014**, *343*, 1370–1372.

[2] Nagata, Y.; Takeuchi, N. *Odor Measurement Review, Office of Odor, Noise and Vibration Environmental Management Bureau, Ministry of the Environment, Government of Japan, Tokyo, Japan* **2003**, 118–127.

[3] Sarrafchi, A.; Odhammer, A. M.; Salazar, L. T. H.; Laska, M. **2013**,

[4] Sela, L.; Sobel, N. *Experimental brain research* **2010**, *205*, 13–29.

[5] Jehl, C.; Royet, J.; Holley, A. *Perception & psychophysics* **1995**, *57*, 1002–1011.

[6] Rabin, M. D. *Perception & Psychophysics* **1988**, *44*, 532–540.

[7] Melker, R.; Dennis, D. Application of biosensors for diagnosis and treatment of disease. 2005; http://www.google.com.ar/patents/US6974706, US Patent 6,974,706.

[8] Mohapatra, H.; Phillips, S. T. *Angewandte Chemie* **2012**, *124*, 11307–11310.

[9] Nicklin, S.; Cooper, M.; D, S. Whole cell biosensor using the release of a volatile substance as reporter. 2007; http://google.com/patents/WO2007083137A1?cl=ja, WO Patent App. PCT/GB2007/000,171.

[10] Wang, Z.; Johns, V. K.; Liao, Y. *Chemistry-A European Journal* **2014**, *20*, 14637–14640.

[11] Xu, Y.; Zhang, Z.; Ali, M. M.; Sauder, J.; Deng, X.; Giang, K.; Aguirre, S. D.; Pelton, R.; Li, Y.; Filipe, C. D. *Angewandte Chemie International Edition* **2014**, *53*, 2620–2622.

[12] Zhang, Z.; Wang, J.; Ng, R.; Li, Y.; Wu, Z.; Leung, V.; Imbrogno, S.; Pelton, R.; Brennan, J. D.; Filipe, C. D. *Analyst* **2014**, *139*, 4775–4778.

[13] Wang, J.; Wang, L.; Liu, X.; Liang, Z.; Song, S.; Li, W.; Li, G.; Fan, C. *Advanced Materials* **2007**, *19*, 3943–3946.

[14] Yang, N.-C.; Ho, W.-M.; Chen, Y.-H.; Hu, M.-L. *Analytical biochemistry* **2002**, *306*, 323–327.

[15] Greenman, J.; El-maaytah, M.; Duffield, J.; Spencer, P.; Rosenberg, M.; Corry, D.; Saad, S.; Lenton, P.; Majerus, G.; Nachnani, S. *The Journal of the American Dental Association* **2005**, *136*, 749–757.

[16] Sahu, R. K.; Prakash, V. *International Journal of Food Properties* **2008**, *11*, 613–623.

[17] Vagenende, V.; Yap, M. G.; Trout, B. L. *Biochemistry* **2009**, *48*, 11084–11096.

[18] Wang, W. *International journal of pharmaceutics* **2005**, *289*, 1–30.

[19] Feng, S.; Yan, Y.-B. *Proteins: Structure, Function, and Bioinformatics* **2008**, *71*, 844–854.

[20] Gekko, K.; Timasheff, S. N. *Biochemistry* **1981**, *20*, 4667–4676.

[21] Cheng, K.-C.; Demirci, A.; Catchmark, J. M. *Applied microbiology and biotechnology* **2011**, *92*, 29–44.

[22] Farris, S.; Introzzi, L.; Fuentes-Alventosa, J. M.; Santo, N.; Rocca, R.; Piergiovanni, L. *Journal of agricultural and food chemistry* **2012**, *60*, 782–790.

[23] Farris, S.; Unalan, I. U.; Introzzi, L.; Fuentes-Alventosa, J. M.; Cozzolino, C. A. *Journal of Applied Polymer Science* **2014**, *131*.

[24] Gounga, M.; Xu, S.-Y.; Wang, Z.; Yang, W. *Journal of food science* **2008**, *73*, E155–E161.

[25] Boridy, S.; Takahashi, H.; Akiyoshi, K.; Maysinger, D. *Biomaterials* **2009**, *30*, 5583–5591.

[26] Kaneo, Y.; Tanaka, T.; Nakano, T.; Yamaguchi, Y. *Journal of controlled release* **2001**, *70*, 365–373.

[27] San Juan, A.; Bala, M.; Hlawaty, H.; Portes, P.; Vranckx, R.; Feldman, L. J.; Letourneur, D. *Biomacromolecules* **2009**, *10*, 3074–3080.

[28] Jahanshahi-Anbuhi, S.; Pennings, K.; Leung, V.; Liu, M.; Carrasquilla, C.; Kannan, B.; Li, Y.; Pelton, R.; Brennan, J. D.; Filipe, C. D. *Angewandte Chemie International Edition* **2014**, *53*, 6155–6158.

[29] Jadhav, S. B.; Singhal, R. S. *Carbohydrate polymers* **2014**, *105*, 49–56.

[30] Pelton, R. *TrAC Trends in Analytical Chemistry* **2009**, *28*, 925–942.

[31] di Salvo, M. L.; Hunt, S.; Schirch, V. *Protein expression and purification* **2004**, *36*, 300–306.

[32] Erez, T.; Gdalevsky, G. Y.; Hariharan, C.; Pines, D.; Pines, E.; Phillips, R. S.; Cohen-Luria, R.; Parola, A. H. *Biochimica et Biophysica Acta (BBA)-Protein Structure and Molecular Enzymology* **2002**, *1594*, 335–340.

[33] Metzler, C. M.; Viswanath, R.; Metzler, D. E. *Journal of Biological Chemistry* **1991**, *266*, 9374–9381.

[34] Davies, M. J. *Biochemical and biophysical research communications* **2003**, *305*, 761–770.

[35] Gregory, J.; Kirk, J. *Journal of Food Science* **1978**, *43*, 1801–1808.

[36] others,, et al. *Science* **1976**, *191*, 468–469.

[37] Saidi, B.; Warthesen, J. J. *Journal of Agricultural and Food Chemistry* **1983**, *31*, 876–880.

[38] Standard practice for determining odor and taste thresholds by a forced-choice ascending concentration series method of limits. 2008.

[39] Garcia-Galan, C.; Berenguer-Murcia, Á.; Fernandez-Lafuente, R.; Rodrigues, R. C. *Advanced Synthesis & Catalysis* **2011**, *353*, 2885–2904.

[40] Gupta, R.; Chaudhury, N. *Biosensors and Bioelectronics* **2007**, *22*, 2387–2399.

[41] Rodrigues, R. C.; Berenguer-Murcia, Á.; Fernandez-Lafuente, R. *Advanced Synthesis & Catalysis* **2011**, *353*, 2216–2238.

[42] Sassolas, A.; Blum, L. J.; Leca-Bouvier, B. D. *Biotechnology Advances* **2012**, *30*, 489–511.

[43] Sheldon, R. A. *Advanced Synthesis & Catalysis* **2007**, *349*, 1289–1307.

[44] Rasi, M. Permeability properties of paper materials. Ph.D. thesis, University of Jyväskylä, 2013.

Electronic Supplement Information for

Bi-Enzymatic Odour-Generating Biosensor with Enhanced Stability: Pullulan Based Smell-Tell Tablets for On-Site ATP detection

Zhuyuan Zhang,[a] Paul Wigmore,[a] Xudong Deng,[a] Sana Jahanshahi-Anbuhi,[a] Vincent Leung,[a]

Robert Pelton,[a] Yingfu Li,[b] Carlos D. M. Filipe[*a]

* Corresponding author

[a] Department of Chemical Engineering, McMaster University, 1280 Main Street West,

Hamilton, ON, Canada; **E-mail:** filipec@mcmaster.ca; **Fax:** +1 905 521-1350; **Tel:** +1

905 525-9140 ext. 27278

[b] Department of Biochemistry and Biomedical Sciences, McMaster University, 1200

Main Street West, Hamilton, ON, Canada
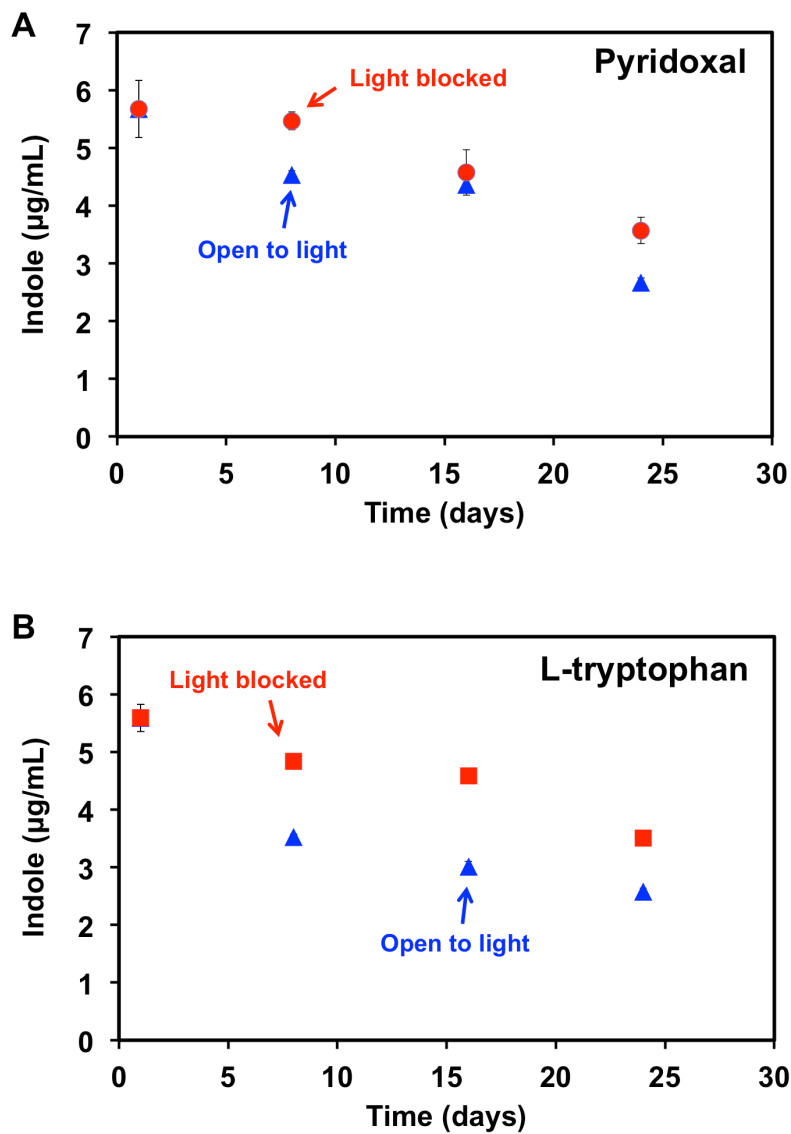
Fig. S1. Light sensitivity of pyridoxal and L-tryptophan. (A) Pyridoxal immobilized in pullulan tablets stored open to the light and with light blocked (in a carton). (B) L-tryptophan immobilized in pullulan tablets stored open to the light and with light blocked.
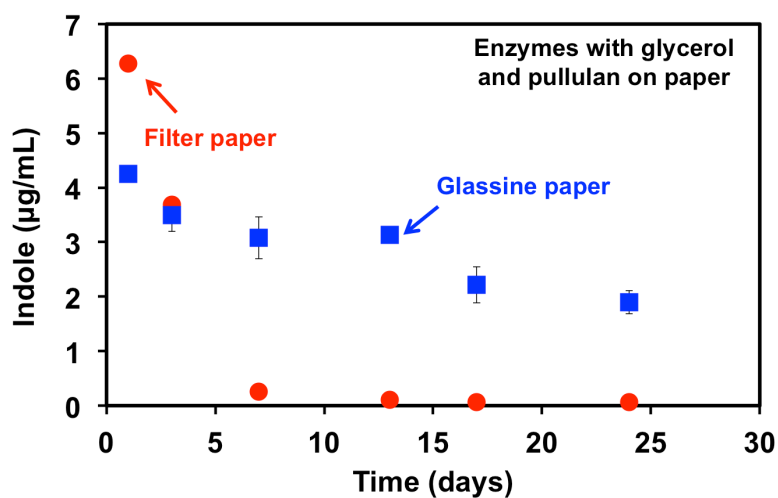
Fig. S2. Enzymes immobilized on paper substrates with glycerol and pullulan. 47 μL

PKase (0.34 mg/mL) in glycerol (50% v/v) and pullulan (12% w/w) mixed solution, and

16 μL Apo-TPase (1.4 mg/mL) in glycerol (50% v/v) and pullulan (12% w/w) mixed

solution were pipetted onto filter paper or glassine paper stripes to prepare the samples

for bienzyme reaction.

Table S1. Human smell test for samples in pullulan tablets on day 1

Panelist	Judgments [a]							
	Concentrations of ATP (µM)						BET	
	0.026	0.15	0.93	5.56	33.3	200	Value	Log_{10} of Value
1	0	1	1	1	1	1	0.06	-1.21
2	1	1	1	1	1	1	0.01	-1.99
3	1	1	1	1	1	1	0.01	-1.99
4	1	0	0	0	1	1	13.61	1.13
5	0	0	0	0	1	1	13.61	1.13
1	1	1	1	0	1	1	13.61	1.13
2	0	0	1	1	1	1	0.37	-0.43
3	1	1	1	1	0	1	81.61	1.91
4	1	1	0	1	0	1	81.61	1.91
5	1	0	0	0	1	1	13.61	1.13
Group BET = geometric mean, µM ATP							Average of log_{10} = 0.27	
							BET = $10^{0.27}$ = 1.88	
							Log Stand. Dev. = 1.46	

[a] "0" indicates that the panelist identified the wrong sample in the set; "1" indicates the panelist selected the correct sample.

Table S2. Human smell test for samples in pullulan tablets on day 60

Panelist	Judgments [a]							
	Concentrations of ATP (µM)						BET	
	0.026	0.15	0.93	5.56	33.3	200	Value	Log_{10} of Value
1	1	1	1	1	1	1	0.01	-1.99
2	1	0	1	1	1	1	0.37	-0.43
3	0	0	1	0	0	1	81.61	1.91
4	0	1	1	0	1	1	13.61	1.13
5	1	1	1	1	0	1	81.61	1.91
1	1	1	1	1	1	1	0.01	-1.99
2	0	1	1	1	1	1	0.06	-1.21
3	0	0	1	0	1	1	13.61	1.13
4	1	0	0	0	1	1	13.61	1.13
5	0	0	1	1	0	1	81.61	1.91
Group BET = geometric mean, µM ATP							Average of log_{10} = 0.35	
							BET = $10^{0.35}$ = 2.25	
							Log Stand. Dev. = 1.60	

Table S3. Human smell test for samples in solution on day 1

Panelist	Judgments [a]							
	Concentrations of ATP (µM)						BET	
	0.026	0.15	0.93	5.56	33.3	200	Value	Log$_{10}$ of Value
1	0	0	1	1	1	1	0.37	-0.43
2	1	1	1	1	1	1	0.01	-1.99
3	0	1	1	1	1	1	0.06	-1.21
4	0	0	1	1	1	1	0.37	-0.43
5	0	0	1	1	1	1	0.37	-0.43
1	0	0	0	1	1	1	2.27	0.36
2	0	0	1	1	1	1	0.06	-1.21
3	1	1	0	1	1	1	2.27	0.36
4	0	1	1	1	0	1	81.61	1.91
5	0	0	1	1	1	1	0.37	-0.43
Group BET = geometric mean, µM ATP							Average of log$_{10}$ = -0.35	
							BET = $10^{-0.35}$ = 0.45	
							Log Stand. Dev. = 1.07	

Table S4. Human smell test for samples in solution on day 60

Panelist	Judgments [a]							
	Concentrations of ATP (µM)						BET	
	0.026	0.15	0.93	5.56	33.3	200	Value	Log$_{10}$ of Value
1	1	1	1	1	1	1	0.01	-1.99
2	0	1	0	1	1	1	5.57	0.75
3	0	0	1	0	0	1	13.61	1.13
4	1	0	1	0	1	1	13.61	1.13
5	0	0	0	1	1	1	2.27	0.36
1	1	1	1	1	1	1	0.01	-1.99
2	0	0	0	1	1	1	13.61	1.13
3	0	0	0	0	1	1	13.61	1.13
4	1	0	0	1	1	1	2.27	0.36
5	0	0	0	1	1	1	2.27	0.36
Group BET = geometric mean, µM ATP							Average of log$_{10}$ = 0.24	
							BET = $10^{0.24}$ = 1.73	
							Log Stand. Dev. = 1.22	

Table S5. Human smell test using Smell-Tell tablets in day 1

Panelist	Judgments [a]							
	Concentrations of ATP (μM)						BET	
	0.026	0.15	0.93	5.56	33.3	200	Value	Log_{10} of Value
1	0	1	0	0	1	1	13.61	1.13
2	0	0	0	1	0	1	81.61	1.91
3	0	1	1	1	1	1	0.06	-1.21
4	1	0	0	1	1	1	2.27	0.36
5	1	1	1	1	1	1	0.01	-1.99
1	0	1	0	0	0	1	81.61	1.91
2	0	0	0	1	1	1	2.27	0.36
3	1	0	1	1	1	1	0.37	-0.43
4	0	0	0	1	1	1	2.27	0.36
5	0	1	1	1	1	1	0.06	-1.21
Group BET = geometric mean, μM ATP							Average of log_{10} = 0.12	
							BET = $10^{0.12}$ = 1.31	
							Log Stand. Dev. = 1.26	

Table S6. Human smell test using Smell-Tell tablets in day 30

Panelist	Judgments [a]							
	Concentrations of ATP (μM)						BET	
	0.026	0.15	0.93	5.56	33.3	200	Value	Log_{10} of Value
1	1	1	1	1	1	1	0.01	-1.99
2	0	1	1	1	1	1	0.06	-1.21
3	1	0	0	0	1	1	13.61	1.13
4	1	0	0	0	1	1	13.61	1.13
5	0	1	1	1	0	1	81.61	1.91
1	1	1	1	1	1	1	0.01	-1.99
2	0	1	1	1	1	1	0.06	-1.21
3	0	0	1	0	1	1	13.61	1.13
4	0	0	0	0	1	1	13.61	1.13
5	1	0	0	1	0	1	81.61	1.91
Group BET = geometric mean, μM ATP							Average of log_{10} = 0.20	
							BET = $10^{0.20}$ = 1.57	
							Log Stand. Dev. = 1.60	

Table S7. Human smell test using Smell-Tell tablets in day 60

Panelist	Judgments [a]							
	Concentrations of ATP (µM)						BET	
	0.026	0.15	0.93	5.56	33.3	200	Value	Log_{10} of Value
1	1	1	1	1	0	1	81.61	1.91
2	0	1	0	0	1	0	489.90	2.69
3	0	0	0	0	0	1	81.61	1.91
4	1	0	0	0	1	1	13.61	1.13
5	0	0	0	0	1	1	13.61	1.13
1	1	1	1	1	0	1	81.61	1.91
2	0	0	0	0	1	0	489.90	2.69
3	0	0	0	0	0	1	81.61	1.91
4	1	0	0	1	0	1	81.61	1.91
5	0	0	0	1	1	1	2.27	0.36
Group BET = geometric mean, µM ATP							Average of log_{10} = 1.76	
							BET = $10^{1.76}$ = 57.1	
							Log Stand. Dev. = 0.71	

Chapter 4

Application of Statistical Method for Optimization of an Odour-Generating Bio-Sensing System

4.1 Abstract

Olfactory signals have demonstrated great potential to be used as a reporting signal for sensing systems. In order to improve the efficiency of odour-generating biosensors, optimization of the sensing systems is necessary. In this work, we report an effective way to optimize an odour-generating sensing system for ATP detection. In the optimization process, fractional factorial design (FFD) and statistical software R were used for experimental design and data analysis; triangular forced-choice smell tests were applied in signal determination tests. For the studied odour-based sensing system, we investigated the influence of 11 factors on the detection efficiency of the sensing system and the reaction conditions were optimized. The optimization process was able to reduce the quantity of expensive materials by at least 30% while maintaining similar detection limits of ATP.

4.2 Introduction

Biosensor technology has been regarded as a tool to be used in the areas of environmental monitoring, food quality control and clinical bio-analysis since the mid-1990s.[1,2] Typically, a biosensor system has two associated elements: target recognizer and signal transducer, which consists of biomaterials such as enzyme,[3,4] antibody,[5] nucleic acid probe,[6] cell,[7] and tissue[8]. Recently, much attention has been brought to the study of detectable signals generated by the biosensor systems. There has been an increasing amount of research work reported on how to convert the physical or chemical changes to electrochemical,[9] optical,[10] piezoelectric,[11] magnetic,[12] and mass change[13] signals. One example of such work, which has received a great amount of

attention, is generating human detectable odour signals that can be directly detected by the human nose.[14–16]

The detection of certain odour signals by the human nose could be used for the determination of threats such as fire, gas leakage, spoiled fish and even early disease diagnosis.[17] Inspired by this, odour-generating biosensors, which generate human detectable odour signals when specific target analytes appear, have been of interest. Differing from the signals involved in most commercial biosensors and prototypes, an odour signal has several unique features. The odour signal is able to diffuse and reach the analytical facilities by itself. For many odour molecules, the human olfactory system has extremely low detection thresholds at the part-per-trillion (ppt) level,[18,19] which makes the human nose a "free analytical instrument". Detecting odour signals by human noses has another special advantage since smell is an involuntary sensation. The sense of smell is always active because a person cannot stop breathing.[20,21] During the last couple of years, there have been two groups working on the development of the odour-generating biosensing system. In 2012, Mohapatra's group,[16] used glucose oxidase and specially designed molecules to detect enzymes via generating the odour signal, volatile ethanethiol. Based on this method, they could detect β-D-galactosidase with a detection limit of 21 nM. Our group recently reported a tryptophanase (TPase) based odour generating reporter,[15] to generate methyl mercaptan/indole in the presence of analytes such as antibodies. In addition, pyridoxal kinase (PKase) was coupled with TPase in our system for detection of adenosine triphosphate (ATP), an important biological marker. The odour signals could be detected by the human nose with a detection limit of 0.32 µM ATP.[15] However, although both of the studies have developed effective bio-analysis strategies based on

odour generation, the biomaterials used in these systems are either expensive or hard to prepare. It is therefore important that a robust and extensive optimization strategy be developed to reduce the cost without sacrificing the low detection limit of the sensing systems.

Herein, we proposed and developed a robust optimization strategy for the odour-generating bio-sensing system. The biosensor system used in this study was designed by our group for ATP detection,[15] which consists of two enzymes, PKase and Apotryptophanase (Apo-TPase) (Fig. 4.1). When target ATP presents, PKase generates pyridoxal 5'-phosphate (PLP), which can convert Apo-TPase (inactive status) to Holo-TPase (active status). Holo-TPase produces odourous methyl mercaptan (CH_3SH) by consuming S-methyl-L-cysteine (SMLC), generating an odour signal that can be detected by humans directly. As reported in the previous studies,[14,15] triangular forced-choice human smell test was applied here for participants to determine the odour signal.
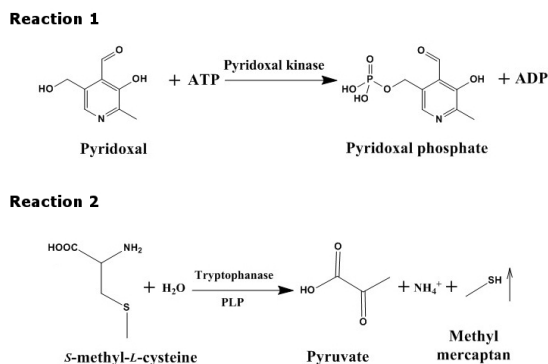
Figure 4.1 Reaction mechanisms of the ATP sensing system.[14,15] Reaction 1: the reaction mechanism for PLP produce based on PKase; Reaction 2: the reaction mechanism for CH_3SH produce based on TPase and PLP generated from Reaction 1.

The variables which could affect the sensitivity and therefore effectiveness of the sensing system, often include enzyme concentrations, pH, temperature, reaction time. To explore all the possible variables for the biosensor system, optimization methods based on optimizing a single factor each time would involve a substantial amount of sample preparation and tests, making the optimization tests costly and time consuming.[22] It is therefore desirable that statistical strategies are applied to develop a statistically significant and robust optimization strategy. Fractional factorial designs (FFD) were applied as such a statistical analysis strategy to evaluate the influence of different factors. FFD is a class of experimental designs which are very useful in identifying the important factors and interactions between two or more factors using fewer experiments when compared with conventional optimization of single factor.[22,23] After selecting the important factors to improve the detection limit, it was possible to optimize the sensing system using less time and overall costs. In this study, we combined triangular forced-choice human smell tests with FFD to explore the effect of multiple variables and to optimize the odour-generating sensing system.

4.3 Materials and Methods

4.3.1 Materials

ATP disodium salt, pyridoxal and SMLC were purchased from Sigma-Aldrich (Oakville, ON). KDP buffer contained 0.2 M potassium phosphate and 6.7 mM ammonium sulfate. Glass bottles with a volume of 40 mL were purchased from a local chemical store. PKase (EC 2.7.1.35) and Apo-TPase from *Escherichia coli* (EC 4.1.99.1) were prepared as reported in previous studies.[24–26] Ultrapure (UP) water was prepared

with a Nanopure purification system (Barnstead Nanopure D11901 from Thermo Scientific) to a specific resistance of 18MΩ/cm. Tap water was directly collected from the faucet in the lab.

4.3.2 Variables for Sensing System Optimization

Based on the previous work[14,15] and enzymatic kinetic models (see supplementary information), there were 11 variables (Table 4.1) chosen to be investigated: the amount of enzymes (PKase & Apo-TPase), temperature, pH, the ion cofactor for the enzymes ($MgCl_2$), the concentrations of substrates (SMLC, pyridoxal and ATP), reaction time, liquid: gas ratio (the volume ratio of liquid phase to gas phase in the reaction bottle) and the solvent water type (to see the influence of solvent background). These variables were selected as they were thought to have an effect on the odour-generating sensing system. The low levels and high levels were selected to cover enough of a range that the variable would have an effect and on the basis of previous studies.[14,15] These are initial low and high levels and a preliminary point to start the FFD experiments to screen for which factors might be truly significant.

Table 4.1 Variables and their values for the preliminary screening test.

Variables	Factors	Low Level Value	High Level Value
A	Temperature	4°C	23°C
B	pH	5.5	7.8
C	Apo-TPase	10 µg/mL	100 µg/mL
D	Conc. of SMLC	0.05 mM	1 mM
E	Conc. of $MgCl_2$	0	0.2 mM
F	Conc. of Pyridoxal	1 µg/mL	0.1 mg/mL
G	Conc. of ATP (target)	0.1 µM	10 µM
H	PKase	0.1 µg/mL	20 µg/mL
I	Reaction Time	10 mins	60 mins
J	Liquid: Gas Ratio	1:79	1:15
K	Water Type	UP water	Tap water

FFD for Statistical Analysis

FFD, which consists of an adequate fraction of experimental runs required for a complete factorial experiment, was applied to reduce the cost of the optimization process. In this study, to reduce cost, a two-level FFD (Table 4.1) was employed first for a screening purpose to identify which factors affected the system significantly. Following the approach described in [23?] , this two-level FFD was generated using a full four factor factorial design involving factors **A**, **B**, **C**, **D** and constructing the remaining factors by the generating relations shown in Table 4.2.

Table 4.2 Design of the two level fractional factorial experiments.

Variables	Confounding
E	**= ABC**
F	**= BCD**
G	**= ACD**
H	**= ABD**
I	**= ABCD**
J	**= AB**
K	**= AC**

To include all of the combinations of the 11 factors at two levels, a 2^7 fraction of the full factorial design (2^{11} different sets) was selected, resulting in 2^4 (2^{11-7}) sets of experiments. Because of the low reliability in human smell based analysis, a complementary 2^4 experiment sets were also carried out to increase the accuracy of results. In the complementary experiment sets, the factor signs were reversed (for example, in the first set **E = ABC**, in the complementary set **E = - ABC**). In total, 2^5 experiment sets (details shown in the left part of Table 4.3, with six additional replicates to ensure the tests are repeatable) were studied for preliminary screening purposes. The levels for two-level FFD (Table 4.1) were chosen on the basis of previous studies,[14,15] and theoretical predications using the reported coefficients.[27,28] FFDs at multi-level were also involved in this study to further determine the individual and interacting effects of different variables. The details are shown in the following sections.

Table 4.3 Design and result of the two-level fractional factorial design as the preliminary screening test. "1" is the high level value of the variables; "-1" is the low level. The experiments were done in random order. The table is reported in standard order. The last three columns are the outcomes of the experiments.

A	B	C	D	E	F	G	H	I	J	K	Average Score	Standard Deviation	% Correct Detection
-1	-1	-1	-1	-1	-1	-1	-1	1	1	1	3.00	0.00	33
1	-1	-1	-1	1	-1	1	1	-1	-1	-1	4.33	2.31	33
-1	1	-1	-1	1	1	-1	1	-1	-1	1	2.00	1.00	0
1	1	-1	-1	-1	1	1	-1	1	1	-1	3.67	1.15	33
-1	-1	1	-1	1	1	1	-1	-1	1	-1	3.00	0.00	0
1	-1	1	-1	-1	1	-1	1	1	-1	1	3.00	0.00	0
-1	1	1	-1	-1	-1	1	1	1	-1	-1	2.67	0.58	67
1	1	1	-1	1	-1	-1	-1	-1	1	1	3.00	0.00	33
-1	-1	-1	1	-1	1	1	1	-1	1	1	5.00	0.00	100
1	-1	-1	1	1	1	-1	-1	1	-1	-1	4.33	2.31	67
-1	1	-1	1	1	-1	1	-1	1	-1	1	2.67	0.58	0
1	1	-1	1	-1	-1	-1	1	-1	1	-1	3.33	1.53	33
-1	-1	1	1	1	-1	-1	1	1	1	-1	3.67	1.15	100
1	-1	1	1	-1	-1	1	-1	-1	-1	1	3.67	1.15	67
-1	1	1	1	-1	1	-1	-1	-1	-1	-1	3.67	1.15	33
1	1	1	1	1	1	1	1	1	1	1	6.33	1.15	100
-1	-1	-1	-1	-1	-1	-1	-1	1	1	1	2.67	0.58	67
1	1	1	1	1	1	1	1	1	1	1	6.33	1.15	100
1	1	1	1	1	1	1	1	-1	-1	-1	4.33	2.31	100
-1	1	1	1	-1	1	-1	-1	1	1	1	2.33	1.15	0
1	-1	1	1	-1	-1	1	-1	1	1	-1	3.33	1.53	33
-1	-1	1	1	1	-1	-1	1	-1	-1	1	4.33	2.31	33
1	1	-1	1	-1	-1	-1	1	1	-1	1	3.67	1.15	67
-1	1	-1	1	1	-1	1	-1	-1	1	-1	4.33	2.31	67
1	-1	-1	1	1	1	-1	-1	-1	1	1	2.00	0.00	0
-1	-1	-1	1	-1	1	1	1	1	-1	-1	2.33	1.15	33
1	1	1	-1	1	-1	-1	-1	1	-1	-1	3.33	1.53	67
-1	1	1	-1	-1	-1	1	1	-1	1	1	3.00	0.00	33
1	-1	1	-1	-1	1	-1	1	-1	1	-1	3.00	0.00	67
-1	-1	1	-1	1	1	1	-1	1	-1	1	3.00	0.00	33
1	1	-1	-1	-1	1	1	-1	-1	-1	1	2.67	0.58	0
-1	1	-1	-1	1	1	-1	1	1	1	-1	3.00	0.00	33
1	-1	-1	-1	1	-1	1	1	1	1	1	3.67	2.31	67
-1	-1	-1	-1	-1	-1	-1	-1	-1	-1	-1	2.67	0.58	33
1	1	1	1	1	1	1	1	-1	1	-1	4.67	2.52	67
-1	-1	-1	-1	-1	-1	-1	-1	-1	-1	-1	3.67	1.15	33
-1	-1	-1	-1	-1	-1	-1	-1	1	1	1	3.00	2.00	33
1	1	1	1	1	1	1	1	1	1	1	6.33	1.15	100

4.3.3 Triangular Forced-Choice Human Smell Test and Scoring System

A triangular forced-choice smell test was done following ASTM (E679-04)[29] with slight modification. For each experiment set there were three samples given to a human participant, of which only one was positive (with ATP). Five participants were required to identify the ATP-positive sample from the two other samples that were negative for ATP. Participants were forced to indicate a response even if no olfactory difference was detected. Participants were also asked to fill out an answer form and indicate their confidence level in their response, with level choices of 1, 2, and 3. A confidence level of 1 indicated that the participant randomly guessed their response, a confidence level of 3 indicated that the participant could detect the generated odour and they were very sure in their response, while a level of 2 was used to indicate the situation between levels of 1 and 3.

Meanwhile, a scoring system was developed to analyze results effectively and reduce the noise due to random guessing. The scoring system is not only based on the participant's accuracy of response, but also their confidence levels. The method of scoring is shown in Table 4.4: if a participant got the correct response and had the highest confidence, he/she would get the highest score (7); if a participant got the incorrect response and still had the highest confidence, he/she would get the lowest score (1); if the participant had low confidence, he/she could get a moderate score (2, 3 and 5) based on the correctness of the response. The scores were averaged out between five participants for each experiment.

Table 4.4 Scoring system in the triangular forced-choice human smell test.

Response	Confidence Level	Score
Correct	3	7
Correct	2	5
Correct	1	3
Wrong	3	1
Wrong	2	2
Wrong	1	3

4.3.4   Analysis of the Influence of Different Variables

Both the averaged score and the standard deviation of scores were used in the data analysis for the optimization. The averaged score shows the participants' detection ability of the odour signal generated. The standard deviation of the scores from different participants demonstrates the repeatability, or the robustness, of the results, which works as a complementary index for the efficiency determination. A higher average score indicates that the sensing system is more effective, while a higher standard deviation of scores indicates that the result has lower repeatability.

Programming language and environment R (version 3.0.2) was used for statistical computing. The linear regression model **lm** in R was used in this study. The **lm** function was used to fit data using multiple linear regression. For N variables, the model used was:

$$\hat{y} = \beta_0 + \beta_1 X_1 + \beta_2 X_2 + ... + \beta_N X_N$$

where X_i denotes the explanatory variables used in the analysis, $\hat{y}$ denotes the predicted response variable modeled as a function of the explanatory variables and

β_i denotes the coefficients computed by the **lm** function.

To evaluate how the model fits, **summary** function was invoked. The metrics from the **summary** function indicate the fit quality and include the significance of the β_i coefficients.

4.3.5 Best Estimation of Threshold (BET) for ATP Detection

The best estimation of threshold (BET) was determined and calculated following the previous reports[14,15,29]. The BET of each panelist is the geometric mean of the highest concentration of ATP that was identified incorrectly and next higher concentration recognized correctly. Five panelists were asked to finish the triangular forced-choice human smell test two times to calculate the BET for the entire group, which was determined as the geometric mean of individual BETs. BETs for ATP detection were determined to evaluate the detection ability of the sensing system before and after optimization.

4.4 Results and Discussion

4.4.1 Preliminary Screening Test

FFD based preliminary screening test was applied for quick determination of important variables, to eliminate variables that were not significantly influential. The results of human smell test are shown in the right part of Table 4.3. The significant coefficients from the FFD results are shown as a Pareto Plot in Fig. 4.2 (detailed results shown in Table S1). From these results, we can interpret that a high level of

factor **D** (SMLC) leads to high averaged scores but low repeatability; high levels of factors **F** (pyridoxal) and **K** (water type) lead to high repeatability. Also, high level of **H** (PKase) leads to more accurate responses from participants (Table S2). From this, we conclude that factors **D**, **F**, **H**, and **K** might have a significant influence on the sensing system and they were investigated in the next step of study. Other variables that did not show significant influence, factors **B**, **C**, **E** and **J**, were removed from the following tests based on the previous reported results[15] and theoretical estimation of CH_3SH produced and diffused. Factors **A**, **G** and **I** were kept for further studies (but not as key factors) for the following reasons: factor **A** (temperature) was kept because it is important to demonstrate future application conditions of the sensor, which is unpredictable since no report has been found on the activity of these two enzymes at low temperature; factors **G** (target ATP) and **I** (reaction time) were kept because they could be significant, as estimated by the enzymatic reaction equations. The influence of these two factors might be mistakenly represented due to the fluctuation of human olfactory perception, which can be influenced by factors such as participants current emotional state,[30] background light[31] or noise level,[32] cognitive ability after extended testing,[33] etc.
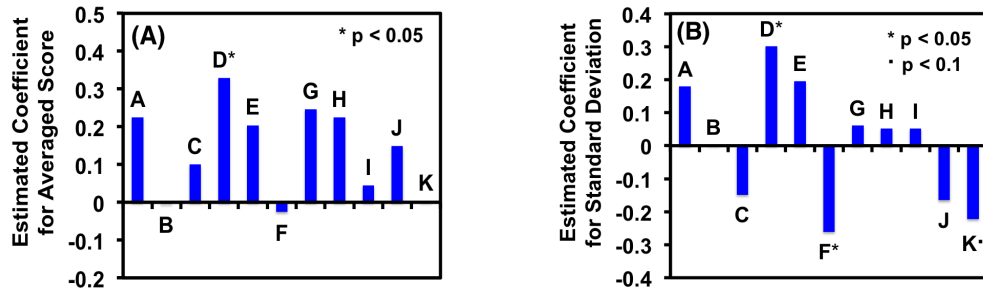
109

Figure 4.2 Estimated coefficient results in the preliminary screening test. (A) Estimated coefficients based on averaged scores; (B) Estimated coefficients based on standard deviations of scores. The p-value is the probability that the null hypothesis is actually correct.

4.4.2 FFDs for Exploratory Tests

A second FFD (Table S2) was run to determine the influence of the factors **A**, **D**, **H**, **F**, **K**, and **I**. There were 6 different levels for factors **D**, **F**, and **H**;(high resolution for the potential important factors shown in the preliminary test) 3 different levels for factors **A** and **I**;(low resolution for the potential important factors by theoretical estimation, but not shown in the preliminary test) and 2 different levels for **K** (only UP water and Tap water were studied) to further check their influence. The remaining factors were set to values where each factor was the average value of its previous high value and low value.

Fig. 4.3 (detailed results shown in Table S3) shows the averaged scores and standard deviations of scores. The analysis based only on the factors: **D**, **F**, **H** and **K**, which are the significant factors determined from the screening test. The results show that only factor **K** (water type) might have a significant effect for both the detectability and repeatability of the sensing system. Tap water might lead to higher averaged scores but lower repeatability, compared with UP water.
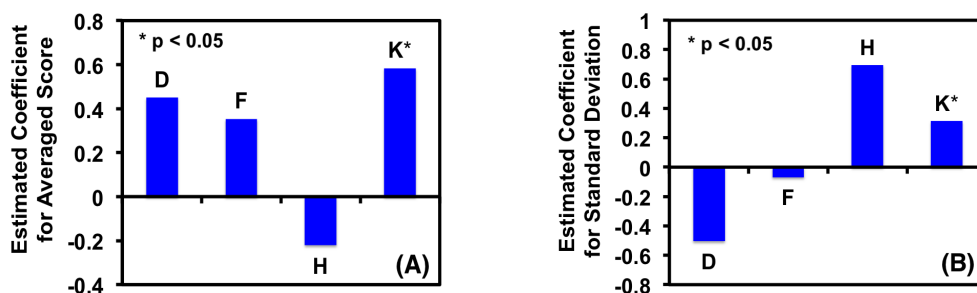
Figure 4.3 Estimated coefficient results for factors **D**, **F**, **H** and **K**. (A) Estimated coefficients based on averaged scores; (B) Estimated coefficients based on standard deviations of scores.

However, for experiment sets in which factor **K** (water type) varied between low and high levels, factors **A** (temperature) and **I** (reaction time) also varied at the low and high levels. Thus, the following set of experiments was done to determine the individual influence and interactions of factors **A**, **K**, and **I**. The only variables that changed in this round were **A**, **K**, and **I**, with the other variables remaining at the baseline (Table S4). For each experiment, a replicate for each set of experiments was done to increase the accuracy of the test. All experiments were done in random order.

The results analysis is shown in Fig. 4.4 and Table S5. Increasing the value of factor **I** (reaction time) leads to higher averaged score, but factor **I** also shows a strong positive effect on the standard deviation of scores. The interactions between the different factors were also investigated. The results show there is a significant interaction between factor **A** (temperature) and **I** for the averaged composite score: higher levels of factors **A** and **I** together lead to improved detection. Higher levels of factors **I** and **K** (UP water) together lead to improved detection.
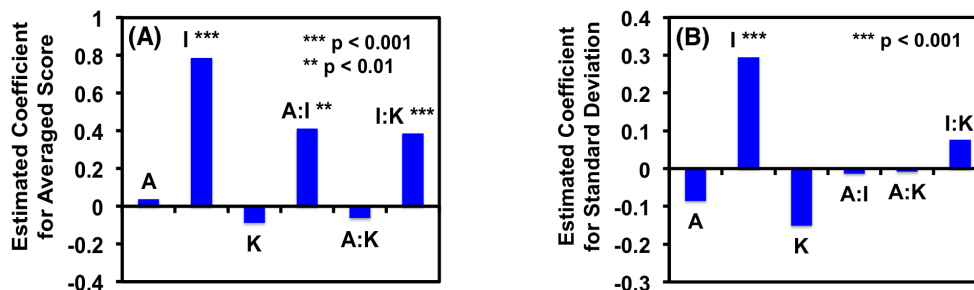
Figure 4.4 Estimated coefficient results for factors **A**, **K** and **I**. (A) Estimated coefficients based on averaged scores; (B) Estimated coefficients based on standard deviations of scores.

A new round of smell tests (Table S6) was designed to further explore the influence of variables, since some of the previous experiment results showed conflicting conclusions. Compared to the previous sections, larger changes of factors **D**, **H** and **F** values were applied in this round as shown in Table S6. In addition, this round contains a FFD for factors **A** and **I**, because the **A** and **I** interaction (higher temperature and longer time) is significant at improving detection, without affecting repeatability.

Fig. 4.5 and Table S7 show the analysis results based on the experiment sets of Table S6. Increased levels of factors **G** (target ATP) and **I** (reaction time) lead to increased detectability, with increased factor **I** values being significant. Increased levels of **I** and decreased levels of **A** (temperature) lead to lower repeatability. Also, the results show that factors **D** (SMLC) and **F** (pyridoxal) do not have significant influence on the sensing system.
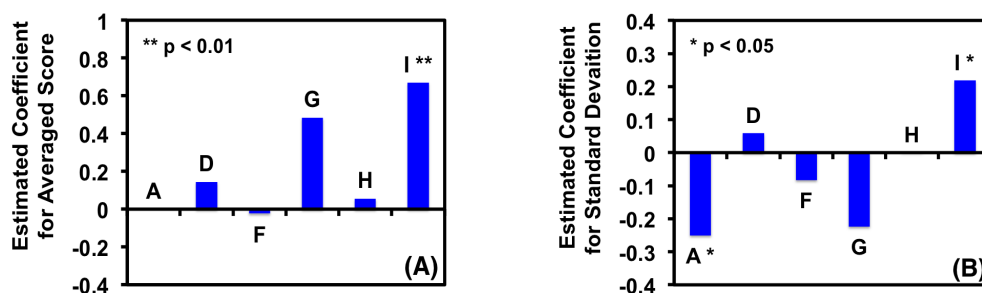
Figure 4.5 Estimated coefficient results for factors **A**, **D**, **F**, **G**, **H**, and **I**. (A) Estimated coefficients based on averaged scores; (B) Estimated coefficients based on standard deviations of scores.

4.4.3 Optimized Sensing System

From the experiments in the previous sections, we know how different factors influence the performance of this sensing system. Based on the results, this sensing system is quite robust in the studied conditions. Factor **I** (reaction time) has the most significant influence on the sensing system in the ranges investigated. Surprisingly, tap water works better than UP water as the solvent to improve detection ability. This is probably because the tap water has more volatile organic compounds than UP water does, and the increasing stimulus complexity actually decrease the odour signal threshold value, the conclusion reported by scientists.[34–36] For the other factors, their values in the studied ranges did not show significant influence on the performance of the sensing system. Thus, for these factors, the reaction conditions of the sensing system were optimized based on the principles of cost saving and preparation simplification. The optimized values of different factors are shown in Table 4.5. The quantity of expensive materials (PKase and TPase) is reduced. The sensing system was also prepared in a more practical manner, using tap water (instead of UP water)

and an easier achievable liquid: gas ratio (1:39 compared to 0.7:39.3).

Table 4.5 Values of different factors before and after optimization.

Variables	Factors	Before Optimization[15]	After Optimization
A	Temperature	23°C	23°C
B	pH	7.8	6.7
C	Apo-TPase	57 µg/mL	27.5 µg/mL
D	Conc. of SMLC	1 mM	4 mM
E	Conc. of $MgCl_2$	0.6 mM	0.1 mM
F	Conc. of Pyridoxal	0.1 mg/mL	0.05 mg/mL
G	Conc. of ATP (target)	BET of 0.32 µM	To be determined
H	PKase	71 µg/mL	25 µg/mL
I	Reaction Time	60 mins	Significant influencer, negatively correlated to detection limit
J	Liquid: Gas Ratio	0.7: 39.3	1: 39
K	Water Type	UP water	Tap water

4.4.4   BETs of the Optimized System

BET tests of the optimized sensing system were carried out to determine the efficiency of the optimized system. In total, three groups of experiments with different reaction times (factor **I**) were carried out. The reaction times were 20, 60 and 110 mins, with no longer reaction time studied since biosensors require short reaction time. In each group, the concentrations of ATP (factor **G**) were varied, with ascending concentration series started at 0.01 µM and spaced by a factor of 4 (shown in Fig. 4.6). All of the triangular forced-choice smell tests were run in random order. The results (Fig. 4.6 and Table S8) show reaction time negatively correlates to the ATP detection limit in the studied reaction time range, which is in accordance with the previous conclusion shown by Fig. 4.4 & 4.5. With a 20 mins reaction time,

smell test participants had difficulty in detecting the samples, even with the highest ATP concentration. The BET of ATP with 20 mins reaction time is 0.91 µM. With a 60 mins reaction time, BET of ATP is 0.37 µM. With reaction time increased to 110 mins, participants could detect the positive samples at even lower ATP concentrations, with BET of 0.18 µM. Compared with the previous reported system,[15] the optimized system requires less amount of expensive materials and is easier to prepare, but still resulted in a BET (0.37 µM with 60 mins reaction time) not significantly different from the previously reported BET (0.32 µM with 60 mins reaction time).
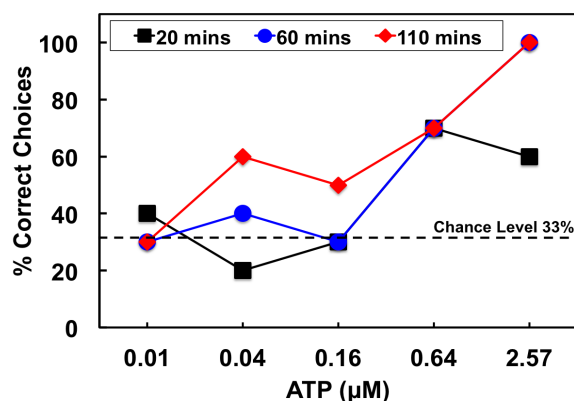
Figure 4.6 BETs with different reaction times (20, 60, 110 mins) using the optimized system. The black dashed line is the chance level for participants to get the right answer by chance, 33%.

4.5 Conclusion

Triangular forced-choice human smell test and fractional factorial designs were employed to set up a statistical method to optimize an odour-generating bio-sensing system. To our best knowledge, this is the first report on how to optimize an odour-generating bio-sensing system. Influence of 11 different variables (temperature, pH,

Apo-TPase, S-methyl-L-cysteine, $MgCl_2$, pyridoxal, ATP, PKase, reaction time, liquid: gas ratio, and water type) of the reported bienzyme sensing system were studied in this case. The required experiment sets were largely reduced (for example, 2^{11} sets were reduced to 2^5 sets in the preliminary screening test) by using fractional factorial designs. Even with multiple verifications, this pioneering optimization work encountered the fluctuations of human olfactory sensitivity, indicating it is better to involve more human related factors in the future studies. In this research, the reaction time factor, showed the most significant influence on the system: with reaction time increased, the detection ability of target, ATP, increases significantly. Tap water works better than UP water as the solvent, which shows the potential for this system to be utilized in a complex background. This system demonstrates its robustness since factors such as temperature, pH and water type did not show significant influence on the sensing efficiency. The sensing system was therefore optimized based on the principles of cost saving and preparation simplification. The detecting efficiency of the optimized system was determined by the best estimations of threshold (BETs) before and after system optimization. With detection limits of ATP almost the same, the quantity of expensive materials is reduced (30% for Apo-TPase and 50% for PKase) and the preparation processes are simplified after the optimization.

4.6   Acknowledgments

References

[1] Arugula, M. A.; Simonian, A. *Measurement Science and Technology* **2014**, *25*, 032001.

[2] Sassolas, A.; Blum, L. J.; Leca-Bouvier, B. D. *Biotechnology Advances* **2012**, *30*, 489–511.

[3] Moyo, M.; Okonkwo, J. O.; Agyei, N. M. *Sensors* **2012**, *12*, 923–953.

[4] Wang, J. *Electroanalysis* **2001**, *13*, 983.

[5] Zeng, X.; Shen, Z.; Mernaugh, R. *Analytical and bioanalytical chemistry* **2012**, *402*, 3027–3038.

[6] Song, K.-M.; Lee, S.; Ban, C. *Sensors* **2012**, *12*, 612–631.

[7] Su, L.; Jia, W.; Hou, C.; Lei, Y. *Biosensors and Bioelectronics* **2011**, *26*, 1788–1799.

[8] Campàs, M.; Carpentier, R.; Rouillon, R. *Biotechnology advances* **2008**, *26*, 370–378.

[9] Wu, Z.-S.; Chen, C.-R.; Shen, G.-L.; Yu, R.-Q. *Biomaterials* **2008**, *29*, 2689–2696.

[10] Ali, M. M.; Li, Y. *Angewandte Chemie* **2009**, *121*, 3564–3567.

[11] Bunde, R. L.; Jarvi, E. J.; Rosentreter, J. J. *Talanta* **1998**, *46*, 1223–1236.

[12] Wirix-Speetjens, R.; Reekmans, G.; De Palma, R.; Liu, C.; Laureyn, W.; Borghs, G. *Sensors and Actuators B: Chemical* **2007**, *128*, 1–4.

[13] Elsom, J.; Lethem, M. I.; Rees, G. D.; Hunter, A. C. *Biosensors and Bioelectronics* **2008**, *23*, 1259–1265.

[14] Zhang, Z.; Wang, J.; Ng, R.; Li, Y.; Wu, Z.; Leung, V.; Imbrogno, S.; Pelton, R.; Brennan, J. D.; Filipe, C. D. *Analyst* **2014**, *139*, 4775–4778.

[15] Xu, Y.; Zhang, Z.; Ali, M. M.; Sauder, J.; Deng, X.; Giang, K.; Aguirre, S. D.; Pelton, R.; Li, Y.; Filipe, C. D. *Angewandte Chemie International Edition* **2014**, *53*, 2620–2622.

[16] Mohapatra, H.; Phillips, S. T. *Angewandte Chemie* **2012**, *124*, 11307–11310.

[17] Liddell, K. *Postgraduate medical journal* **1976**, *52*, 136–138.

[18] Reed, R. R. *Neuron* **1992**, *8*, 205–209.

[19] Dunkel, A.; Steinhaus, M.; Kotthoff, M.; Nowak, B.; Krautwurst, D.; Schieberle, P.; Hofmann, T. *Angewandte Chemie International Edition* **2014**, *53*, 7124–7143.

[20] Sela, L.; Sobel, N. *Experimental brain research* **2010**, *205*, 13–29.

[21] Hoover, K. C. *American journal of physical anthropology* **2010**, *143*, 63–74.

[22] Fang, X.-L.; Han, L.-R.; Cao, X.-Q.; Zhu, M.-X.; Zhang, X.; Wang, Y.-H. *PloS one* **2012**, *7*, e38421.

[23] others,, et al. **1978**,

[24] di Salvo, M. L.; Hunt, S.; Schirch, V. *Protein expression and purification* **2004**, *36*, 300–306.

[25] Metzler, C. M.; Viswanath, R.; Metzler, D. E. *Journal of Biological Chemistry* **1991**, *266*, 9374–9381.

[26] Erez, T.; Gdalevsky, G. Y.; Hariharan, C.; Pines, D.; Pines, E.; Phillips, R. S.; Cohen-Luria, R.; Parola, A. H. *Biochimica et Biophysica Acta (BBA)-Protein Structure and Molecular Enzymology* **2002**, *1594*, 335–340.

[27] Yoshida, Y.; Sasaki, T.; Ito, S.; Tamura, H.; Kunimatsu, K.; Kato, H. *Microbiology* **2009**, *155*, 968–978.

[28] Hoch, S. O.; DeMoss, R. *Journal of bacteriology* **1973**, *114*, 341–350.

[29] Standard practice for determining odor and taste thresholds by a forced-choice ascending concentration series method of limits. 2008.

[30] Chen, D.; Dalton, P. *Chemical Senses* **2005**, *30*, 345–351.

[31] Yeshurun, Y.; Sobel, N. *Annual review of psychology* **2010**, *61*, 219–241.

[32] Seo, H.-S.; Hähner, A.; Gudziol, V.; Scheibe, M.; Hummel, T. *Experimental brain research* **2012**, *222*, 89–97.

[33] Dalton, P.; Doolittle, N.; Breslin, P. A. *Nature neuroscience* **2002**, *5*, 199–200.

[34] Guadagni, D.; Buttery, R. G.; Okano, S.; Burr, H. *Nature* **1963**, *200*, 1288–1289.

[35] Patterson, M. Q.; Stevens, J. C.; Cain, W. S.; Cometto-Muñiz, J. E. *Chemical Senses* **1993**, *18*, 723–734.

[36] Laska, M.; Hudson, R. *Chemical Senses* **1991**, *16*, 651–662.

Supplementary Information for

Application of Statistical Method for Optimization of an Odour-generating Bio-sensing System

Zhuyuan Zhang, Robin Ng, Kevin Dunn, Robert Pelton, Carlos D. M. Filipe*

Department of Chemical Engineering, McMaster University, 1280 Main Street West, Hamilton, Canada

* **E-mail:** filipec@mcmaster.ca

Kinetic modeling of the smell generating bienzymatic system

A kinetic model based on the Michaelis-Menten kinetics was created to predicate and explain the influence of different factors. There are two enzymatic reactions included in this process: generation of PLP by Pkase (Reaction 1). Based on the reaction conditions, we assume there is no product and substrate inhibition and the concentration of pyridoxal is much more than its Michaelis constant[1], the generating rate of PLP would be

$$\frac{dC_{PLP}}{dt} = \frac{K_{cat,ATP} \cdot C_{ATP}}{K_{m,ATP} + C_{ATP}} \cdot E_P$$

where E_p is the concentration of PKase. This reaction rate will depend on the concentrations of detecting target (ATP) and the enzyme (PKase).

Reaction 2 is the generation of CH_3SH by Holo-TPase. Considering the concentration of SMLC is low[2], the reaction rate would be

$$R_2 = \frac{V_{max,S} \cdot C_S}{K_{m,S} \cdot (1 + \frac{C_P}{K_{I,P}}) + C_S}$$

where C_S is the concentration of substrate (SMLC), $K_{I,P}$ is the inhibition effect of product. At the beginning of the reaction, the concentration of Holo-TPase would be in proportion to the concentration of PLP generated in reaction 1, since there is no enough PLP to transfer Apo-TPase to Holo-TPase. Meanwhile, there is no product inhibition during the initial stage of reaction. Assume the coefficient of concentration of PLP to concentration of holo-tryptophanase is K_1, the reaction rate for the initial reaction period would be:

$$\frac{dC_P}{dt} = K_1 \frac{K_{cat,S} \cdot C_S}{K_{m,S} + C_S} \int_0^t \frac{K_{cat,ATP} \cdot C_{ATP}}{K_{m,ATP} + C_{ATP}} \cdot E_P \, dt$$

After the initial time, there will be enough PLP to active all of the apo-tryptophanase to holo-tryptophanase, so the concentration of holo-tryptophanase $E_{T,H}$ will be the same as that of apo-tryptophanase $E_{T,A.}$ Also, there might be product inhibition, so the reaction rate would be:

$$\frac{dC_P}{dt} = \frac{K_{cat,S} \cdot C_S}{K_{m,S} \cdot (1 + \frac{C_P}{K_{I,P}}) + C_S} \cdot E_{T,A}$$

From these two stages reaction rate, we can see the concentration of SMLC, Apo-TPase and reaction time could influence the odour signal generating rate, which constant with the previous studies[2-4].

Table S1-1 Analysis based on averaged scores in preliminary screening test

	A	B	C	D	E	F	G	H	I	J	K
Estimated Coefficient	0.225	-0.00417	0.100	0.329	0.204	-0.0250	0.246	0.225	0.0441	0.1483	0.00247
Pr(>|t|)	0.170	0.979	0.536	0.049 *	0.211	0.877	0.135	0.170	0.7779	0.349	0.987

'***' denotes a 99.9-100% confidence interval for which we expect the variable to be related to $\bar{y}$
'**' denotes a 99-99.9% confidence interval for which we expect the variable to be related to $\bar{y}$
'*' denotes a 95-99% confidence interval for which we expect the variable to be related to $\bar{y}$
'.' denotes a 90-95% confidence interval for which we expect the variable to be related to $\bar{y}$
' ' denotes a 0-90% confidence interval for which we expect the variable to be related to $\bar{y}$

Table S1-2 Analysis based on standard deviation of scores in preliminary screening test

	A	B	C	D	E	F	G	H	I	J	K
Estimated Coefficient	0.179	0.00245	-0.132	0.301	0.196	-0.261	0.0610	0.0513	0.0512	-0.165	-0.222
Pr(>|t|)	0.151	0.984	0.287	0.0201 *	0.119	0.0415 *	0.620	0.676	0.669	0.175	0.0731 .

Table S1-3 analysis based on percentages of correct response in preliminary screening test

	A	B	C	D	E	F	G	H	I	J	K
Estimated Coefficient	0.0438	-0.0188	0.0438	0.0854	0.0229	-0.0604	0.0438	0.106	0.0540	0.0540	-0.0501
Pr(>|t|)	0.391	0.711	0.391	0.1003	0.651	0.239	0.391	0.0438 *	0.279	0.279	0.315

Table S2. Design and results for exploratory tests round 1. The experiments were carried out in random order. Values are in coded units.

A	B	C	D*	E	F*	G	H	I	J	K	Average Score	Standard Deviation	% Detected
-1	-1	-1	-1	-1	-1	-1	-1	1	1	1	4.2	2.17	60
1	1	1	1	1	1	1	1	-1	-1	-1	4.2	1.79	60
0	0	0	0	0	0	0	0	0	0	0	3	1.41	60
0	0	0	1.3	0	0	0	1	0	0	-1	3.6	1.34	40
1	0	0	1.3	0	0	0	1	-1	0	1	5.8	1.79	80
0	0	0	2.7	0	0	0	2	0	0	-1	4.2	1.10	60
1	0	0	2.7	0	0	0	2	-1	0	1	4.4	1.34	80
0	0	0	4	0	0	0	3	0	0	-1	5	2.00	100
1	0	0	4	0	0	0	3	-1	0	1	5	2.00	100
0	0	0	1.3	0	-0.9	0	1	0	0	-1	3.4	0.89	40
1	0	0	1.3	0	-0.9	0	1	-1	0	1	4.6	2.61	80
0	0	0	2.7	0	-1.8	0	2	0	0	-1	2.4	0.89	20
1	0	0	2.7	0	-1.8	0	2	-1	0	1	4	2.00	60
0	0	0	4	0	-2.7	0	3	0	0	-1	3.6	1.95	40
1	0	0	4	0	-2.7	0	3	-1	0	1	5.4	2.19	60

* Values of factor D: "1.3" represents 1.16 mM, "2.7" represents 1.79 mM, "4" represents 2.43 mM; Values of factor F: "-0.9" represents 6.5 μg/mL, "-1.8" represents 1 μg/mL (minimal value), "-2.7" represents 1 μg/mL (minimal value).

Table S3-1 Analysis based on averaged scores in exploratory test round 1

	D	F	H	K
Estimated Coefficient	0.4503	0.3536	-0.2206	0.5833
Pr(>|t|)	0.8240	0.1346	0.9327	0.0189 *

Table S3-2 Analysis based on standard deviation of scores in exploratory test round 1

	D	F	H	K
Estimated Coefficient	-0.50409	-0.06859	0.69595	0.31281
Pr(>|t|)	0.7074	0.6434	0.6881	0.0468 *

Table S4 Design and results of the experiment for exploratory tests round 2

A	B	C	D	E	F	G	H	I	J	K	Average Score	Standard Deviation	% Detected
-1	0	0	0	0	0	0	0	-1	0	-1	4.2	1.79	60
-1	0	0	0	0	0	0	0	-1	0	-1	3.6	1.34	60
1	0	0	0	0	0	0	0	-1	0	-1	3.4	1.52	40
1	0	0	0	0	0	0	0	-1	0	-1	3.2	1.1	40
-1	0	0	0	0	0	0	0	1	0	-1	3.8	1.79	80
-1	0	0	0	0	0	0	0	1	0	-1	4	2	60
1	0	0	0	0	0	0	0	1	0	-1	4.8	2.28	60
1	0	0	0	0	0	0	0	1	0	-1	5	1.41	100
-1	0	0	0	0	0	0	0	-1	0	1	2.4	0.89	0
-1	0	0	0	0	0	0	0	-1	0	1	3.8	1.1	100
1	0	0	0	0	0	0	0	-1	0	1	2.2	0.84	20
1	0	0	0	0	0	0	0	-1	0	1	2.2	1.1	20
-1	0	0	0	0	0	0	0	1	0	1	4.2	1.79	60
-1	0	0	0	0	0	0	0	1	0	1	5	2	60
1	0	0	0	0	0	0	0	1	0	1	5.8	1.1	100
1	0	0	0	0	0	0	0	1	0	1	5	2	100

Table S5-1 Analysis based on averaged score in exploratory tests round 2

	A	I	K	A:I	A:K	I:K
Estimated Coefficient	0.0375	0.7875	-0.0875	0.4125	-0.0625	0.3875
Pr(>|t|)	0.74915	6.88×10^{-5} ***	0.46138	0.00551 **	0.59599	0.00778 ***

Table S5-2 Analysis based on standard deviation of scores in exploratory tests round 2

	A	I	K	A:I	A:K	I:K
Estimated Coefficient	-0.085246	0.293952	-0.151229	-0.013216	-0.008651	0.076339
Pr(>|t|)	0.3633	0.0092 **	0.1236	0.8853	0.9247	0.4134

Table S6-1 Design and results for exploratory tests round 3 part 1 (factors D and F influence determination). Values are in coded units.

A	B	C	D	E	F*	G	H	I	J	K	Average Score	Standard Deviation	% Detected
0	0	0	0	0	0	0	0	1	0	1	2.6	0.55	40
0	0	0	-1	0	1	0	0	1	0	1	2.4	0.89	0
0	0	0	-1	0	2	0	0	1	0	1	3	0.00	40
0	0	0	-1	0	4	0	0	1	0	1	3	0.00	20
0	0	0	-1	0	8	0	0	1	0	1	2.6	0.55	60

* Values of factor F: "2" represents 0.15 mg/mL, "4" represents 0.25 µg/mL, "8" represents 0.45 µg/mL.

Table S6-2 Design and results for exploratory tests round 3 part 2 (factors D and H influence determination). Values are in coded units.

A	B	C	D*	E	F	G	H*	I	J	K	Average Score	Standard Deviation	% Detected
0	0	0	2.6	0	0	0	2	1	0	1	4.6	1.67	60
0	0	0	5.2	0	0	0	4	1	0	1	3.4	1.52	40
0	0	0	7.8	0	0	0	6	1	0	1	5	2.00	80
0	0	0	10.4	0	0	0	8	1	0	1	4.2	1.79	80

* Values of factor D: "2.6" represents 1.76 mM, "5.2" represents 3.00 mM, "7.8" represents 4.23 mM, "10.4" represents 5.47 mM; Values of factor H: "2" represents 14.98 µg/mL, "4" represents 24.93 µg/mL, "8" represents 24.88 µg/mL.

Table S6-3 Design and results for exploratory tests round 3 part 3. Values are in coded units.

A	B	C	D*	E	F	G*	H*	I	J	K	Average Score	Standard Deviation	% Detected
-1	0	0	9.25	0	0	0	7	-1	0	1	3.2	1.10	40
-1	0	0	11.7	0	0	0	7	1	0	1	5	1.41	80
-1	0	0	9.25	0	0	0	9	1	0	1	4	2.00	80
-1	0	0	11.7	0	0	0	9	-1	0	1	4.6	1.67	80
1	0	0	9.25	0	0	0	7	1	0	1	4.6	1.67	60
1	0	0	11.7	0	0	0	7	-1	0	1	3	0.00	40
1	0	0	9.25	0	0	0	9	-1	0	1	3.6	1.34	60
1	0	0	11.7	0	0	0	9	1	0	1	6.6	0.89	100
-1	0	0	9.25	0	0	-0.5	7	-1	0	1	3	1.22	40
-1	0	0	11.7	0	0	-0.5	7	1	0	1	4.2	1.79	40
-1	0	0	9.25	0	0	-0.5	9	1	0	1	4.2	1.10	100
-1	0	0	11.7	0	0	-0.5	9	-1	0	1	4.2	1.79	100
1	0	0	9.25	0	0	-0.5	7	1	0	1	6.6	0.89	100
1	0	0	11.7	0	0	-0.5	7	-1	0	1	2	1.00	0
1	0	0	9.25	0	0	-0.5	9	-1	0	1	2.6	0.55	40
1	0	0	11.7	0	0	-0.5	9	1	0	1	6.2	1.10	100
-1	0	0	9.25	0	0	-1	7	-1	0	1	4.8	2.28	60
-1	0	0	11.7	0	0	-1	7	1	0	1	4	2.00	60
-1	0	0	9.25	0	0	-1	9	1	0	1	4.4	1.95	60
-1	0	0	11.7	0	0	-1	9	-1	0	1	3.4	0.89	40
1	0	0	9.25	0	0	-1	7	1	0	1	3.4	1.52	40
1	0	0	11.7	0	0	-1	7	-1	0	1	4.2	1.79	100
1	0	0	9.25	0	0	-1	9	-1	0	1	2.2	0.45	20
1	0	0	11.7	0	0	-1	9	1	0	1	4	2.00	40

* Values of factor D: "9.25" represents 4.92 mM, "11.7" represents 6.08 mM; Values of factor G: "-0.5" represents 2.58 μg/mL; Values of factor H: "7" represents 39.85 μg/mL, "9" represents 49.8 μg/mL.

Table S7-1 Analysis based on averaged scores in exploratory tests round 3

	A	D	F	G	H	I
Estimated Coefficient	0.000	0.14473	-0.02206	0.48445	0.05617	0.66982
Pr(>|t|)	1.000	0.195597	0.874849	0.289161	0.705097	0.001311 **

Table S7-2 Analysis based on standard deviation of scores in exploratory tests round 3

	A	D	F	G	H	I
Estimated Coefficient	-0.2502245	0.0585991	-0.0827548	-0.2236631	0.0006022	0.2181084
Pr(>|t|)	0.0263 *	0.3391	0.2899	0.3740	0.9941	0.0434 *

Table S8-1 Estimated human threshold for reaction time of 20 mins

Panelist	Judgments [a]						
	Concentrations of ATP (µM)					BET	
	0.01	0.04	0.16	0.64	2.57	Value	Log_{10} of Value
1	1	0	0	1	1	0.320	-0.49
2	1	0	1	1	0	5.140	0.71
3	0	0	0	0	0	5.140	0.71
4	0	1	1	0	1	1.282	0.11
5	0	0	0	1	1	0.320	-0.49
1	1	0	0	0	1	1.282	0.11
2	1	0	0	1	0	5.140	0.71
3	0	0	0	1	0	2.570	0.41
4	0	1	1	1	1	0.020	-1.70
5	0	0	0	1	1	0.320	-0.49
Group BET = geometric mean, µM ATP						Average of log_{10} = -0.04	
						BET = $10^{-0.37}$ = 0.91	
						Log Stand. Dev. = 0.77	

[a] "0" indicates that the panelist identified the wrong sample in the set; "1" indicates the panelist selected the correct sample.

Table S8-2 Estimated human threshold for reaction time of 60 mins

Panelist	Judgments						
	Concentrations of ATP (µM)					BET	
	0.01	0.04	0.16	0.64	2.57	Value	Log_{10} of Value
1	1	0	0	1	1	0.320	-0.49
2	0	0	0	0	1	1.282	0.11
3	0	0	0	1	1	0.320	-0.49
4	1	1	1	0	1	1.282	0.11
5	1	0	0	1	1	0.320	-0.49
1	0	1	1	1	1	0.020	-1.70
2	0	0	0	1	1	0.320	-0.49
3	0	0	0	1	1	0.320	-0.49
4	0	1	1	0	1	1.282	0.11
5	0	1	0	1	1	0.320	-0.49
Group BET = geometric mean, µM ATP						Average of log_{10} = -0.43	
						BET = $10^{-0.37}$ = 0.37	
						Log Stand. Dev. = 0.53	

Table S8-3 Estimated human threshold for reaction time of 110 mins

Panelist	Judgments						
	Concentrations of ATP (µM)					BET	
	0.01	0.04	0.16	0.64	2.57	Value	Log_{10} of Value
1	0	0	0	0	1	1.282	0.11
2	1	1	0	0	1	1.282	0.11
3	1	0	1	1	1	0.080	-1.10
4	1	1	1	1	1	0.005	-2.30
5	0	1	0	1	1	0.320	-0.49
1	0	0	0	1	1	0.320	-0.49
2	0	1	1	0	1	1.282	0.11
3	0	0	1	1	1	0.08	-1.10
4	0	1	1	1	1	0.02	-1.70
5	0	1	0	1	1	0.32	-0.49
Group BET = geometric mean, µM ATP						Average of log_{10} = -0.74	
						BET = $10^{-0.74}$ = 0.18	
						Log Stand. Dev. = 0.81	

Reference

1.   di Salvo ML, Hunt S, Schirch V. Expression, purification, and kinetic constants for human and Escherichia coli pyridoxal kinases. Protein Expression Purif. 2004;36(2):300-6. doi: http://dx.doi.org/10.1016/j.pep.2004.04.021.

2.   Yoshida Y, Sasaki T, Ito S, Tamura H, Kunimatsu K, Kato H. Identification and molecular characterization of tryptophanase encoded by tnaA in Porphyromonas gingivalis. Microbiology-Sgm. 2009;155:968-78. doi: 10.1099/mic.0.024174-0. PubMed PMID: WOS:000264515100032.

3.   Hoch SO, De Moss RD. Catalytic studies on tryptophanase from bacillus-alvei. J Bacteriol. 1973;114(1):341-50. PubMed PMID: BIOSIS:PREV197356045259.

4.   Hoch JA, Simpson FJ, DeMoss RD. Purification and some properties of tryptophanase from Bacillus alvei. Biochemistry. 1966;5((7)):2229-37. doi: 10.1021/bi00871a011. PubMed PMID: BIOSIS:PREV19664700103224.

Chapter 5

Detecting and Locating Water Leaks Using Odour and Colour Signals Based on Pullulan Film

In chapter 5, all experiments were conducted by myself and Robin Ng (undergraduate student). Xudong Deng, Vincent Leung, Dr. Sana Jahanshahi-Anbuhi and Paul Wigmore assisted in the design and verification of the proposed system. Dr. Junhua Zhang, Dr. Robert Pelton, Dr. Yingfu Li, Dr. John D. Brennan, and Dr. Carlos D. M. Filipe contributed many helpful suggestions on my experiments and paper writing.

5.1 Abstract

A simple water leak detection system is presented, which releases a human detectable odour signal for remote detection and a colour signal for spatial identification of water leaks. It is fabricated using two parts: one component has 3-methyl-1-butanethiol sealed in a Smell-Tell water detector using a pullulan film to release an odour signal once the pullulan film is dissolved by leaked water, and the second uses immobilized allura red dye in a second pullulan film tag to release a colour signal when the film is dissolved by leaked water. The system is extremely simple to prepare and use, and could be exploited in resource poor settings.

5.2 Communication Submission

Many processes and applications rely heavily on the use of water or aqueous solutions. These liquids are either stored in tanks, and then transported to process stations by piping lines, or, stored in smaller containers, such as bags and bottles, which are then transported to end-users. In any of these applications, it is desirable to be aware of any leakage, not only from a material loss standpoint, but also from the standpoint of safety and environmental considerations if such aqueous solutions contain hazardous materials. Previous water detecting proposals[1–3] and commercial products[4–8] for water leakage detection on surfaces mostly use electrical reporters, which employed power supplies and different types of electrically-conductive probes, such as circuit,[4] wire,[3,5] pad,[6] etc., and usually provide audible alarms[1,3,5] and/or visual indicators.[3,6] However, these systems required materials and instruments that were either relatively expensive, complicated and bulky, or difficult to set up. To

overcome these drawbacks, here we present an alternative method by that relies on our human senses (nose and eye) for detection. It is a dual-signal reporting system for detecting (by smell) and locating (by eye) water leakage, based on dissolution of pullulan films containing both odour and colour generating reagents. The use of this reporting system requires minimal training and no power, and thus should be practical in resource-limited situations.

Odour detection is already widely used for detection of natural gas leaks, with low levels of volatile sulphides added to the gas to produce the odour. Humans are extremely sensitive to sulfide odours,[9,10] which was exploited by Mohapatra as a detection method in 2012[11] as well as utilized by our group in previous reports.[12,13] In the current work, we utilized 3-methyl-1-butanethiol (3M1B), one of the main composites of skunk spray[14] which has a low health hazard level (HMIS health hazard level of 0[15]), as the odour-reporting signal. It has a very low threshold detection limit which is at the level of parts per trillion.[16] Compared with the aforementioned sulphide gases, 3M1B has two advantages: 3M1B remains in the liquid phase under ambient conditions, so it contains higher concentrations of odourous molecules and is easier to handle; and, its odour can be removed by common oxidizing agents such as H_2O_2.[14] To seal 3M1B and release it in the presence of water, a pullulan film entrap the odour-generating compound to produce the water leak-reporting device, which we call the "Smell-Tell" water detector.

Pullulan was chosen as it is a water dissolvable and biodegradable polysaccharide,[17] that can form a gas impermeable film[18–21] and dissolve quickly in the presence of a small amount of water.[17,22] Incorporation of a coloured dye into the sensor allows for localization of the leak once an odour is detected, providing a dual-purpose

detection system.

The Smell-Tell water detector was fabricated as shown in Fig. 5.1A.
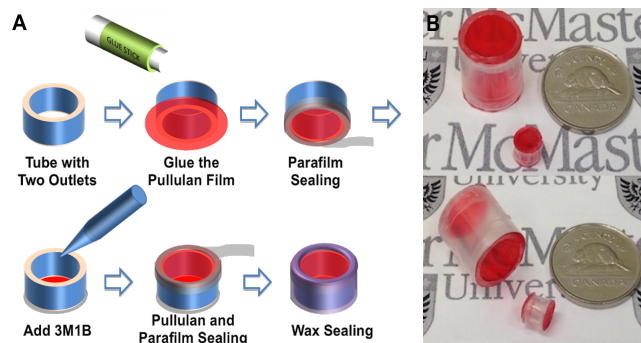
Figure 5.1 (A): Fabrication scheme of odour based water-detecting capsule. 3M1B is dropped into a plastic tube base. The plastic base is sealed with a dyed pullulan film (preparation method shown in following section) using a glue stick, Parafilm and molten wax sequentially; (B): Photos of the water-detecting capsules in two different sizes, with a 5-cent Canadian coin.

A plastic tube is used with a top and bottom outlet. A layer of glue was applied to the bottom edge of the plastic base. The pullulan film was placed on top of the glue and excess film was trimmed. The base bottom was then sealed with Parafilm. A small amount of pure or diluted 3M1B was dropped into the base on top of the pullulan film, followed by sealing the top outlet using a pullulan film and Parafilm as before. The sealed tube was then wax coated to further seal all of the gaps, without covering the pullulan film.

To access performance, ten people were asked to sniff the Smell-Tell water detector, which contained 100 μL 0.01% 3M1B (in ethanol), before and after the pullulan film was broken by adding a water drop. No detectable odour signal was obtained when the Smell-Tell water detector was sealed, and an easily detectable signal was released when the sealing film was dissolved by water, which was reported by all ten panelists.

This shows pullulan films could form an impermeable film for 3M1B that could be broken by a single drop of water (50 µL).

With a view on practical applications, the mechanical properties of pullulan films in various temperature and humidity conditions were studied, to test whether pullulan films could stay as a strong solid film under typical working conditions.

Pullulan films of 1µm60 µm thickness (thinner pullulan films such as 20 µm were difficult for the mechanical testing instrument to process the tensile test) were prepared and kept under different conditions to reach water absorption equilibrium (detailed procedure shown in Chapter 2 – 4 in ESI†). The conditions included: 23 °C, 50% relative humidity (RH); 23°C, 75% RH; 23°C, 90% RH; 4°C, $\sim$ 100% RH (a 4°C refrigerator with uncapped water inside, as an example of general operational fridges and cold-chain transportation); - 20°C; and also by rotating between these temperature and humidity conditions every 2 days. The mechanical characteristics were determined under each condition, with data shown in in Fig. 5.2 & Fig. S2. Tensile tests were performed following the previous reports,[23,24] with INSTRON using a load cell of 50 N and deformation rate of 10 mm/min. Young's modulus (E) (Fig. 5.2), tensile strength (Fig. S2A†) and elongation at break (Fig. S2B†) were tested and calculated using the INSTRON Series IX software. The results show that humidity had a more significant influence on the mechanical characteristics of pullulan films compared to temperature. This is likely due to the increased water content of pullulan films under higher humidity conditions (Fig. S2 & Fig. S3 in ESI†). Even so, pullulan film stored at 23°C, 90% RH could remain a solid film, although it had the lowest Young's modulus, tensile strength and highest value of elongation at break. Also, the pullulan film could be used even after storage conditions changed. These

results demonstrate that pullulan films, even with physical properties influenced by its water content, could function as a sealing film under various conditions.
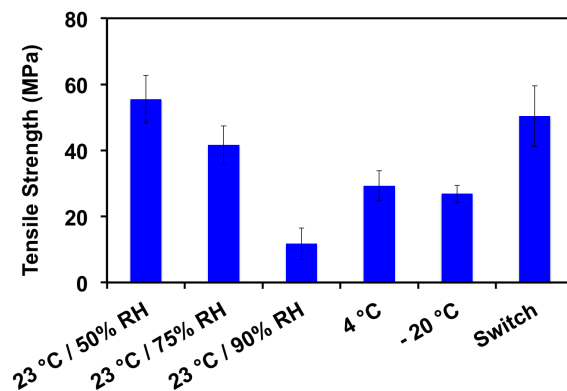
Figure 5.2 Young's modulus of pullulan films after being stored under different conditions. Storage conditions are shown below the horizontal axis, where "Switch" indicates that the temperature and humidity shifted between 4°C, ∼ 100% RH and 23°C, 50% RH by changing storage conditions every 2 days for 12 days. Samples were tested immediately after they were removed from the storage conditions. At least eight replicates were done.

Ideally, even few drops of water can be detected so that the earliest warning signal possible can be produced. Considering this, we optimized this detection system by studying the time required to dissolve pullulan film at 23°C, 50% RH. Results show that pullulan films with a thicknesses of 20 µm worked the best. Films thinner than 20 µm, such as 10 µm, are brittle, hard to cast and handle. The films thicker than 20 µm, such as 40 µm, need a longer time to be dissolved (for example, more than 15 mins, more details shown in chapter 5 in ESI†).The dissolving of pullulan films under other conditions was also studied and the results (Fig. S5†) show the same conclusion. Different amounts of water were tested to find out the minimum amount of water required to dissolve the pullulan films. 25 µL, 50 µL and 100 µL of water were dropped onto 20 µm pullulan film under different conditions. The results show

that 50 µL and 100 µL of water could dissolve the film in 10 mins or less (Table 5.1), while 25 µL of water could not dissolve the film.

Table 5.1 Time required to break up pullulan films under different conditions.

water (µL)	Time required for breaking up (min)			
	23°C, 50% RH	23°C, 75% RH	23°C, 90% RH	4°C, ~ 100% RH
50	6.6 ± 3.9	2.2 ± 1.2	1.9 ± 1.0	9.3 ± 7.0
100	1.7 ± 0.9	0.7 ± 0.5	0.7 ± 0.5	4.8 ± 1.7

50 µL of water was used to examine sensor performance in a human panel test. Following a standard triangular forced-choice test design used in human olfactory tests,[25] we determined the efficacy of the Smell-Tell detector. As shown in Scheme S1†, Three Smell-Tell detectors, containing 100 µL 0.01% 3M1B and sealed by pullulan film with a thickness of 20 µm, were each placed in a styrofoam box with a size of 15 cm × 25 cm × 27 cm for one testing sample set. 50 µL of water was pipetted onto one of the three Smell-Tell detectors to make the positive sample, while the other two were left as blanks. For each sample, a piece of cardboard was used to cover the Smell-Tell detector to block it from human sight before the box was closed. The Smell-Tell detectors remained undisturbed for 20 mins to allow for the dissolution of pullulan film and odour diffusion. Ten participants were then asked to identify the box with the positive sample by opening the lid and sniffing the box. All of the participants were able to identify the box with the positive sample and no detectable leakages were detected from the blanks.

A special advantage for using odour as a reporting signal is that it could easily diffuse to a the remote detecting position. To determine how effective 3M1B could

work as a reporting signal for remote detection, a simulation model was built to predict the diffusion of 3M1B in rooms without significant advective transport. Based on the method illustrated by Geankoplis,[26] the emission rate of 3M1B through the Smell-Tell water detector into the container (Scheme S2†) can be expressed as:

$$q = \frac{DPA}{RTz} ln \frac{P - p_2}{P - p_1} \tag{5.1}$$

where D = diffusivity of odour signal vapour at steady state

in the Smell-Tell detector (m^2/s)

P = total pressure of air (Pa)

A = the emission area through the dissolved hole (m^2)

p_1 = vapour pressure of odour signal at the outlet of

the Smell-Tell detector (Pa)

p_2 = vapour pressure of odour signal at the liquid and

vapour interface in the Smell-Tell detector (Pa)

z = path length of odour signal diffusion from the

phase interface to the outlet (m)

To account for the diffusion of molecules in a rectangular room, Drivas et al.[27] developed a solution for Fick's second law of diffusion to incorporate the three-dimensional boundary effect, which is caused by the reflection of diffused chemical molecules at six wall surfaces. Drivas's solution includes both dispersion process of

the source and general concentration decay process due to room ventilation and surface deposition. He also proved the model is valid even without taking into account of the diffusion decay process in a room, which has no significant advective transport, by comparing experimental measurements with model predictions. Cheng et al.[28] recently modified Drivas's solution to determine the concentration as a function of position and time for a continuous point releasing source, by integrating Drivas's solution over time:

$$c(x, y, z, t) = \int_0^t \frac{q}{(4\pi Kt)^{3/2}} R_x R_y R_z dt \tag{5.2}$$

where $c(x, y, z, t) =$ odour signal concentration at position x,

y, z and time $\boldsymbol{t}$ (mol/m^3)

$q =$ odour signal emission rate from the

Smell-Tell water detector (mol/s)

$K =$ odour signal diffusion coefficient in

the container (m^2/s)

The R_x, R_y and R_z terms in Eq. 5.2 are wall reflection terms and reported by Drivas,[27] which involves reflection by a set of infinite image sources (expansions shown in Chapter 9, ESI†).

Since a quick response is important for a sensing system, we are interested in a relatively short diffusion duration and just add the closest image source for each wall

(to account for the reflection of 3M1B from the wall surfaces), which was stated and proven by Cheng.[28] Take into account the time required for pullulan film to break up, derived from Eq. 5.1 and Eq. 5.2, the evaporation and diffusion process can be simulated and predicted using Eq. 5.3 (expansion shown in Chapter 10, ESI†):

$$c(x,y,z,t) = \int_{t_0}^{t} \sum_{j=0}^{6} \exp(\frac{-[(x-x_j)^2 + (y-y_j)^2 + (z-z_j)^2]}{4\pi K(t-t_0)})$$
$$ln\frac{P-p_2}{P-p_1} \frac{DPA}{RTz\left[4\pi K(t-t_0)\right]^{3/2}} dt \tag{5.3}$$

where t_0 = time required to break up pullulan film *(s)*

Assuming the released 3M1B is well mixed in the closed room after long time, according to mass balance, the final concentration of 3M1B in the room (in terms of N-fold $C_{Threshold}$) follows the relation of

$$\frac{V_{3M1B}}{V_{Room}} = \frac{NC_{Threshold}}{C_{3M1B}} \tag{5.4}$$

where V_{3M1B} and C_{3M1B} are the volume and concentration of 3M1B in resource, respectively, while V_{Room} is the volume of room, and $C_{Threshold}$ is the human detection threshold concentration. According to the previous study,[16] the least sensitive human participant could only smell 3M1B when its concentration reached to 10-fold (N = 10) of the mean threshold value. We calculated five values of V_{3M1B}/V_{Room} when N = 1, 3, 10, 33 and 100, ±1 order of the 10-fold threshold value (Fig. 5.3A). The results show, even when the concentration reaches to 100 fold of the threshold concentration, V_{3M1B}/V_{Room} is an extremely small number, 7×10^{-17}.
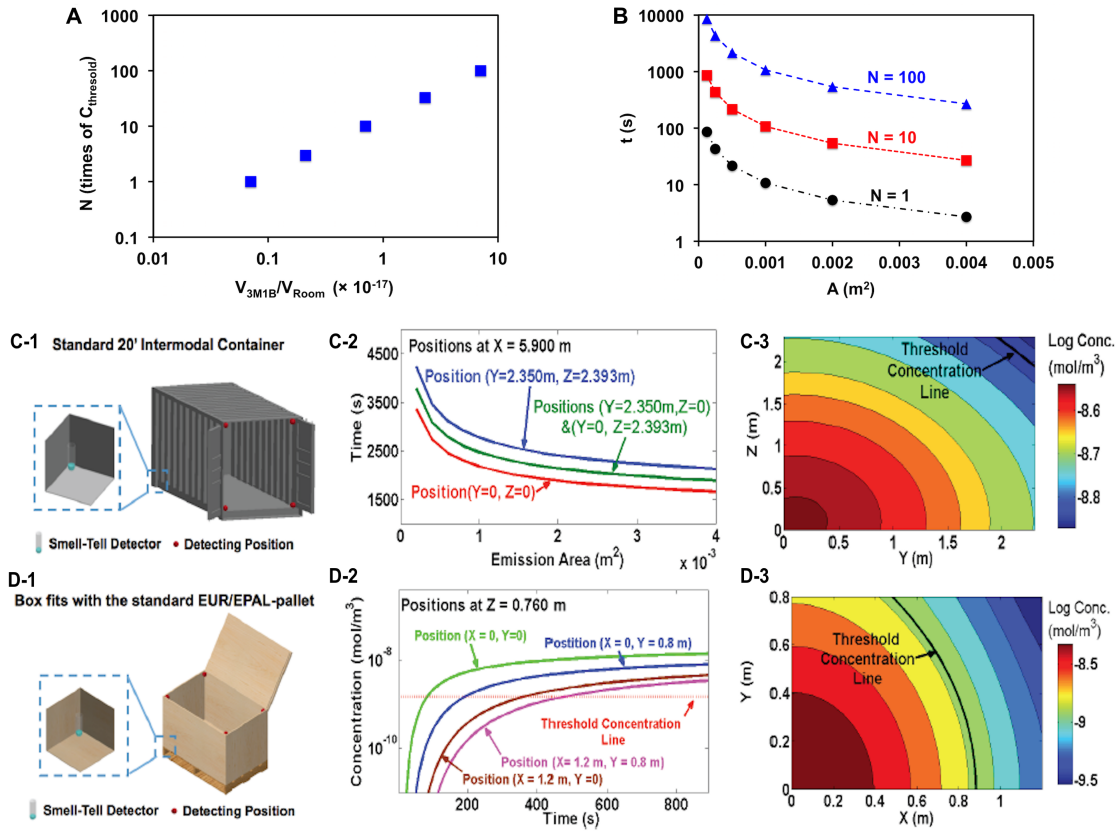
Figure 5.3 Odour signal diffusion in estimated conditions. (A) Relationship between N and V_{3M1B}/V_{Room} when N = 1, 3, 10, 33 and 100. (B) Relationship between emission area, $\boldsymbol{A}$ and the required time, $\boldsymbol{t}$ to reach certain concentration a standard 20' intermodal container. (C) & (D) Diffusion in a standard 20' intermodal container (C) and a box fits with fits with the standard EUR/EPAL-pallet (D). The source position (x_0 = 0 m, y_0 = 0 m, z_0 = 0 m) is determined from where the Smell-Tell water detector sits. (C-1) Scheme of the case of standard 20' intermodal container (length L: X = 5.900 m; width W: Y = 2.350 m; height H: Z = 2.393 m) for Fig. 5.3C-2 and Fig. 5.3C-3. Assuming pure 3M1B is sealed in a Smell-Tell water detector with z = 0.1 m. (C-2) Time required for concentrations at the four corners on the door plane (X = 5.900 m) to reach threshold concentration as a function of emission area, A. (C-3) Concentrations of the positions on the door plane (Y-Z plane at X = 5.900 m) at 5.5 h with $\boldsymbol{A} = 4 \times 10^{-4} m^2$. (D-1) Scheme of the case of a box fits with the standard EUR/EPAL-pallet (length L: X = 1.200 m; width W: Y = 0.800 m; height H: Z = 0.760 m) for Fig. 5.3D-2 and Fig. 5.3D-3. 2% 3M1B is assumed to be sealed in a Smell-Tell water detector with z = 0.02 m. (D-2) Concentrations at the four corners at the lid plane (Z = 0.760 m) as a function of time, with $\boldsymbol{A}$ assumed to be $2 \times 10^{-4} \ m^2$. (D-3) Concentrations of the positions on the lid plane (X-Y plane at Z = 0.760 m) at 4 mins.

140

Meanwhile, the relationship between dissolved area of the pulluan film (emission area, $\boldsymbol{A}$) and the required time ($\boldsymbol{t}$) to reach certain concentration in the room is studied. Assuming the room is well ventilated and the released 3M1B immediately realizes fully diffusion, the relationship between $\boldsymbol{A}$ and $\boldsymbol{t}$ is shown in Eq. 5.5:

$$q \cdot t = \frac{DPA}{RTz} ln \frac{P - p_2}{P - p_1} \cdot t = V_{Room} \cdot N \cdot C_{Threshold} \tag{5.5}$$

Fig. 5.3B illustrated the relationship between $\boldsymbol{A}$ and $\boldsymbol{t}$ in a standard twenty-foot intermodal container ($V_{Room} = 33.2$ m^3), D = 0.09 cm^2/s (calculation shown in ESI), with N = 1, 10 and 100, assuming P = 1 bar, z = 0.1 m, T = 311 K, p_1 = 133 pa, $p_2 \approx 0$.

Two cases were studied to show the possibility of the Smell-Tell water detector working in practical conditions. The containers in the two cases are assumed to be isothermal and without mechanical ventilation, where advective transport is negligible. 3M1B deposition onto the surface of the containers is also assumed to be negligible. The first case is in a standard twenty-foot intermodal container (Fig. 5.3C-1), For diffusion in the freight container with passive vents during transport, the diffusion coefficient is estimated as K = 0.001 m^2/s, by comparing the reported air change rate in this type of container.[29] Extreme situations are studied, in which the Smell-Tell water detector sits at one of the far corners and the odour signal would be detected at the four corners of the door wall. In these extreme situations, the odour signal has to go through the longest path (diagonals) to reach the detection positions. The diffusion process of 3M1B from the Smell-Tell water detector into the container was simulated by MATLAB. Even using the extreme situation variables, diffused 3M1B at

the four corners on the door plane can reach human detection threshold concentration in hours (Fig. 5.3C-2, with details shown in Chapter 11, ESI†). As emission area (A) increases, the required time for diffused 3M1B to reach threshold concentration could decrease. The threshold concentration is also reached more quickly at positions closer to the source. The concentrations of positions on the door wall at 5.5 h after pullulan film broken by water, are shown in Fig. 5.3C-3 with $A = 4 \times 10^{-4}\ m^2$.

Another practical case is about a box, which fits with the standard EUR/EPAL-pallet (Fig. 5.3D-1). After simulation (Chapter 12, ESI†), Fig. 5.3D-2 shows that the concentrations depend on the detecting positions and released time. For positions closer to the source, the threshold concentration can be reached much faster. The odour concentrations right below the lid surface, 4 mins after odour signal released, are shown in Fig. 5.3D-3. From the predicted results, the concentration in the box can easily reach the threshold concentration in minutes, even for the farthest corner from the source and using a diluted signal source. This is because of the short distance between the detection position with the source, due to the small size of the box.

Odour signal can show whether the liquid has leaked, but it is not effective for determining the site of leakage. A complimentary part of the reporting system, combined with the odour signal generation was fabricated based on a colour signal generation. To release colour signal when the pullulan film is dissolved by water, a dye was immobilized into the films. 1 g/L allure red dye was dissolved into 25 mg/mL pullulan solution and cast to form a coloured pullulan film, which then used to prepare the water detector. In order to show a positive signal when water appears, the detector was attached onto a filter paper sheet (Whatman #1), on which a wax barrier could be printed (Fig. 5.4A).
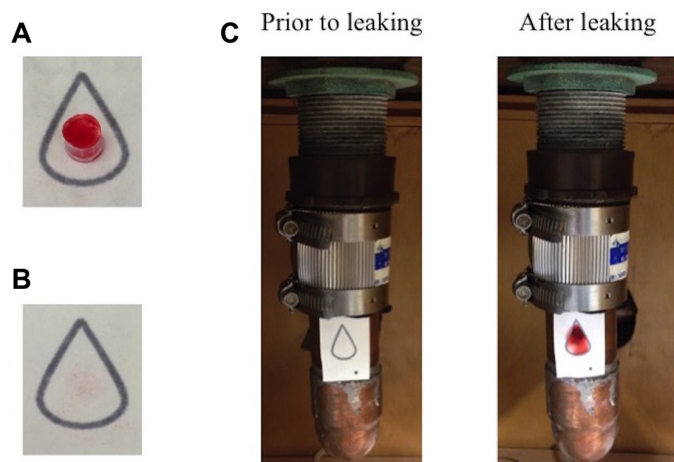
Figure 5.4 Demonstration of colour signal generation for water leakage detection. (A) Reporter consists of a water leakage detector and filter paper with wax barrier printed on. (B) Front side of the reporter. (C) An example showing how colour reporter works. 50 µL water was dropped onto the reporter, which was attached to the pipeline under a sink.

The front side of the reporter only contains the penetrated wax barrier (Fig. 5.4B). In the presence of water, it will dissolve the film and the colour signal will be transferred onto the filter paper with the water flow and show up in the wax barrier pattern (Fig. 5.4C). A demonstration is shown in Fig. 5.4C, with 50 µL water used.

Conclusions

In summary, we have developed an extremely simple and low cost water leakage detection system by generating an odour signal that is detectable by the human nose. To the best of our knowledge, this is the first report of an odour generating water leakage detection system. This detector could report the occurrence of water with a volume as little as 50 µL by releasing a strong, human-detectable odour signal. Results show the pullulan film could be used in various conditions. The simulation model shows

that the smell signal could reach to the remote detection positions and be detected by human noses, even in a large room such as a standard 20' intermodal container. This detector also provides a complementary colour signal to the smell signal, helping the locating of the leaking sites. This water leakage detection system may be used in detecting water and water-related liquid leakages under hidden, visually obstructed locations such as, water leaking from conduit pipes below kitchen sinks, blood leakage in chilled meat transportation, etc. The detection system could be easily prepared in different shapes and is easy to implement by an appliance installer or a homeowner.

Acknowledgements

References

[1] Krebs, R. G. US5188143 A. 1993.

[2] Tacilauskas, A. V. Fluid detection apparatus and kit, and method of installation thereof. 2006; US Patent 7,084,776.

[3] Hill, C. D. Moisture sensing strips. 2011; US Patent 7,956,760.

[4] DORLEN PRODUCTS INC. http://www.wateralert.com, Accessed: 2014-10-30.

[5] THE HOME DEPOT. http://www.homedepot.com, Accessed: 2014-10-30.

[6] ARJAY ENGINEERING. http://www.arjayeng.com, Accessed: 2014-10-30.

[7] GIZMODE INNOVATIONS. http://www.thewateralarm.com, Accessed: 2014-10-30.

[8] AQUILAR LEAK DETECTION SOLUTIONS. http://aquilar.co.uk, Accessed: 2014-10-30.

[9] Yeshurun, Y.; Sobel, N. *Annual Review of Psychology*; Annual Review of Psychology; Annual Reviews: Palo Alto, 2010; Vol. 61; pp 219–241, ISI Document Delivery No.: 547KE Times Cited: 12 Cited Reference Count: 218 Yeshurun, Yaara Sobel, Noam Review; Book Chapter 4139 el camino way, po box 10139, palo alto, ca 94303-0139 usa.

[10] Sela, L.; Sobel, N. *Experimental Brain Research* **2010**, *205*, 13–29, Times Cited: 8.

[11] Mohapatra, H.; Phillips, S. T. *Angew. Chem. Int. Ed.* **2012**, *51*, 11145–11148.

[12] Zhang, Z.; Wang, J.; Ng, R.; Li, Y.; Wu, Z.; Leung, V.; Imbrogno, S.; Pelton, R.; Brennan, J. D.; Filipe, C. D. M. *Analyst* **2014**, *139*, 4775–4778.

[13] Xu, Y.; Zhang, Z.; Ali, M. M.; Sauder, J.; Deng, X.; Giang, K.; Aguirre, S. D.; Pelton, R.; Li, Y.; Filipe, C. D. M. *Angew. Chem. Int. Ed.* **2014**, *53*, 2620–2622.

[14] Wood, W. *Journal of Chemical Ecology* **1990**, *16*, 2057–2065.

[15] Sigmaaldrich, MSDS of 3-methyl-1-butanethiol. 2014.

[16] Sarrafchi, A.; Odhammer, A. M. E.; Hernandez Salazar, L. T.; Laska, M. *PLoS ONE* **2013**, *8*, e80621, with human ethics statement 3-methyl-1-butanethiol human detection threshold.

[17] Rajewski, R. A.; Rajewski, L. G.; Haslam, J. L. US Patent 20,130,005,831. 2013.

[18] Prajapati, V. D.; Jani, G. K.; Khanda, S. M. *Carbohydr. Polym.* **2013**, *95*, 540–549, 145PQ Times Cited:0 Cited References Count:73.

[19] Cheng, K. C.; Demirci, A.; Catchmark, J. M. *Applied Microbiology and Biotechnology* **2011**, *92*, 29–44, 819JM Times Cited:11 Cited References Count:161.

[20] Kristo, E.; Biliaderis, C. G. *Carbohydr. Polym.* **2007**, *68*, 146–158, 144UJ Times Cited:71 Cited References Count:59.

[21] Farris, S.; Introzzi, L.; Fuentes-Alventosa, J. M.; Santo, N.; Rocca, R.; Piergiovanni, L. *Journal of Agricultural and Food Chemistry* **2012**, *60*, 782–790, 880KC Times Cited:4 Cited References Count:37.

[22] Jahanshahi-Anbuhi, S.; Pennings, K.; Leung, V.; Liu, M.; Carrasquilla, C.; Kannan, B.; Li, Y.; Pelton, R.; Brennan, J. D.; Filipe, C. D. M. *Angew. Chem. Int. Ed.* **2014**, 6155–6158.

[23] Trovatti, E.; Fernandes, S. C. M.; Rubatat, L.; Freire, C. S. R.; Silvestre, A. J. D.; Neto, C. P. *Cellulose* **2012**, *19*, 729–737, 934QF Times Cited:4 Cited References Count:25.

[24] Tang, X.; Alavi, S.; Herald, T. J. *Carbohydr. Polym.* **2008**, *74*, 552–558.

[25] ASTM, *Standard practice for determining odor and taste thresholds by a forced-choice ascending concentration series method of limits, E-679-04*; ASTM International: Conshocken, 2008; Vol. 15.08.

[26] Geankoplis, C. *Transport processes and separation process principles*; Prentice Hall Press, 2003; pp 417 – 420.

[27] Drivas, P. J.; Valberg, P. A.; Murphy, B. L.; Wilson, R. *Indoor Air* **1996**, *6*, 271–277.

[28] Cheng, K.-C.; Acevedo-Bolton, V.; Jiang, R.-T.; Klepeis, N. E.; Ott, W. R.; Fringer, O. B.; Hildemann, L. M. *Environ. Sci. Technol.* **2011**, *45*, 4016–4022.

[29] Goedecke, T. Temperature and Air Change Rates in Freight Containers During Transport Between Eupore and Destinations in Asia and Australia. 2008.

Electronic Supplementary Information for

Detecting and Locating Water Leaks Using Odour and Colour Signals Based on Pullulan Film

Zhuyuan Zhang,[a] **Robin Ng,**[a] **Xudong Deng,**[a] **Vincent Leung,**[a] **Sana Jahanshahi-Anbuhi,**[a] **Paul Wigmore,**[a] **Junhua Zhang,**[d] **Robert Pelton,**[a] **Yingfu Li,**[b] **John D. Brennan,**[c] **and Carlos D. M. Filipe**[*a]

* Corresponding author

[a] Department of Chemical Engineering, McMaster University, 1280 Main Street West, Hamilton, ON, Canada. Fax: +1 905 521-1350; Tel: +1 905 525-9140; E-mail: filipec@mcmaster.ca

[b] Department of Biochemistry and Biomedical Sciences, McMaster University, 1280 Main Street West, Hamilton, ON, Canada.

[c] Biointerfaces Institute & Department of Chemistry and Chemical Biology, McMaster University, 1280 Main Street West, Hamilton, ON, Canada.

[d] Air Quality Research Division, Environment Canada, 4905 Dufferin Street, Toronto, ON, Canada.

Contents

2

1 Materials and apparatus

Pullulan from *Escherichia coli* was purchased from Polysciences (CAT 21115). 3-methyl-1-butanethiol and allura red dye was purchased from Sigma Aldrich (Oakville, Ontario). Parafilm and Petri dishes were obtained from a local chemical supplies store. INSTRON machine was with Model 4400 Universal Testing system and Model 4411 Load Frame. Digital Micrometer was from Testing Machines Inc. The temperature and humidity chamber was from ESPEC (Model: ESL-2CA).

2 General procedure to prepare pullulan films

Pullulan powder was dissolved in deionized water at different concentrations (200, 100, 50, and 25 mg/mL) to make films of different thicknesses (160, 80, 40, and 20 μm, respectively). Films were made by casting 2 mL of pullulan solution in small Petri dishes (3.6 cm in diameter) and let to air dry. Once dried, films were removed and cut into appropriate sizes. In some cases, 0.5 g/L of allura red dye was added to the pullulan solution for visualization. Thickness of casted films was measured at five different points with a digital micrometer and an average value was obtained. The thickness of casted film was normalized to the designed one if they are different in the studies.
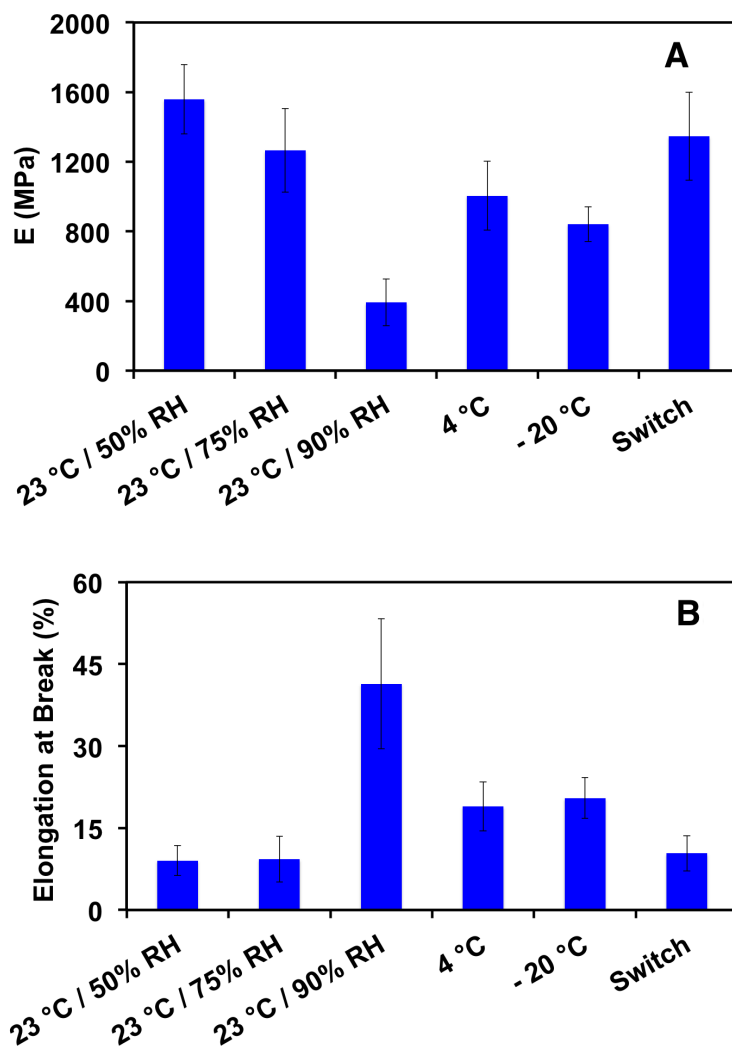
3   Tensile test results

Figure S1. Tensile tests of pullulan film after being stored under different conditions. Maximum tensile strength (A) and elongation at break (B) were tested and calculated using INSTRON. Storage conditions are shown below the horizontal axis, where "Switch" indicates that the temperate and humidity shifted by changing storage conditions every 2 days for 12 days. Samples were tested immediately after they were removed from the storage conditions. At least eight replicates were done.

4   Determination of the water absorption of pullulan films

To determine properties of pullulan films for water detection in various conditions, water absorption was investigated first by studying the time required for pullulan film to reach moisture content equilibrium under different conditions. Films with thicknesses of 20, 40, 80 and 160 μm were cast. The moisture content of samples was determined by drying the films at 110°C for 2 h and derived from the weight change. The water content for the films stored at 23°C, 50% relative humidity (RH) was determined to be 14.5 g water per 100 g dry matter. Films stored under 23°C, 50% RH for at least 72 hours were then placed in ESPCO chamber under the conditions of 23°C, 75% RH; 23°C, 90% RH and in a fridge at 4°C, $\sim$ 100% RH. After storage under required conditions, the films were taken out to measure water absorption by determining the weight change. The water absorption curve is shown in Fig. S2 and Fig. S3.
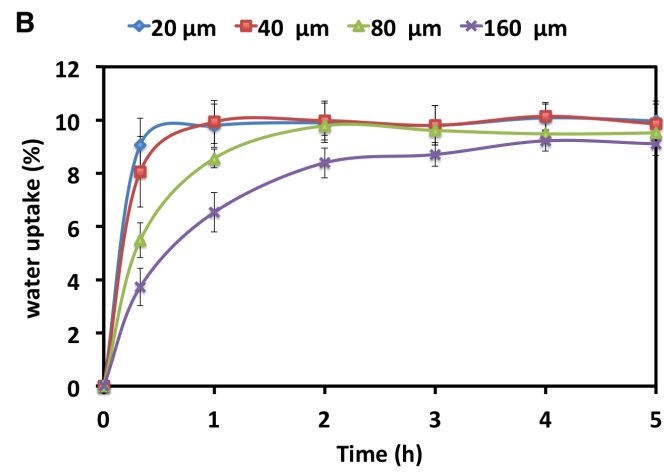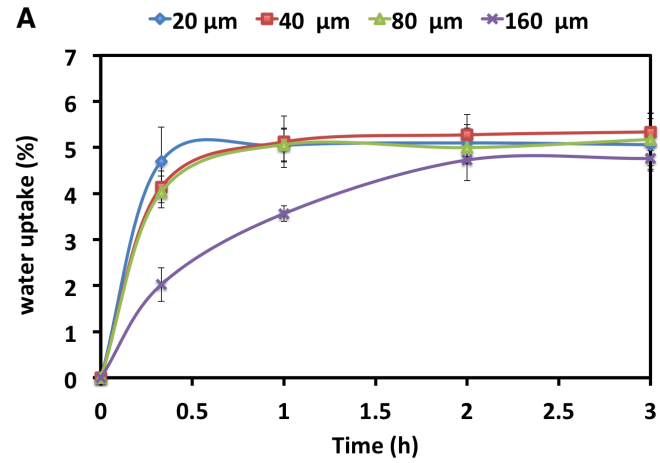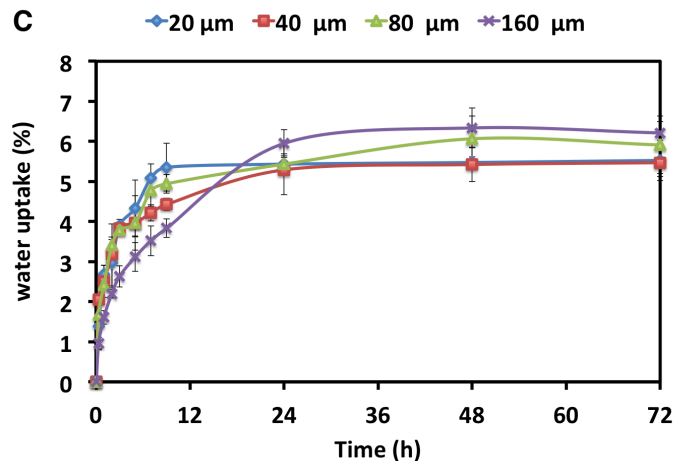
Figure S2. Water absorption of pullulan films under different conditions. (A) 23°C, 75 % RH; (B) 23°C, 90% RH; (C) 4°C, $\sim$ 100% RH. The initial point is based on the weight of films stored at 23°C 50% RH for 72h. Measurements represent an average of three samples.
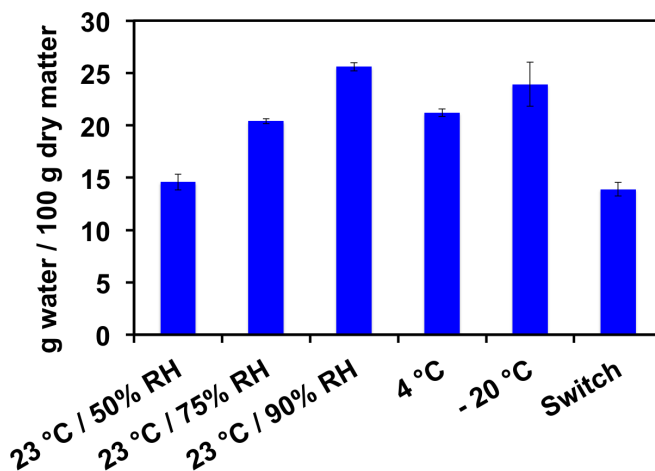

Figure S3. Water contents of pullulan films after stored under different conditions. Storage conditions are shown below the horizontal axis, where "Switch" indicates that the temperate and humidity shifted by changing storage conditions every 2 days for 12 days. At least eight replicates were done.

Required storage time to reach moisture content equilibrium under different conditions

The pullulan films were stored at 23°C, 50% RH for 72 h before transferred into different conditions. From Fig. S2, the least storage time to reach moisture content equilibrium for films under different conditions were, 23°C, 75% RH : 2 h; 23°C, 90% RH : 4 h; 4°C, $\sim$ 100% RH : 24 h. For the samples stored under -20°C, the time was designed to be 72 h.

5   Determination of time required for pullulan films to break up by water dissolving

Films of variable thicknesses were taped onto a 48-well plate (Fig. S4) and placed under different storage conditions. 50 μL or 100 μL water were pipetted onto the films. The films were then monitored to determine the time taken for the water droplet to dissolve them.
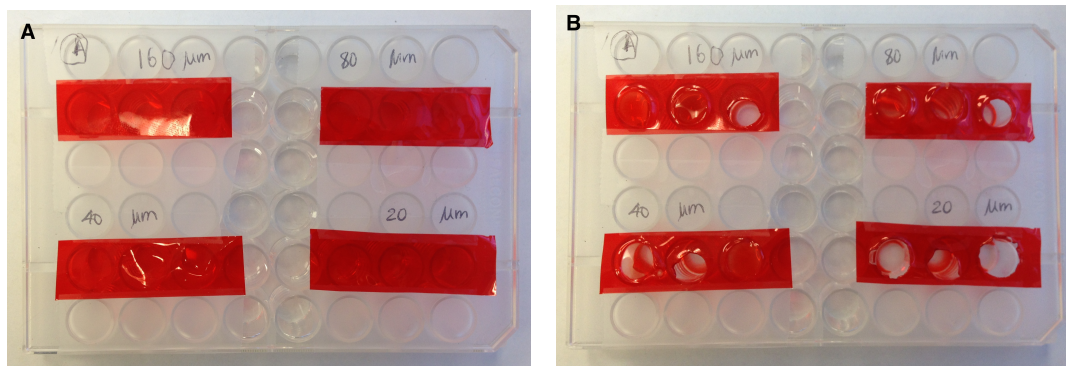

Figure S4. Photos of pullulan films taped onto 48-well plate. The films in photo A are before adding water, while films in photo B are after dropped 50 μL water for 30 mins. In this set of experiments, films with 4 different thicknesses (20, 40, 80 and 160 μm as marked) were attached to the plate, and each of them covered three wells to work as three replicates.

6   The dissolve of pullulan films

| Water (µL)	Conditions	Thicknesses of pullulan film (µm)				Break up ratio	
		160	80	40	20	< 20%	☐
50	23 ºC 50% RH					30% - 40%	☐
	23 ºC 75% RH					50% - 60%	☐
	23 ºC 90% RH					70% - 80%	☐
	4 ºC					90% -100%	■
100	23 ºC 50% RH						
	23 ºC 75% RH						
	23 ºC 90% RH						
	4 ºC						

Figure S5. The dissolve of pullulan films with different thicknesses under different conditions in 30 mins. Ten replicates for each situation were studied. Break up ratio means how much percentage of samples had water that dissolved through the pullulan film.

7 Human smell test
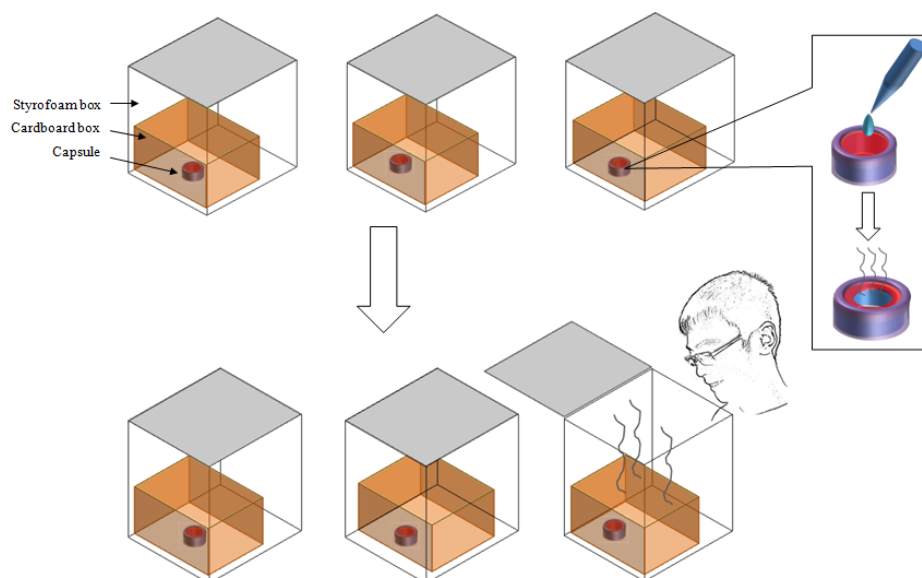
Scheme S1. The design of triangular forced choice test. In one set of testing samples, three detectors were put in styrofoam boxes and covered by a small cardboard box (with holes on its top and sides). 50 μL of water was dropped onto one of the three detectors to make one positive sample while the other two detectors were blanks. The styrofoam boxes were closed and left undisturbed for 20 minutes. Panelists were asked to identify the positive sample by sniffing the three boxes.

8 Scheme for diffusion from the Smell-Tell water detector to the container
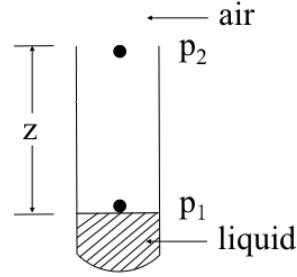
Scheme S2. The diffusion from the Smell-Tell water detector to the container.

9 Equation Expansion for Eq. 2

$$R_x = \sum_{i=-\infty}^{\infty} \left[e^{-\frac{(x+2iL-x_0)^2}{4Kt}} + e^{-\frac{(x+2iL+x_0)^2}{4Kt}} \right]$$

$$R_y = \sum_{i=-\infty}^{\infty} \left[e^{-\frac{(y+2iW-y_0)^2}{4Kt}} + e^{-\frac{(y+2iW+y_0)^2}{4Kt}} \right]$$

$$R_z = \sum_{i=-\infty}^{\infty} \left[e^{-\frac{(z+2iH-z_0)^2}{4Kt}} + e^{-\frac{(z+2iH+z_0)^2}{4Kt}} \right]$$

10 Equation Expansion for Eq. 3

$$\sum_{j=0}^{6} \exp\left(\frac{-\left[(x-x_j)^2 + (y-y_j)^2 + (z-z_j)^2\right]}{4\pi K(t-t_0)}\right)(\text{assume } t_0 = 0)$$

$$= \exp\left(\frac{-\left[(x-x_0)^2 + (y-y_0)^2 + (z-z_0)^2\right]}{4Kt}\right)$$

$$+ \exp\left(\frac{-\left[(x-(2L-x_0))^2 + (y-y_0)^2 + (z-z_0)^2\right]}{4Kt}\right)$$

$$+ \exp\left(\frac{-\left[(x-(-x_0))^2 + (y-y_0)^2 + (z-z_0)^2\right]}{4Kt}\right)$$

$$+ \exp\left(\frac{-\left[(x-x_0)^2 + (y-(2W-y_0))^2 + (z-z_0)^2\right]}{4Kt}\right)$$

$$+ \exp\left(\frac{-\left[(x-x_0)^2 + (y-(-y_0))^2 + (z-z_0)^2\right]}{4Kt}\right)$$

$$+ \exp\left(\frac{-\left[(x-x_0)^2 + (y-y_0)^2 + (z-(2H-z_0))^2\right]}{4Kt}\right)$$

$$+ \exp\left(\frac{-\left[(x-x_0)^2 + (y-y_0)^2 + (z-(-z_0))^2\right]}{4Kt}\right)$$

11 Simulation for Case 1: diffusion in a standard 20' intermodal container

Calculation example of diffusion coefficient D

D can either be found from the experimental data or estimated following the reported method, which was stated by Fuller et al. [1] and recommended by Smith [2]. A calculation example is shown below:

$$D_{AB} = \frac{0.00143T^{1.75}}{PM_{AB}^{1/2}\left[\left(\sum_A v_i\right)^{1/3} + \left(\sum_B v_i\right)^{1/3}\right]^2} \tag{1}$$

where $M_{AB} = 2\left[(1/M_A) + (1/M_B)\right]^{-1}$, M_i = the molecular weight of chemical i

$\qquad P = \text{pressure}(bar)$

$\qquad T = \text{temperature}(K)$

$\qquad D_{AB} = \text{resulting diffusion coefficient}(cm^2/s)$

Take A : 3-methyl-1-butanethiol; B: air. From the reported atomic diffusion volumes data [1]: $\sum_A = 130.12; \sum_B = 19.70$, under the condition of T= 311 K, P = 1 bar, substitute these values into Eq. 1:

$$M_{AB} = 2\left[(1/M_A) + (1/M_B)\right]^{-1} = 2\left[(1/130.12) + (1/19.70)\right]^{-1} = 34.3 \; g/mol$$

$$
\begin{aligned}
D_{AB} &= \frac{0.00143 T^{1.75}}{P M_{AB}^{1/2} \left[(\sum_A v_i)^{1/3} + (\sum_B v_i)^{1/3}\right]^2} \\
&= \frac{0.00143 * 311^{1.75}}{1 * 34.3^{1/2} \left[(130.12)^{1/3} + (19.70)^{1/3}\right]^2} \\
&= 0.09 \; cm^2/s
\end{aligned}
$$

Diffusion in a standard 20' intermodal container

Assume pure 3-methyl-1-butanethiol is sealed in a capsule with evaporation path length of 0.1 m, which sits in a standard shipping container with length L: X = 5.900 m, width W: Y = 2.350 m, height H: Z = 2.393 m and temperature 311 K. The hole on the capsule dissolved by water ($\boldsymbol{A}$) has a size of $4 \times 10^{-4} \; m^2$, diffusion coefficient of 3-methyl-1-butanethiol in the capsule (D) is about 0.09 cm^2/s with estimation details shown above. For diffusion in the freight container with passive vents during transport, diffusion coefficient in the container is assumed to be K = 0.001 m^2/s, estimated by comparing the reported air change rate in this type of container [3] with similar well studied indoor gas molecular diffusion situations [4] [5] . Because the capsule is a thin tube, in this case, air exchange in the intermodal container (K = $0.001 m^2/s$) will not influence the diffusion in the tube, which means $K \gg D$, and $p_2 \ll p_1$. The saturated

3-methyl-1-butanethiol vapour pressure at 311 K is 133 Pa [6]. The diffusion rate of odour signal from capsule into the container is q = 1.9×10^{-9}mol/s, which can be easily calculated by substituting the aforementioned values to Eq. 3 (assume the change of z is negligible).

Extreme situations are studied here, in which the capsule sits at one of the far corners and the people detect the odour signal at the four corners of the door wall (Fig. 3C-1). In these extreme situations, the odour signal needs to go through the longest path to reach the threshold concentration at detecting positions. The source position ($x_0 = 0$ m, $y_0 = 0$ m, $z_0 = 0$ m) is determined from where the Smell-Tell detector sits. The diffusion process from capsule into the container, was simulated by MATLAB. Four corners on the door are the detecting positions. In Fig. 3C-3, we can see the concentration at the four corners can reach human detecting threshold concentration in 5.5 hours. At that time, the released amount of odour signal will cause path length increases by 0.0002 cm, which is negligible as assumed for q calculation.

12   Simulation for Case 2: diffusion in a box which fits with the standard EUR/EPAL-pallet

A box, which fits with the standard EUR/EPAL-pallet, has a size of length L: X = 1.200 m, width W: Y = 0.800 m, height H: Z = 0.760 m. 2% (V/V) 3M1B in anhydrous ethanol is assumed to be sealed in a Smell-Tell detector with path length (z) of 0.02 m. The hole on the capsule dissolved by water has a size ($\boldsymbol{A}$) of 2×10^{-4} m^2. In this case, diffusion coefficient in the box (K) is assumed to be $0.001 m^2/s$, which means $K \gg D$, and $p_2 \ll p_1$. Diffusion coefficient of 3-methyl-1-butanethiol in the capsule (D) is about 0.086 cm^2/s. Estimate p_1 is 2.26 Pa based on the molar ratio of 3-methyl-1-butanethiol in the dilute solution. The diffusion rate of odour signal from capsule into the box can be easily calculated: $q = 4.6 \times 10^{-11}$mol/s. Assume the capsule is placed at one of the bottom corners of the box. Set the bottom corner, where the detector sits, as $x = 0, y = 0, z = 0$, which means the source position is $x_0 = 0$ $m, y_0 = 0$ $m, z_0 = 0$ m. After simulation, we can see the diffusion results in Fig. 3D-2 and Fig. 3D-3.

References

1. Fuller EN, Ensley K, Giddings JC (1969) Diffusion of halogenated hydrocarbons in helium. the effect of structure on collision cross sections. The Journal of Physical Chemistry 73: 3679-3685.

2. Smith RL (2000) Predicting evaporation rates and times for spills of chemical mixtures. Annals of Occupational Hygiene 45: 437-445.

3. Goedecke T (2008). Temperature and air change rates in freight containers during transport between eupore and destinations in asia and australia. URL `http://www.ista.org/forms/GOEDECKE_THOMAS_08PAPER.pdf`.

4. Drivas PJ, Valberg PA, Murphy BL, Wilson R (1996) Modeling indoor air exposure from short-term point source releases. Indoor Air 6: 271-277.

5. Cheng KC, Acevedo-Bolton V, Jiang RT, Klepeis NE, Ott WR, et al. (2011) Modeling exposure close to air pollution sources in naturally ventilated residences: Association of turbulent diffusion coefficient with air change rate. Environmental science technology 45: 4016-4022.

6. ChemSpider. Isoamylthiol. URL `http://www.chemspider.com/Chemical-Structure.10462.html`.

Chapter 6

Concluding Remarks

6.1   Conclusions

This work focuses on the development of practical odour-generating sensors. The results push the boundaries of limitation for odour-generating biosensors and pave the way for the utilization of odour signals in multi-sensory sensors. The research objectives proposed in Chapter 1 were fulfilled and the major contributions of this work are listed as below:

1. The efficiency of the bi-enzymatic (PKase and TPase) odour-generating biosensor was fully characterized. The best estimated threshold for instrument-free ATP detection using this biosensor was determined to be 0.32 µM.

2. The first odour-generating paper sensor, named "Smell-Tell" paper, was developed. The two enzymes (PKase and TPase) were printed on filter paper using a commercial printer, the scalable technology. A practical swab version of the paper sensor, named Smell-Tell swab, was developed. The paper sensor and swab sensor were stable for at least one month in the fridge. These sensors were also proven to

be reliable in complex background and open space cases.

3. The first odour-generating biosensor suitable for room temperature storage was obtained. Every component of the bi-enzymatic biosensor was immobilized and stabilized in pullulan tablets. The prepared Smell-Tell tablets were easy to use and handle, retaining activity for at least two months at room temperature. This product provided an uncomplicated platform for easy-to-run single step ATP assay suitable for resource-limited areas.

4. The bi-enzyme system was optimized using a low-cost statistical method. The influence of 11 variables was investigated. After optimization, the material cost of the biosensor was reduced by at least 30%, while maintaining the same detection limits of ATP.

5. A dual-signal water detector was proposed by generating both odour and colour signals was proposed. The detection limit of water was determined to be 50 µL. This detector demonstrated the compatibility of odour signal and colour signal, paving the way for the development of instrument-free multi-sensory sensors employing odour signal.

6. The evaporation and diffusion of the odour signal were simulated, demonstrating the possibility of using an odour as the reporting signal in a large room, such as a standard 20' intermodal container.

6.2   Proposed Work

Detection of microorganisms using the bi-enzymatic sensor

As mentioned in chapter 1, microbial cells contain a substantial amount of intracellular ATP. Some previously reported ATP assay methods have been used for the detection of microorganisms and organic contaminations. The bi-enzymatic odour-generating biosensor was tested for this purpose but the results showed that this biosensor was not effective enough for bacteria detection. For high concentrations of bacteria cells, the smell of bacteria by itself was very strong; for low concentration of bacteria cells, the ATP concentration in the sample was lower than the detection limit of the bi-enzymatic odour-generating biosensor. A potential solution to this problem is to regenerate ATP by a new enzyme, such as pyruvate kinase, to decrease the detection limit of the biosensor.

Development of multi-sensory sensors

Chapter 5 of this thesis has demonstrated the compatibility of odour signal and colour signal. This illustrates that one prospective type of odour-generating sensors could be multi-sensory sensors. In this type of sensors, odour signal could either work as a final reporting signal as shown in chapter 5, or as the primary signal, since it could self-diffuse and be easily transferred to other types of signals by the artificial noses as presented in Chapter 1.

Controlled release of different volatiles

Since humans can smell many odours with low thresholds, there are numerous odourous chemicals that could be involved in odour-generating sensors. The odour signals

utilized in this project are all repugnant, which are effective for detection of hazards. However, in other less threatening situations, the ideal signals should be easily detectable yet not displeasing to smell. Perfume chemicals could be used in such situations. Also, the perfume-generating sensors may find practical applications in perfume industry, by prolonging the longevity of perfume/fragrance.

In the larger scheme of sensor development, the vapours that are beyond the human detecting range could also be used for sensor development. Controlled release of pesticide, pheromone, or other special vapours intended for animals with highly developed sense of smell (e.g. dogs and cats), may be applied in areas of pest control, hazards alerting for pets, etc.